

DISS. ETH. NO.: 15378

# **ASSESSMENT OF THE FATE OF ORGANIC GROUNDWATER CONTAMINANTS USING THEIR ISOTOPIC SIGNATURES**

A dissertation submitted to the

SWISS FEDERAL INSTITUTE OF TECHNOLOGY ZURICH

for the degree of

Doctor of Sciences

presented by

LUC ZWANK

Dipl. Umweltnatw. ETH

born 02.01.1975

citizen of

Luxembourg

accepted on recommendation of

Prof. Dr. René P. Schwarzenbach, examiner

Prof. Dr. Stefan B. Haderlein, co-examiner

Prof. Dr. Daniel Hunkeler, co-examiner

2004



# TABLE OF CONTENTS

DANK .....	V
SUMMARY .....	VI
ZUSAMMENFASSUNG .....	IX
GENERAL INTRODUCTION .....	1
1.1 Contaminant Hydrology .....	2
1.2 <i>Classical</i> Methods in Contaminant Hydrology .....	3
1.3 Stable Isotope Based Investigations - Prospects and Limitations .....	4
1.4 Scope of the Present Work .....	7
SIMULTANEOUS DETERMINATION OF FUEL OXYGENATES AND BTEX USING DIRECT AQUEOUS INJECTION GAS CHROMATOGRAPHY MASS SPECTROMETRY (DAI-GC/MS).....	9
2.1 Introduction .....	10
2.2 Experimental Section .....	12
2.2.1 Reagents and Materials. ....	12
2.2.2 Standard Solutions. ....	13
2.2.3 Sampling and Sample Preparation. ....	14
2.2.4 DAI-GC/MS Analysis. ....	14
2.2.5 Absolute and Relative Recoveries and Method Detection Limits. ....	15
2.3 Results and Discussion .....	16
2.3.1 Chromatographic Separation. ....	16
2.3.2 Quality Assurance: Calibration, Recoveries, Method Detection Limits, and Accuracy. ....	16
2.3.3 Optimization of Injection Volume and Injection Speed. ....	19
2.3.4 Robustness of the Method. ....	19
2.4 Applications to Environmental Samples. ....	20
2.4.1 Application Example 1: Monitoring of Pollutant Degradation in a Gasoline-Contaminated Aquifer. ....	21
2.4.2 Application Example 2: Advanced Oxidation Treatment of MTBE in Drinking Water. ....	21
2.4.3 Application Example 3: Characterization of Various Gasoline Brands. ....	23
2.5 Conclusions .....	24

COMPOUND-SPECIFIC CARBON ISOTOPE ANALYSIS OF VOLATILE ORGANIC COMPOUNDS IN THE LOW-MICROGRAM PER LITER RANGE .....	25
3.1 Introduction.....	26
3.2 Experimental Section.....	28
3.2.1 Reagents and Materials. ....	28
3.2.2 Gas Chromatography-Combustion-Isotope Mass Spectrometry. ....	29
3.2.3 $\delta^{13}\text{C}$ Determination of the Pure Liquid Analytes. ....	30
3.2.4 $\delta^{13}\text{C}$ Determination of the Analytes with GC-IRMS. ....	30
3.2.5 Influence of the Oxidation Capacity of the Combustion Unit. ....	30
3.2.6 Liquid Injections. ....	31
3.2.7 SPME Measurements. ....	31
3.2.8 Purge and Trap Measurements. ....	32
3.2.9 Determination of Method Detection Limits. ....	33
3.2.10 Determination of Extraction Efficiencies. ....	33
3.2.11 Assumptions for Calculation of P&T Extraction Efficiency. ....	33
3.3 Results and Discussion .....	34
3.3.1 Liquid Injection. ....	34
3.3.2 Solid-Phase Microextraction. ....	35
3.3.3 Purge and Trap. ....	37
3.3.4 Comparison and Validation of Different Injection and Extraction Techniques. ....	39
3.3.5 Environmental Application of CSIA at Trace Levels. ....	42
3.4 Conclusions .....	43
VARIABILITY OF THE CARBON ISOTOPIC FRACTIONATION DURING THE REDUCTIVE DEHALOGENATION OF CARBON TETRACHLORIDE BY SURFACE-BOUND FERROUS IRON..	45
4.1 Introduction.....	46
4.2 Experimental Section.....	48
4.2.1 Reagents and Materials .....	48
4.2.2 Preparation of Solutions for Transformation Experiments .....	49
4.2.3 Preparation of Mineral Suspensions. ....	50
4.2.4 Preparation of Transformation Experiments. ....	50
4.2.5 Sampling and Analytical Procedures .....	51
4.3 Results and Discussion .....	53
4.3.1 Reaction Kinetics and Isotopic Enrichment. ....	53
4.3.2 Product Yields and Isotopic Enrichments - Mechanistic Considerations. ....	58
4.4 Conclusions .....	61
DIFFERENTIATION BETWEEN ABIOTIC AND MICROBIALLY MEDIATED REDUCTIVE DEHALOGENATION OF CHLORINATED ETHENES BASED ON STABLE CARBON AND HYDROGEN ISOTOPIC ANALYSIS .....	63
5.1 Introduction.....	64
5.2 Experimental Section.....	67
5.2.1 Reagents and Materials .....	67
5.2.2 Microbial Degradation Experiment .....	67
5.2.3 FeS Experiments .....	68
5.2.4 Sampling and Analytical Procedures .....	69
5.3 Results and Discussion .....	70
5.3.1 Microbial Reductive Dehalogenation .....	70
5.3.2 Abiotic Reductive Dehalogenation in the Presence of FeS .....	72
5.3.3 Hydrogen Isotopic Data of Dehalogenation Products .....	74
5.4 Conclusions .....	75

DETECTION OF ANAEROBIC MTBE DEGRADATION AND HINTS ON REACTION MECHANISM USING COMPOUND-SPECIFIC STABLE ISOTOPE ANALYSIS.....	77
6.1 Introduction .....	78
6.2 Experimental Section .....	81
6.2.1 Site Description .....	81
6.2.2 Sample Collection and Storage .....	83
6.2.3 Analytical Methods .....	83
6.2.4 Quantification of Biodegradation .....	84
6.2.5 Determination of $^{12}\text{k}/^{13}\text{k}$ and $^1\text{k}/^2\text{k}$ Values from Enrichment Factors .....	85
6.2.6 Complete MTBE-Hydrolysis under Acidic Conditions .....	87
6.3 Results and Discussion .....	88
6.3.1 Qualitative Assessment of <i>In Situ</i> Biodegradation of MTBE .....	88
6.3.2 Quantification of Biodegradation .....	93
6.3.3 Identification of Mechanism of Anaerobic MTBE Biodegradation .....	98
6.4 Conclusions .....	102
REFERENCES .....	105
Appendix A1 THEORETICAL BACKGROUND .....	I
1.1 Definitions and Calculations .....	II
1.2 General Rules for the Correction of “Statistical” Effects in the Reevaluation of $\epsilon$ -Data .....	IV
1.2.1 Ratios of Isotopes and Isotopic Molecules .....	IV
1.2.2 Zero Fractionation at Non-Reacting Positions Inside a Molecule .....	VI
1.2.3 Intramolecular Isotopic Competition .....	VII
1.2.4 General derivation of the proposed evaluation scheme .....	VII
1.3 Enzymatic Effect on Kinetic Isotope Effects - “Commitment to Catalysis” .....	XI
1.4 References .....	XIV
Appendix A2 ISOTOPIC ENRICHMENT FACTORS REPORTED FOR TRANSFORMATION REACTIONS OF ENVIRONMENTAL CONTAMINANTS.....	XV
2.1 References .....	XXI
Appendix A3 HYDROGEN ISOTOPIC SIGNATURES OF PRODUCTS FROM THE MICROBIAL DEGRADATION OF PER AND TCE BY DEHALOSPIRILLUM MULTIVORANS.....	XXV
3.1 Experiments Spiked with Tetrachloroethene (PER) .....	XXVI
3.2 Experiments Spiked with Trichloroethene (TCE).....	XXVI
CURRICULUM VITAE.....	XXIX



# DANK

Ein herzliches Dankeschön möchte ich den Betreuern meiner Arbeit Prof. Dr. René Schwarzenbach und Prof. Dr. Stefan Haderlein aussprechen. Sie haben es mir ermöglicht an der EAWAG an einem neuen Forschungsgebiet selbstständig zu arbeiten, mir das wissenschaftliche Rüstzeug für den erfolgreichen Abschluss dieser Dissertation mitgegeben und mich auch in schwierigen Situationen in meiner Vorgehensweise unterstützt. Ich möchte mich auch bei Prof. Dr. Daniel Hunkeler bedanken, dass er mir bereits am Anfang meiner Arbeit mit Tips, Tricks und ersten Isotopenmessungen zur Seite stand und auch zum Abschluss als Koreferent sehr wertvolle Inputs für meine Arbeit gegeben hat.

Bei den allzu häufigen "kleinen" Problemen im Labor und mit den manchmal sehr widerspenstigen analytischen Geräten konnte ich jeder Zeit auf den Input von Michael Berg und Torsten Schmidt zählen. Ohne ihren grossen Erfahrungsschatz wäre der Fortschritt in der Analytik wohl nie richtig aus dem Stocken gekommen. Bei Anna Aeberhardt, Jakov Bolotin, Martin Elsner, Thomas Erhart, Maik Jochmann und Samuel Luzi möchte ich mich für eine tolle Zusammenarbeit und ihr grosses Engagement in unseren gemeinsamen Projekten bedanken.

Allen weiteren ständigen wie temporären Mitgliedern der Schadstoffhydrologie (Marianne Erbs, Irene Hanke, Andreas Kappler, Thomas Hofstetter, Caroline Stengel, Thomas Kellerhals, Akané Hartenbach, Nicole Tobler, Anke Neumann) wie auch allen Mitgliedern von W+T, vom GruFo, den Unihockey- und (Tisch)-FussballspielerInnen, die unsere gemeinsamen Diskussionen, Sitzungen, Exkursionen, etc. hoffentlich genauso genossen haben wie ich, danke ich für die einmalige Arbeitsatmosphäre.

Schliessen möchte ich mit einem herzlichen Dankeschön an meine Eltern weil sie mir das Studium ermöglicht haben und mich zu jeder Zeit unterstützt haben. Sophie danke ich für ihre Geduld und ihre Unterstützung während den intensiveren und auch manchmal weniger erfolgreichen Arbeitsphasen.

## SUMMARY

Groundwater contaminations with organic pollutants are frequently found in industrialized countries, and occur when anthropogenic chemical compounds enter the subsurface through point sources (e.g., accidental spills, illegal disposal, leaking underground storage tanks) or diffuse inputs (e.g. rain, street runoff). For a reliable assessment and eventually a successful remediation of contaminated sites, it is important (i) to identify the sources of the contamination, (ii) to understand the transport and fate of the compounds in the groundwater, (iii) to evaluate potential *in situ* transformation processes and, (iv) to assess the fate and toxicity of the products of this transformation. In recent years, compound-specific stable isotope analysis (CSIA) has been increasingly used for the assessment of the fate of organic pollutants in groundwater. This new technique potentially allows the identification of different contamination sources based on the fact that organic chemicals may have significantly different isotopic signatures depending on the raw materials and pathways used in the synthesis. Furthermore, CSIA may allow the distinction between physical processes, such as transport, sorption and evaporation of the pollutants, and their (bio)chemical transformation, because the latter is commonly associated with a significant shift in the isotopic composition between the parent compound and its degradation products, known as isotopic fractionation. As a consequence, the remaining fraction of the contaminant becomes more and more enriched in the heavy isotope as the reaction proceeds along the groundwater flow path. The major goal of this thesis was to further develop, apply and evaluate prospects and limitations of compound-specific stable carbon and hydrogen isotope analysis in contaminant hydrology .

In the first part, two analytical methods were developed that allow (i) for the simultaneous quantification of gasoline oxygenates, major degradation products of methyl *tert*-butyl ether (MTBE) and BTEX compounds (Chapter 2), and (ii) for the determination of compound-specific isotope signatures of volatile organic compounds in the low  $\mu\text{g/L}$ -range (Chapter 3). The developed direct aqueous injection (DAI) GC/MS method was shown to be a robust analytical tool for the routine determination of a variety of important groundwater pollutants found at gasoline spill sites. The method detection limits (MDLs) are  $<2 \mu\text{g/L}$  for most analytes and  $<0.2 \mu\text{g/L}$  for MTBE, benzene and toluene. The method is accurate as



determined from comparison with headspace-GC/MS and purge-and-trap GC/MS and versatile as shown by its application in various environmental studies. Chapter 3 further addresses the development of extraction methods that allowed to reduce MDLs of CSIA significantly. Purge-and-trap (P&T) was the most efficient preconcentration technique reaching MDLs from 0.25 µg/L - 5 µg/L for frequently found groundwater contaminants, corresponding to the lowest MDLs reported so far for continuous-flow isotope ratio determinations. The isotopic fractionation caused by P&T and solid-phase microextraction (SPME) were shown to be small and highly reproducible and can, therefore, be corrected for. Hence, using P&T, the use of CSIA becomes accessible to study degradation processes of pollutants at concentration ranges that are frequently found at contaminated sites, even in the fringe zones of extended contaminant plumes.

Isotopic fractionation factors of dehalogenation reactions have frequently been determined for biotransformations, while data from abiotic reactions are more scarce. The study presented in Chapter 4, focusses on abiotic dehalogenation reactions that potentially occur in contaminated aquifers under iron-reducing conditions. The results show that the abiotic dehalogenation of tetrachloromethane (CCl<sub>4</sub>) by Fe(II) adsorbed to the surface of different iron-containing minerals (mackinawite, goethite, magnetite, lepidocrocite, hematite and siderite) is associated with significant carbon isotopic enrichments (ε). These observed enrichments spanned from -15.9‰ to -32.0‰. Furthermore, the results emphasize that isotopic fractionation of a given reaction type may be influenced by factors such as several concurrent reaction pathways and/or shifts in the relative positions of the transition state on the reaction coordinate. The simultaneous measurement of the concentrations and isotopic signatures of chloroform, a major and highly toxic degradation product of CCl<sub>4</sub>, showed that the mechanisms governing isotopic fractionation are complex, even in the transformation reaction of a “simple” compound.

In order to evaluate if abiotic and microbial dehalogenation could be distinguished based on the isotopic fractionation associated with the respective reaction, carbon isotopic enrichments of microbially mediated and abiotic transformations of tetrachloroethene (PER) and trichloroethene (TCE) under sulfate-reducing conditions were determined in Chapter 5. The still rather preliminary results show that, in the case of PER, the isotopic enrichment (ε = -1.0‰) observed during the microbial degradation by a pure culture of *dehalospirillum multivorans* differed significantly from the enrichment associated with the abiotic dehalogena-

tion of PER in the presence of FeS (-14.7‰). In the case of TCE, an unambiguous distinction of both processes based on carbon isotopic enrichments ( $\epsilon = -12.6\text{‰}$  to  $-20.9\text{‰}$  and  $\epsilon = -9.6\text{‰}$  for the microbial dehalogenation and the abiotic reaction, respectively) was not possible. Furthermore, it was shown that stable hydrogen isotopic signatures of TCE and *cis*-1,2-dichloroethene (*cis*-DCE) can be used to infer the source of these lower chlorinated compounds in a contaminant plume. This is possible because manufactured chlorinated ethenes are usually enriched in  $^2\text{H}$  ( $> +500\text{‰}$  for TCE and,  $> +300\text{‰}$  for *cis*-DCE), while the compounds originating from the degradation of higher chlorinated ethenes are depleted by 50‰ for TCE and 100‰ for *cis*-DCE, relative to the bulk  $\text{H}_2\text{O}$ .

Finally, in Chapter 6, *in situ* biodegradation of MTBE was successfully identified and quantified based on the simultaneous determination of stable carbon and hydrogen isotopic signatures of MTBE and its major degradation product *tert*-butanol (TBA), despite a complex hydrogeological setting and the presence of multiple contamination sources. Carbon and hydrogen isotopic signatures of MTBE increased from  $-26.4\text{‰}$  (carbon) and  $-73.1\text{‰}$  (hydrogen), in the source regions to signatures of up to  $+40.0\text{‰}$  (carbon) and  $+60.3\text{‰}$  (hydrogen) downgradient of the major source. Carbon isotopic signatures of TBA remained more or less invariant throughout the plume, suggesting the absence of TBA-degradation. The quantification of the biodegradation based on isotopic enrichments revealed the relevance of an additional process (potentially evaporation) for the observed MTBE-concentration decline. The reevaluation of isotopic enrichments reported for anaerobic and aerobic biodegradation of MTBE as intrinsic kinetic isotope effects, yielded for the first time hints that the anaerobic biodegradation occurs via a  $\text{S}_{\text{N}}2$ -type reaction mechanism.

# ZUSAMMENFASSUNG

In industrialisierten Ländern kommt es häufig zu Grundwasserkontaminationen durch organische Substanzen. Diese treten auf, wenn chemische Verbindungen anthropogenen Ursprungs über Punktquellen (z. Bsp. Unglücksfälle, illegale Entsorgung oder Leckagen an un-terirdischen Tankanlagen) respektive über diffuse Quelle (z. Bsp. Regen oder Strassenabläufe) in den Untergrund gelangen. Um solche kontaminierte Standorte richtig charakterisieren und schlussendlich erfolgreich sanieren zu können bedarf es (i) einer klaren Identifizierung der Kontaminationsquellen, (ii) eines guten Verständnisses des Transportes und des Verhaltens der Schadstoffe im Untergrund, (iii) einer Charakterisierung und Quantifizierung eventuell vorhandener Transformationsprozesse und (iv) einer Beurteilung des Verhaltens und der Toxizität der Abbauprodukte aus diesen Prozessen. In den letzten Jahren, wurde die Bestimmung substanzspezifischer Isotopensignaturen organischer Verbindungen vermehrt zur Untersuchung des Verhaltens von Grundwasserschadstoffen eingesetzt. Mit Hilfe dieser neuen Technik, können verschiedene Kontaminationsquellen unterschieden werden, da synthetische Chemikalien unter Umständen je nach Synthese und verwendeter Rohstoffe ganz unterschiedliche isotopische Zusammensetzungen aufweisen können. Des Weiteren kann anhand von substanzspezifischen Isotopensignaturen möglicherweise zwischen physikalischen Prozessen, wie zum Beispiel Transport, Sorption und Evaporation der Schadstoffe und biologischen oder chemischen Transformationsprozessen unterschieden werden. Dies wird ermöglicht, da die (bio)chemischen Prozesse üblicherweise mit einer signifikanten Verschiebung der isotopischen Zusammensetzung zwischen Edukt und Produkt verbunden sind. Dieser Effekt wird als Isotopenfraktionierung bezeichnet. Als Folge dieser Fraktionierung, werden die schweren Isotope in dem Anteil des Eduktes, welches noch nicht reagiert hat, im Laufe der Reaktion angereichert. Ziel dieser Dissertation war es Methoden zu entwickeln, welche es ermöglichen substanzspezifische Isotopenbestimmungen unter Feldbedingungen durchzuführen, diese Methoden anzuwenden sowie die Perspektiven und Limiten dieser Technik in der Schadstoffhydrologie aufzuzeigen.

Die zwei analytischen Methoden, welche im ersten Teil der Arbeit entwickelt wurden, erlauben (i) eine gleichzeitige Quantifizierung von Benzininhaltstoffen, Methyl-*tert*-butylether (MTBE), dessen wichtigsten Abbauprodukten sowie von BTEX-Komponenten (Kapitel 2) und (ii) eine Bestimmung der substanzspezifischen Isotopensignaturen flüchtiger organischer Verbindungen im tiefen  $\mu\text{g/L}$ -Bereich (Kapitel 3). Es wurde gezeigt, dass die entwickelte direkte wässrige Injektion-GC/MS Methode eine robuste analytische Methode zur routine-mässigen Bestimmung einer Reihe wichtiger Grundwasserschadstoffe ist. Die Nachweisgrenzen für die meisten Analyten waren  $<2 \mu\text{g/L}$  und  $<0.2 \mu\text{g/L}$  für MTBE sowie Benzen und Toluol. Die Genauigkeit der Methode wurde einerseits anhand von Vergleichsmessungen mit Headspace GC/MS sowie Purge-and-Trap GC/MS gezeigt. Die Anwendung der Methode in ganz unterschiedlichen Studien unterstreicht die Vielseitigkeit der direkten wässrigen Injektion. Kapitel 3 behandelt die Entwicklung von Extraktionstechniken, welche die Sensitivität der substanzspezifischen Isotopenbestimmung deutlich verbessert haben. Dabei hat sich Purge-and-Trap (P&T) als effizienteste Extraktionstechnik erwiesen, welche die bislang tiefsten berichteten Nachweisgrenzen ( $0.25 - 5 \mu\text{g/L}$ ) für häufige Grundwasserschadstoffe ermöglicht. Es wurde gezeigt, dass die Isotopenfraktionierung welche durch P&T und Festphasenmikroextraktion (SPME) hervorgerufen wird, gering und äusserst reproduzierbar und somit auch, mit Hilfe externer Standards, korrigierbar, ist. Die Verwendung von P&T erlaubt demnach die Bestimmung der stabilen Isotopensignaturen von Schadstoffen in einem Konzentrationsbereich, der häufig an kontaminierten Standorten und sogar an den Randzonen von Schadstofffahnen gefunden wird.

Im Vergleich zu mikrobiellen Dehalogenierungsreaktionen gibt es für die abiotische Transformation von chlorierten organischen Verbindungen nur wenige Daten über Isotopenfraktionierungen. In Kapitel 4 wurden abiotische Dehalogenierungsreaktionen untersucht. Diese Reaktionen können in kontaminierten Aquiferen unter eisenreduzierenden Bedingungen eine wichtige Rolle spielen. Es wurde gezeigt, dass die abiotische Dehalogenierung von Tetrachlormethan ( $\text{CCl}_4$ ) durch, an eisenhaltige Mineralien (Mackinawit, Goethit, Magnetit, Lepidocrocit, Hematit und Siderit) adsorbiertes Fe(II), mit einer deutlichen Isotopenfraktionierung verbunden ist. Die beobachteten Anreicherungsfaktoren ( $\epsilon$ ) lagen zwischen  $-15.9\%$  und  $-32.0\%$ . Diese Resultate unterstreichen, dass die Isotopenfraktionierung einer gegebenen Reaktion durch Faktoren, wie parallel verlaufende

Reaktionswege und/oder Verschiebungen in der Lage des Übergangszustandes auf der Reaktionskoordinate, stark beeinflusst wird. Die gleichzeitige Bestimmung des Konzentrationsverlaufs sowie der isotopischen Zusammensetzung von Chloroform, eines wichtigen und toxischen Abbauprodukts von  $\text{CCl}_4$ , hat aufgezeigt dass die Isotopenfraktionierung, selbst bei der Transformation eines "einfachen" Moleküls, auf sehr komplexen Mechanismen beruht.

In Kapitel 5 wurde bestimmt inwiefern sich die Fraktionierung der Kohlenstoffisotope bei der reduktiven Dehalogenierung unter sulfatreduzierenden Bedingungen von Tetrachlorethen (PER) und Trichlorethen (TCE) durch Mikroorganismen, einerseits, und durch abiotische Reaktionen, andererseits, unterscheiden. Die vorläufigen Ergebnisse haben gezeigt, dass, im Fall von PER, die Anreicherung ( $-1\text{‰}$ ) während der mikrobiellen Transformation durch *dehalospirillum multivorans* sich wesentlich von dem Anreicherungsfaktor ( $\epsilon = -14.7\text{‰}$ ) der abiotischen Reaktion mit FeS unterscheidet. Die Resultate im Beispiel von TCE hingegen, erlauben keine eindeutige Unterscheidung zwischen mikrobieller ( $\epsilon = -12.6\text{‰}$  bis  $-20.9\text{‰}$ ) und abiotischer ( $\epsilon = -9.6\text{‰}$ ) Dehalogenierung. Zusätzlich wurde gezeigt, dass die stabilen Wasserstoffisotopensignaturen von TCE und *cis*-1,2-Dichlorethen (*cis*-DCE) verwendet werden können um den Ursprung dieser Substanzen im Grundwasser zu bestimmen. Dies ist möglich, da die synthetisch hergestellten chlorierten Ethene meistens eine starke Anreicherung an  $^2\text{H}$  aufweisen ( $> +500\text{‰}$  für TCE,  $> +300\text{‰}$  für *cis*-DCE) wohingegen die Verbindungen, welche durch die Transformation von PER im Vergleich zum umgebenden Wasser um  $50\text{‰}$  (TCE) bis  $100\text{‰}$  (*cis*-DCE) abgereichert sind.

Schlussendlich, wurde in Kapitel 6 die *in situ* Biodegradation von MTBE mit Hilfe der Bestimmung stabiler Kohlenstoff- und Wasserstoffisotopensignaturen von MTBE und seines Abbauproduktes *tert*-Butanol (TBA) erfolgreich identifiziert und quantifiziert. Dies war möglich obschon die hydrogeologischen Bedingungen sehr komplex waren und mehrere Kontaminationsquellen vorhanden waren. Kohlenstoff- und Wasserstoffisotopensignaturen von MTBE stiegen von  $-26.4\text{‰}$  (C) und  $-73.1\text{‰}$  (H) in den Verschmutzungsherden bis zu Werten von  $+40.0\text{‰}$  (C) und  $+60.3\text{‰}$  (H) in stromabwärts gelegenen Probenahmebrunnen an. Die Kohlenstoffsignaturen von TBA entlang der Schadstofffahne blieben im Grossen und Ganzen unverändert, so dass davon ausgegangen werden konnte dass kein TBA-Abbau stattfindet. Die, auf der beobachteten Isotopenfraktionierung beruhende,

Quantifizierung des Abbaus hat ergeben, dass noch ein weiterer Prozess (möglicherweise Evaporation) für die beobachtete Konzentrationsabnahme von MTBE von Wichtigkeit ist. Die Reevaluation, der für den aeroben respektive anaeroben MTBE-Abbau berichteten, Anreicherungs-faktoren als intrinsische kinetische Isotopeneffekte, hat zum ersten Mal Hinweise darauf geliefert, dass die anaerobe Biotransformation von MTBE über einen  $S_N2$ -Mechanismus abläuft.

**1**

# **GENERAL INTRODUCTION**

## 1.1 Contaminant Hydrology

Groundwater contaminations are frequent in industrialized countries, where high amounts of anthropogenic chemical compounds are used. Organic pollutants may enter the subsurface through various pathways (point sources such as accidental spills, illegal disposal, leaking underground storage tanks or via diffuse inputs such as agriculture, rain, street runoff) and subsequently be transported and transformed by various processes. Hence, the initial contaminants as well as their potential degradation products endanger the most important drinking water resources. In order to conduct successful remediations of contaminated sites, the potential processes that govern the behavior of the contaminants have to be understood and quantified. Figure 1.1 illustrates the major challenges with which contaminant hydrology has to deal.

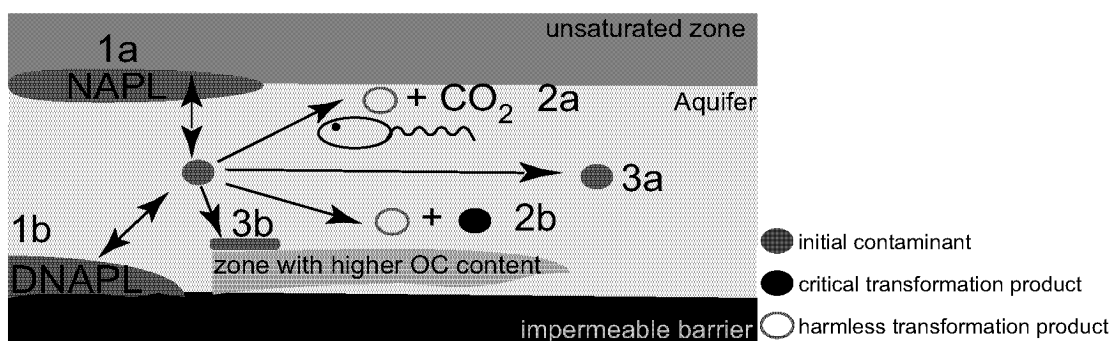


**Figure 1.1: Challenges of Contaminant Hydrology.** Depending on the specific density of the contaminants, non-aqueous phase liquids (NAPLs, (1a) e.g., in the case of gasoline components such as BTEX and MTBE) or dense non-aqueous phase liquids (DNAPLs, (1b) e.g., in the case of solvents such as  $\text{CCl}_4$ , PER or TCE) form in the aquifer. From these phases, the contaminants partition into the groundwater and may be subject to microbial (2a) or abiotic (2b) transformation, dilution (3a) or sorption (3b).

A major problem encountered, once a contamination has been detected, is to localize the source of the contaminant. Next, the different processes that lead to a decrease of the concentration of the contaminant with increasing distance from the source have to be identified and quantified. A decrease of contaminant concentrations along the flow path may be due to various factors including physical processes such as dilution and transport (3a) and sorption (3b) of the organic compound, or to degradation reactions that may be microbially mediated (2a) or abiotic (2b). An acceptable *in situ* remediation requires that a degradation reaction occurs, which will eventually lead to the removal of the contaminant from the contaminant plume. Eventually, once it has been shown that an *in situ* degradation actually occurs, it is important to identify the nature of the degradation to assure that the degradation of the initial contaminant does not lead to recalcitrant or toxic products. To date, most of these



tasks are difficult to fulfill, especially if complex hydrogeological conditions and/or several sources of pollutions are present.

## 1.2 **Classical Methods in Contaminant Hydrology**

The identification of contamination sources (environmental forensics) is always necessary to adopt appropriate means of risk reduction and/or to identify responsible parties in litigation. Traditional approaches in environmental forensics use biomarker analysis, chemometrics and chemical fingerprints. In the latter approach, the chemical composition of contaminant plumes are compared to mixtures used by different manufacturers. Chemical fingerprinting using high-resolution gas chromatography is often used in the source apportionment of contaminations.<sup>1</sup> For example, concentration patterns of polycyclic aromatic hydrocarbons, C<sub>1</sub>-C<sub>5</sub> hydrocarbons or BTEX are used to differentiate between various gasoline or petroleum spills.<sup>2</sup> In this type of investigation complex statistical models are used, but the basic questions about the source of a contamination can often not be answered unambiguously.<sup>3</sup> Chemical fingerprinting is *per definitionem* limited to sites where the contamination is due to a spill of a mixture (e.g. gasoline, petroleum) and cannot be used to distinguish between multiple sources of one single compound (e.g., in the case of solvent spills where only a limited number of compounds such as tetrachloroethene (PER) or trichloroethene (TCE) enter the subsurface). Furthermore, fingerprinting is based on the assumption that all components in a mixture show the same transport and transformation behavior in the aquifer, which is usually not the case.

The occurrence and rate of degradation reactions in subsurface environments are usually described using mass-balances of contaminant and metabolite concentrations, as well as of electron-acceptor concentrations. However, in order to be successful, a set of conditions has to be met: the input of contaminant has to be known, a dense network of monitoring wells has to be used<sup>4</sup> and the analytical techniques must exist to enable the detection of the metabolites at trace levels. As a consequence, intrinsic remediation becomes difficult to monitor in the case of widespread plumes of poorly degradable compounds. For instance the degradation of methyl *tert*-butyl ether (MTBE) was proposed to be estimated by calculating a mass balance of MTBE and *tert*-butanol, its initial metabolite.<sup>5</sup> However, even at a site with well known hydrogeological conditions and a dense network of sample wells, the degradation of a known amount of

injected MTBE could not be unequivocally determined.<sup>6</sup> Hence, the mass balance approach is only reliable in the case of single sources of easily degradable substances and a precise knowledge of the groundwater flow regime.

### 1.3 Stable Isotope Based Investigations - Prospects and Limitations

During the past years stable isotope methods have been introduced in the field of contaminant hydrology. In the beginning these methods focussed on the use of isotopically labelled tracers or the determination of the stable isotope signature of sum parameters such as dissolved inorganic carbon (DIC), carbon dioxide (CO<sub>2</sub>) or methane.<sup>7-12</sup> Recently, compound-specific stable isotope analysis (CSIA) has opened new approaches in the field of contaminant hydrology.<sup>13</sup> The hyphenation of gas chromatographic separation to an isotope ratio mass spectrometer (GC-IRMS) via a combustion/pyrolysis interface allows the on-line determination of stable isotope compositions of single organic compounds (Figure 1.2). The isotopic composition is usually expressed relative to an international standard as defined (for example of carbon) by Equation (1-1).

$$\delta^{13}C = \left( \frac{R_{sample}}{R_{reference}} - 1 \right) \cdot 1000 \quad [‰] \quad (1-1)$$

where  $R_{sample}$  and  $R_{reference}$  are the ratios of the heavy isotope to light isotope in the sample and the international standard, respectively

Source apportionment of groundwater contaminations as well as the determination of the time of contaminant releases by CSIA rely on the fact that isotopic compositions of chemicals show differences between manufacturers depending on the pathways and raw materials used in the synthesis of the chemical. This has already been successfully applied for  $\delta^{13}C$  of BTEX compounds<sup>14</sup>,  $\delta^{13}C$  of MTBE<sup>15</sup>,  $\delta^{13}C$  and  $\delta^{37}Cl$  of polychlorinated biphenyls<sup>16-18</sup>,  $\delta^{13}C$ ,  $\delta^2H$  and  $\delta^{37}Cl$  of chlorinated solvents<sup>19</sup> and  $\delta^{13}C$  and  $\delta^{15}N$  in trinitrotoluene.<sup>20</sup> Often, neither CSIA nor chemical fingerprinting *alone* are conclusive for source apportionment, but the combination of both techniques has resulted in successful source identification.<sup>21</sup> This differentiation could even be enhanced by the determination of the isotopic composition of two or more elements, e.g. the combination of data for  $\delta^{13}C$  and  $\delta^{37}Cl$ <sup>18,19,22</sup> or  $\delta^{13}C$  and  $\delta^2H$ .<sup>19,23,24</sup>

Enhancing the sensitivity of CSIA to the ng/L range, could even provide means to distinguish diffuse from point source immissions into ground-water..

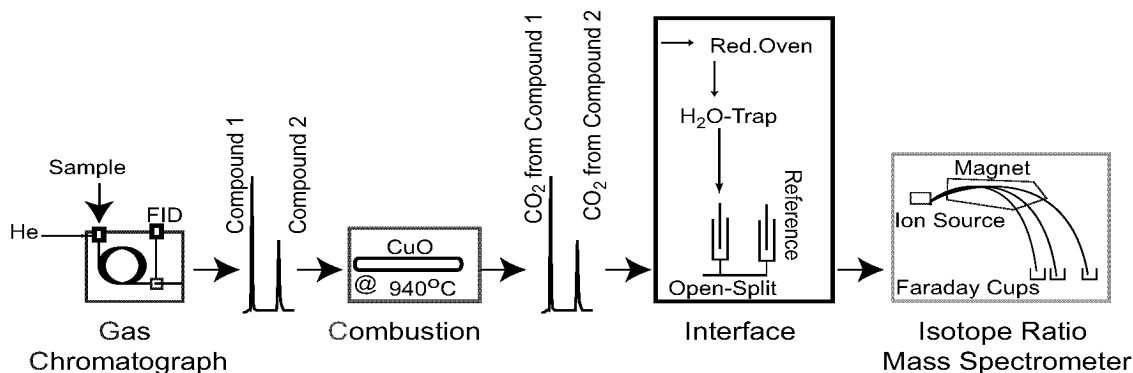


**Figure 1.2: Schematic of GC-IRMS for the Determination of  $\delta^{13}\text{C}$ -values.**

After chromatographic separation the analytes are combusted to  $\text{CO}_2$  and  $\text{H}_2\text{O}$ .  $\text{NO}_x$  that may be formed during the combustion of nitrogen-containing analytes, are completely reduced to  $\text{N}_2$  in the reduction oven and the water is removed by a Nafion™-membrane. The  $\text{CO}_2$  is then ionized in the ion source of the mass spectrometer, the ions ( $m/z$  44  $^{12}\text{CO}_2$ ,  $m/z$  45  $^{13}\text{CO}_2$  and  $m/z$  46  $^{12}\text{C}^{18}\text{O}^{16}\text{O}$ ) are deviated by the magnetic field and detected in separate faraday cups, with an amplification adapted to the natural abundance of the different isotopes. The  $\delta^{13}\text{C}$ -ratio is determined by comparing the relative abundances of mass 44 and 45 of the unknown analyte with a reference gas of known isotopic composition. The determination of mass 46 is used to correct for the relative abundance of  $^{17}\text{O}$  via the determination of the abundance of  $^{18}\text{O}$ .

CSIA also yields information that is useful in the determination of *in situ* transformation, because it allows to distinguish between transport, partitioning and transformation processes. During chemical transformations (e.g., the cleavage or the formation of chemical bonds) a shift in the isotope ratios of the precursor and the product may occur. This effect is known as kinetic isotope fractionation and is due to the fact that bonds between the lighter isotopes are usually weaker than bonds between the heavy isotopes. Thus, if the reacting bond of a molecule contains light isotopes it reacts faster as if an heavy isotope of the element would be present. This leads to a progressive enrichment of the molecules containing heavy isotopes at the reacting bond in the remaining fraction of the precursor, while the degradation product is depleted in the heavy isotopes. In environmental investigations, this fractionation is usually quantified by the “Rayleigh Equation” (Equation (1-2)), since the study of Mariotti et al.<sup>25</sup>

$$\ln\left(\frac{\delta^{13}C_t + 1000}{\delta^{13}C_0 + 1000}\right) = \frac{\varepsilon}{1000} \cdot \ln f = (\alpha - 1) \cdot \ln f \quad (1-2)$$

where  $\delta^{13}C_t$  and  $\delta^{13}C_0$  are the relative isotopic compositions of the investigated compound at time  $t$  in a batch reactor (or at distance  $x$  in the field) and at time  $0$  (or at the contamination source), respectively.  $\alpha$  is commonly known as isotopic fractionation factor, whereas  $\varepsilon$  is referred to as isotopic enrichment factor and  $f$  corresponds to the remaining fraction of the substrate (e.g.  $C_t/C_0$ ), see also Appendix A1 for a more detailed derivation of Equation (1-2).

To date numerous laboratory experiments have been carried out that have demonstrated the usefulness of CSIA in the detection and quantification of transformation reactions of organic groundwater pollutants.<sup>24,26-45</sup> The isotopic enrichment factors determined in these studies are summarized in Appendix A2. In the case of constant  $\alpha$  (or  $\varepsilon$ ) values for a given reaction, such values may be used for the quantification of *in situ* degradation of a given compound.<sup>46-48</sup> In the ideal case, this allows the assessment of *in-situ* remediation without the establishment of mass balances, since the change of isotopic signature is primarily caused by the degradation reaction, and not by physical processes such as evaporation<sup>31,36,49</sup>, transport<sup>22</sup> and sorption<sup>50</sup> that are not, or only to a much lower extent, subject to isotopic fractionation. However, the results from field sites are mostly of qualitative nature because a quantification is only possible if the responsible process and its specific enrichment factor can be identified. Nevertheless, these studies have shown the potential of using CSIA for determining the existence of natural attenuation of a contamination.<sup>32,34,39,42,51-54</sup>

## 1.4 Scope of the Present Work

To date, several issues hamper a wider application of stable isotope investigations, especially at field sites. One of the major obstacles to use CSIA in field investigations are the relatively high method detection limits of GC-IRMS (e.g. >130 ppb of chlorinated methanes, ethanes and ethenes).<sup>55</sup> The distinction between different processes that may lead to isotopic fractionations is not possible, because most field studies are restricted to one element (mostly C) of the contaminant, and hence quantification of natural attenuation is often impossible.

The scope of this thesis was to further develop, apply and evaluate prospects and limitations of multielement compound-specific stable isotope analysis in different fields of contaminant hydrology, ranging from mechanistic laboratory studies to field applications. Within this dissertation the following studies were performed:

Chapter 2 addresses the development and validation of a versatile and robust analytical method for routine determination of methyl *tert*-butyl ether, its major polar degradation products (*tert*-butanol (TBA), *tert*-butyl formate, methyl acetate and acetone), possible MTBE substitutes as gasoline oxygenates as well as BTEX components in aqueous samples.

In Chapter 3, several preconcentration techniques were evaluated to lower method detection limits (MDLs) for the determination of stable isotopic signatures of volatile organic groundwater pollutants. The use of purge and trap extraction as well as solid-phase microextraction prior to the GC-IRMS measurement was compared to different liquid injection techniques and the potential isotopic fractionation caused by each extraction step was carefully evaluated.

Factors influencing the magnitude of isotopic fractionation, due to an environmentally relevant type of abiotic reaction were studied in Chapter 4. The carbon isotopic enrichment of  $\text{CCl}_4$  during the reductive dehalogenation by Fe(II) bound to the surface of different iron-containing minerals was determined. If one single enrichment factor could be assigned to the abiotic reaction, it could be used for differentiating between abiotic and microbial reactions and for the quantification of the abiotic reaction.

In Chapter 5 carbon enrichment factors associated with microbial reductive dehalogenation as well as abiotic dehalogenation reactions of chlorinated ethenes that may coexist under sulfate-reducing conditions are determined. The major goal was to exemplify how stable hydrogen isotopic data of trichloroethene and *cis*-1,2-dichloroethene could be used

to differentiate between anthropogenic contamination sources and degradation products of the higher chlorinated tetrachloroethene.

Finally, in Chapter 6, it is shown how CSIA can be used to assess *in-situ* bioremediation of MTBE at a field site with a complex hydrogeological background and multiple sources of contaminations. Carbon and hydrogen stable isotopic data of MTBE and its major degradation product TBA allowed an identification as well as a quantification of *in situ* degradation.

# **SIMULTANEOUS DETERMINATION OF FUEL OXYGENATES AND BTEX USING DIRECT AQUEOUS INJECTION GAS CHROMATOGRAPHY MASS SPECTROMETRY (DAI-GC/MS)**

*A direct aqueous injection-gas chromatography/mass spectrometry (DAI-GC/MS) method for trace analysis of gasoline components in water is presented. The method allows for the simultaneous quantification of the following solutes: methyl tert-butyl ether (MTBE), its major degradation products (tert-butyl formate, tert-butyl alcohol (TBA), methyl acetate, and acetone), and possible substitutes of MTBE as an octane enhancer in gasoline (tert-amyl methyl ether, ethyl tert-butyl ether) as well as benzene, toluene, ethylbenzene, p-xylene, m-xylene, and o-xylene (BTEX). No enrichment or pre-treatment steps are required, and sample volumes of only 50  $\mu\text{L}$  are needed for analysis. The detection limits in two different matrixes (spiked lake water and contaminated groundwater) are  $<2 \mu\text{g/L}$  for most analytes and  $<0.2 \mu\text{g/L}$  for MTBE, benzene, and toluene. The accuracy of the DAI-GC/MS method was excellent as determined from comparison with headspace-GC/MS and purge-and-trap-GC/MS. The DAI-GC/MS method has been applied to various environmental studies, which demonstrated its versatility. The applications comprised both laboratory (MTBE degradation in water treatment, quantification of polar gasoline components) and field (MTBE degradation at a gasoline spill site) investigations.*

## 2.1 Introduction

Because of the ubiquity and high volume use of fuels and other petroleum products, their components are important environmental contaminants. Accidental spills and leaking underground storage tanks are the most significant point sources of gasoline contamination. Hence, monitoring programs include some priority gasoline-derived contaminants, such as benzene, toluene, ethylbenzene, and the xylene isomers (BTEX). In addition to these compounds, more polar components (e.g., dialkyl ethers used as oxygenates and octane enhancers) are nowadays present in gasoline. Methyl tert-butyl ether (MTBE), for example, is the most widely used fuel oxygenate and is added to gasoline at concentrations of up to 15% (v/v) in gasoline.<sup>56</sup> tert-Butanol (TBA) is considered the major degradation product of MTBE in natural systems<sup>57,58</sup> but can also be found as a gasoline component. Because of the relatively high water solubility of MTBE and TBA as compared to other gasoline components (Table 2.1), these components partition to a higher degree from nonaqueous phase liquids into the groundwater. Consequently, MTBE has been found to be one of the most frequent groundwater contaminants in recent years.<sup>56,59</sup> In addition, diffuse input to groundwater through atmospheric deposition can cause low-level aquifer contaminations with MTBE.<sup>60</sup> Furthermore, MTBE is released to lakes because of boating activities.<sup>60,61</sup> Hence, in addition to the conventionally monitored gasoline-derived contaminants, future environmental monitoring programs must include such highly polar gasoline components as well as their transformation products or their byproducts.

The trace analysis of BTEX<sup>64-66</sup> and dialkyl ethers<sup>67-69</sup> often includes enrichment by solid-phase microextraction (SPME) and purge-and-trap (P&T). However, the sensitivity of these methods is not suitable for more polar components, such as TBA. The lack of a trace analytical method, that allows for the simultaneous determination of all major gasoline derived contaminants with a high groundwater pollution potential, may explain the fact that environmental data on TBA, for example, is relatively scarce. Gaines et al. proposed a headspace SPME extraction coupled to a two-dimensional gas chromatographic separation for the simultaneous detection of oxygenates as well as aromatic compounds.<sup>70</sup> The technical effort necessary hampers the use of this method as a routine analytical tool. The extraction efficiency of SPME and in particular headspace SPME is hardly sufficient for the trace analysis of TBA and other polar compounds.<sup>68,71</sup> SPME is also of limited use for aqueous



samples with a high content of nonpolar organic compounds because cross competition occurs.<sup>72</sup>

**Table 2.1: Gasoline Components with High Water Solubilities and Average Fuel-Water Partition Coefficients**

compound	water solubility [g/L]	fuel-water partition coefficient ( $K_{fw}$ )
TBA	complete <sup>a</sup>	0.15–0.33 <sup>b</sup>
MTBE	48 <sup>a</sup>	15.5 <sup>c</sup>
benzene	1.8 <sup>d</sup>	350 <sup>c</sup>
toluene	0.5 <sup>d</sup>	1250 <sup>c</sup>
ethylbenzene	0.2 <sup>d</sup>	4500 <sup>c</sup>
p-xylene	0.2 <sup>d</sup>	4350 <sup>c</sup>
m-xylene	0.2 <sup>d</sup>	4350 <sup>c</sup>
o-xylene	0.2 <sup>d</sup>	3630 <sup>c</sup>

a. Reference (56)

b. Own work; value depending on MTBE content.

c. Reference (62)

d. Reference (63)

The aim of this study was to develop and validate a robust analytical method for the simultaneous detection of fuel derived water contaminants including their polar degradation products with a high sensitivity for all analytes. A promising approach is the use of direct aqueous injection-gas chromatography (DAI-GC). The applicability of DAI-GC has already been evaluated for various organic compounds.<sup>73-76</sup> For the detection of MTBE, two different DAI-GC/MS methods have been published.<sup>75,76</sup> Using polar columns to retain the water more strongly and a mass spectrometer with high vacuum capacity for the evacuation of the high water vapor volumes, Church et al. reported method detection limits (MDLs) in the sub- $\mu\text{g/L}$  range.<sup>75</sup> This method was applied in various field studies to determine MTBE and its degradation products.<sup>6,77</sup> Hong et al.<sup>76</sup> adapted the method for the use on a benchtop mass spectrometer. The achieved MDLs were only 30-100  $\mu\text{g/L}$ , and the obtained chromatographic resolution was not suitable for environmental samples from contaminated aquifers. None of these DAI methods included the determination of other relevant gasoline components.

We developed a method suited to simultaneously quantify trace levels of fuel oxygenates and their major metabolites as well as BTEX compounds even in small sample volumes. This DAI-GC method allows for low MDLs (ng/L- $\mu\text{g/L}$ ) using a benchtop mass spectrometer and can be

used as a routine analytical tool in monitoring programs and other investigations which require high throughput and minimum handling of samples. The method presented has been validated for 13 analytes (see Table 2.2) and has been successfully applied to monitor a groundwater MTBE plume at a gasoline spill site, to study the product formation in advanced oxidation processes for the elimination of MTBE in drinking water treatment, and to characterize the water-soluble fractions of different gasoline brands.

## 2.2 Experimental Section

### 2.2.1 Reagents and Materials.

Methanol (>99.9%) used to prepare stock solutions was obtained from Scharlau S. A. (Barcelona, Spain). MTBE (99.5%), acetone (99.5%), methyl acetate (99.5%), tert-butyl alcohol (99.5%), benzene (99.9%), perdeuterated benzene (99.9%), toluene (99.5%), m-xylene (99.5%), o-xylene (99.5%), p-xylene (99.5%), and ethylbenzene (99.5%) were purchased from Fluka (Buchs, Switzerland). Ethyl tert-butyl ether (99%), tert-amyl methyl ether (TAME) (>97%), tert-butyl formate (>99%), and MTBE- $d_3$  (>99% atom D) were purchased from Aldrich (Steinheim, Germany). The perdeuterated tert-butyl alcohol (98%) was obtained from Acros Organics (Geel, Belgium). Table 2.2 shows the names, abbreviations and CAS numbers of the analytes and reference compounds used in this paper.

**Table 2.2: Investigated Compounds and Internal Standards, Molecular Weights, Densities and Monitored Mass Traces**

compound	CAS-no.	Abbreviation	mol. wt.	density [kg/L]	target ion <sup>a</sup> [m/z]	reference ions <sup>a</sup> [m/z]
methyl <i>tert</i> -butyl ether	1634-04-4	MTBE	88.15	0.740 <sup>b</sup>	73	43
deuterated MTBE	29366-08-3	MTBE- <i>d</i> <sub>3</sub>	91.17	0.765 <sup>b</sup>	76	43
ethyl <i>tert</i> -butyl ether	637-92-3	ETBE	102.17	0.752 <sup>b</sup>	59	87, 57
<i>tert</i> -amyl methyl ether	994-05-8	TAME	102.17	0.770 <sup>b</sup>	73	87, 55
acetone	67-64-1	AC	58.08	0.790 <sup>b</sup>	58	43
methyl acetate	79-20-9	MA	74.08	0.934 <sup>b</sup>	74	43
<i>tert</i> -butyl alcohol	762-75-4	TBF	102.13	0.879 <sup>c</sup>	59	87, 57
perdeuterated <i>tert</i> -butyl alcohol	75-65-0	TBA	74.12	0.789 <sup>b</sup>	59	57
benzene	53001-22-2	TBA- <i>d</i> <sub>10</sub>	84.20	0.893 <sup>c</sup>	65	
perdeuterated benzene	71-43-2	BENZ	78.11	0.876 <sup>b</sup>	78	55
toluene	1076-43-3	BENZ- <i>d</i> <sub>6</sub>	84.15	0.669 <sup>b</sup>	84	56
ethylbenzene	108-88-3	TOL	92.14	0.867 <sup>a</sup>	91	92
<i>p</i> -xylene	100-41-4	ETHBENZ	106.17	0.867 <sup>b</sup>	91	106
<i>m</i> -xylene	108-38-3	p-XYL	106.17	0.861 <sup>b</sup>	91	106
<i>o</i> -xylene	95-47-6	m-XYL	106.17	0.864 <sup>b</sup>	91	106

a. Used for MS.

b. Reference (78)

c. Specification from manufacturer.

## 2.2.2 Standard Solutions.

Methanolic single compound stock solutions (4000 ppmv) were prepared in 25-mL volumetric flasks. Twenty milliliters of methanol were added, and after drying of the necks, 100  $\mu$ L of the neat analyte were spiked to the methanol using precision glass syringes. The flasks were then filled with methanol to the mark. These primary stock solutions were prepared monthly, transferred to screw cap vials, and stored without headspace at 4 °C. Standard solutions were prepared in fresh tap water from the laboratory that was free of detectable target compounds, whereas HPLC-grade, deionized, and Nanopure water showed low-level contamination with volatile analytes. Tap water stored for several days in the laboratory was often contaminated (<1  $\mu$ g/L) with some of the target compounds, mostly benzene. Aqueous standard solutions (16 ppmv) of single analytes, a mixture of all analytes (S<sub>0</sub>), and internal standards (IS<sub>0</sub>) were prepared by adding 100  $\mu$ L of the primary methanolic stock solutions to 25 mL of tap water as described previously. These concentrated

aqueous standards ( $S_0$  and  $IS_0$ ) were prepared weekly and stored without headspace at 4 °C. However, aqueous concentrated TBF standards were prepared daily because of the rapid hydrolysis of TBF to TBA.<sup>79</sup> Diluted aqueous standards for calibration were prepared daily from the  $S_0$  solutions in fresh tap water. A six-point external calibration curve ranging from 0.16 to 3.2 ppbv or from 1.6 to 160 ppbv, according to the concentration of the analytes, was used for quantification. The internal standard was used to correct for the variations of the injection volume and fluctuations in the ionization efficiency of the mass spectrometer. Alternatively to a deuterated standard, TAME was found a suitable internal standard if absent in the samples.

### 2.2.3 Sampling and Sample Preparation.

Generally, the loss of the volatile analytes has to be minimized during sampling, sample transport, and storage. Lake water from lake Zurich (depth, 2.5 m) and groundwater samples from a gasoline contaminated aquifer were collected in 120-mL glass bottles with Teflon-lined screw caps. These vials were slowly filled from the bottom to top and sealed without headspace. The samples were then stored in the dark at 4 °C until analysis. The only sample preparation required was the addition of an internal standard (e.g., deuterated MTBE). For this purpose, 1 mL of the samples were transferred to 1.8-mL autosampler vials and 5  $\mu$ L of the internal standard were added with a glass syringe from the  $IS_0$  aqueous stock solution. Final concentrations of the deuterated internal standards in the samples were 1.6 or 80 ppbv, depending on the concentration range of the calibration. Tests with 50- $\mu$ L glass inserts for the autosampler vials revealed that, if required, even such low sample volumes are sufficient. However, this was not further investigated because the sample volumes in all of our applications exceeded 1 mL.

### 2.2.4 DAI-GC/MS Analysis.

The water samples were quantified using a gas chromatograph (GC 8000, Fisons, Manchester, U.K.) coupled to a mass spectrometric detector (single quadrupole MD 800, Fisons). The gas chromatograph was equipped with an 8 m  $\times$  0.53 mm guard-column deactivated with OV-1701-04 (BGB, Anwil, Switzerland). The separation of the analytes was achieved on a 60 m  $\times$  0.32 mm Stabilwax fused silica column coated with a 1.0  $\mu$ m crossbonded Carbowax-poly(ethylene glycol) film (Restek, Bellefonte, PA). Helium was used as the carrier gas at a constant column head pressure of 100 kPa. Samples of 1-10  $\mu$ L were injected through a

cold on-column injector, using an autosampler (AS 800, Fisons). A slow and reproducible injection rate of 1  $\mu\text{L/s}$  was necessary to achieve uniform wetting of the precolumn. The following temperature program was used: 6 min standby at 50  $^{\circ}\text{C}$ , 5 min at 50  $^{\circ}\text{C}$ , then to 60  $^{\circ}\text{C}$  at 10  $^{\circ}\text{C/min}$ , 3 min at 60  $^{\circ}\text{C}$ , then to 95  $^{\circ}\text{C}$  at 30  $^{\circ}\text{C/min}$ , 4 min at 95  $^{\circ}\text{C}$ , then to 200  $^{\circ}\text{C}$  at 30  $^{\circ}\text{C/min}$ , and 6 min at 200  $^{\circ}\text{C}$ . The total run time was 30 min. The 6 min standby time at 50  $^{\circ}\text{C}$  was necessary to obtain a stable background signal. The 6 min bake time at 200  $^{\circ}\text{C}$  was required for the complete elimination of water. Detection and quantification of the analytes was performed in the electron impact positive ion mode and selected ion monitoring (SIM), using the compound-specific ions given in Table 2. The identification of the analytes was assured by monitoring additional compound-specific reference ions and by comparing retention times in samples and standards. To reduce the number of simultaneously monitored  $m/z$  ratios, we used three different SIM windows.

### **2.2.5 Absolute and Relative Recoveries and Method Detection Limits.**

The determination of recoveries and method detection limits (MDLs) was performed in two types of natural waters. Series with 1 and 10  $\mu\text{L}$  injections were validated separately. Natural water samples were spiked to analyte concentrations of 3.2 and 80 ppbv for 1  $\mu\text{L}$  injections and 0.8 and 3.2 ppbv for 10  $\mu\text{L}$  injections. Five replicates of each spike level were prepared and quantified, using a six-point calibration curve of concentration versus the ratio of analyte signal intensity to internal standard (MTBE- $d_3$ ) signal intensity. The MDLs were determined as three times the standard deviation derived from these 10 spike samples multiplied with the low spike concentration. Recoveries correspond to the ratios of determined concentrations to spiked concentrations. The absolute recovery is based on concentration measurements using external calibration, whereas the relative recovery is based on internal calibration.<sup>80</sup> Because of the hydrolysis of TBF to TBA, recoveries of TBF were determined in a separate experiment with samples that did not contain TBA initially.

## 2.3 Results and Discussion

### 2.3.1 Chromatographic Separation.

As can be seen in Figure 2.1, the use of a 60-m poly(ethylene glycol) (PEG) analytical column and the chosen chromatographic conditions yielded baseline separation for all investigated compounds. Because of the high polarity of the stationary phase, the water is retained more strongly than the analytes. The “water peak” can be recognized by an elevated background between 16.5 and 19 min. The excellent chromatographic resolution allows for the simultaneous detection of additional compounds that have not been included in the method validation, such as 2-butanone (MEK), 2-propanol (IPA), sec-butanol (2BA), and even ethanol (see Chapter 2.4). To monitor additional analytes, additional SIM windows are necessary to maintain the sensitivity for all analytes.

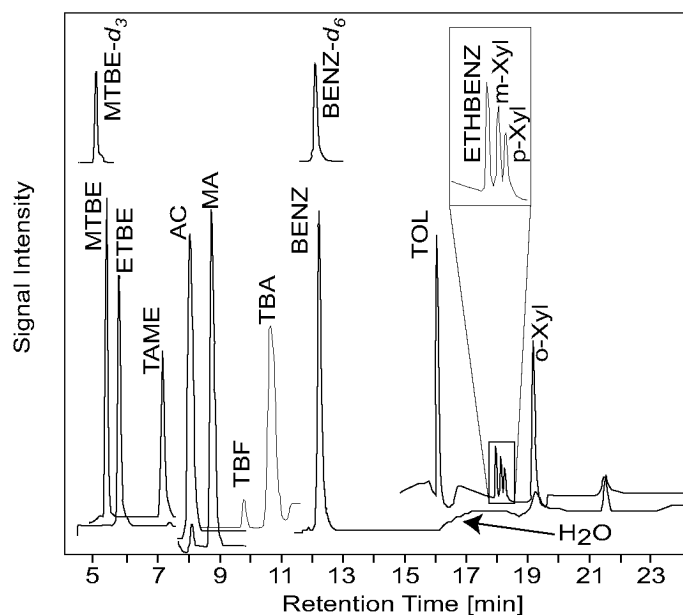


**Figure 2.1:DAI-Chromatogram.** Mass traces of quantification ions derived from a 1  $\mu\text{L}$  injection of a lake water sample spiked with 80 ppbv of the target analytes and internal standards. The water eluting between 16.5 and 19 min., is lowering the signal intensity of ETHBENZ, m-XYL., and p-XYL

### 2.3.2 Quality Assurance: Calibration, Recoveries, Method Detection Limits, and Accuracy.

The linearity of the DAI-GC/MS method was tested for concentration ranges of 1.6-160 ppbv (1  $\mu\text{L}$  injections) and 0.16-3.2 ppbv (10  $\mu\text{L}$  injections). The calibration curves were linear in both concentration ranges ( $R^2 > 0.996$ ). Table 2.3 shows the parameters of the method validation for the 13 investigated analytes. The high recoveries ( $92 \pm 16\%$  absolute,

101 ± 11% relative) reflect the fact that the method does not require any sample preparation apart from the addition of the internal standard. The use of an internal standard improved the overall performance of the method as it corrects for variations in injection volumes and drifting ionization efficiencies. The absence of sample preconcentration steps (e.g., solid-phase extraction or purge-and-trap) helps to avoid sample contamination, which frequently occurs when dealing with volatile analytes. For the 10 µL injections, MDLs of MTBE, ETBE, TAME, BENZ, and TOL were <0.20 µg/L in lake water and 0.45 µg/L in groundwater. The MDLs for ethylbenzene, p-xylene, and m-xylene were significantly higher and might not be sufficient for some applications because these compounds coeluted with the water (solvent). The reduced sensitivity for these compounds can be explained by the elevated background during solvent elution (16.5-19 min). However, as can be seen from the o-xylene peak, the sensitivity for components eluting after the solvent peak is not influenced by the neighboring water peak. In the case of 1 µL injections, MDLs of <2 µg/L were achieved for most analytes. The use of multiple internal standards (e.g., for the different compound classes of the target analytes) such as TBA-*d*<sub>10</sub> and benzene-*d*<sub>6</sub> did not significantly improve either the method detection limits or the relative recoveries, indicating that the ionization conditions remained sufficiently constant throughout a single chromatographic run. In groundwater samples, we observed a suppression of the benzene-*d*<sub>6</sub> signal, which was presumably induced by the matrix. MTBE-*d*<sub>3</sub> was, therefore, used as single internal standard for all measurements. Samples from a gasoline spill site and from Lake Zurich were used for an interlaboratory comparison of DAI-GC/MS with other analytical methods (i.e., headspace-GC/MS and P&T-GC/MS).

Figure 2.2 shows the correlation of our DAI-GC/MS measurements with the concentrations reported by external laboratories. The results agreed over a wide concentration range with an average deviation of 17%.

**Table 2.3: Relative and Absolute Recoveries with Relative Standard Deviations (RSD) and Method Detection Limits (MDL) Determined in Lake Water and Groundwater**

compound	injection vol. [μL]	Lake Water (depth 2.5 m)				Groundwater					
		spike levels [μg/L]	relative recovery <sup>a,b</sup> [%] (RSD)		absolute recovery <sup>a</sup> [%] (RSD)	MDL <sup>b,c</sup> [μg/L]	spike levels [μg/L]	relative recovery <sup>a,b</sup> [%] (RSD)		absolute recovery <sup>a</sup> [%] (RSD)	MDL <sup>b,c</sup> [μg/L]
			100 (8.0)	103 (9.8)				95 (6.8)	0.12		
MTBE	10	0.59; 2.37	100 (8.0)	95 (6.8)	0.12	0.59; 1.18	104 (7.4)	77 (4.5)	0.05 <sup>d</sup>		
ETBE	10	0.60; 2.41	103 (9.8)	95 (9.8)	0.08	0.60; 1.20	103 (7.5)	70 (5.3)	0.13		
TAME	10	0.62; 2.46	97 (9.0)	88 (11.5)	0.10	0.62; 1.23	100 (13.1)	65 (12.2)	0.24		
AC	1	2.53; 63.2	126 (23.2)	111 (14.8)	1.38	2.53; 63.2	109 (13.1)	102 (11.1)	0.99		
MA	1	2.99; 74.7	94 (12.6)	92 (12.3)	1.54	2.99; 74.7	96 (23.6)	89 (11.4)	2.12		
TBF <sup>e</sup>	1	70.3	81 (2.0) <sup>f</sup>	85 (1.0) <sup>f</sup>	2.98	70.3	94 (5.5) <sup>f</sup>	82 (4.7) <sup>f</sup>	11.6		
TBA	1	2.52; 63.1	130 (12.7)	128 (12.1)	1.78	2.52; 63.1	106 (15.8)	109 (11.4)	1.19		
BENZ	10	0.70; 2.80	112 (8.9)	106 (7.6)	0.20	0.70; 1.40	110 (8.5)	60 (13.1)	0.18		
TOL	10	0.69; 2.77	119 (9.7)	111 (8.7)	0.14	0.69; 1.39	88 (7.8)	62 (6.8)	0.16		
ETHBENZ	1	2.53; 69.4	94 (7.4) <sup>f</sup>	93 (4.2) <sup>f</sup>	14.54	2.53; 69.4	95 (3.6) <sup>f</sup>	93 (3.3) <sup>f</sup>	7.50		
p-Xyl	1	2.53; 68.9	93 (13.9) <sup>f</sup>	98 (11.2) <sup>f</sup>	26.56	2.53; 68.9	90 (5.5) <sup>f</sup>	95 (4.2) <sup>f</sup>	11.3		
m-Xyl	1	2.77; 69.1	107 (15.0) <sup>f</sup>	107 (13.4) <sup>f</sup>	33.41	2.77; 69.1	99 (8.4) <sup>f</sup>	97 (5.6) <sup>f</sup>	17.4		
o-Xyl	1	2.82; 70.4	97 (11.3)	97 (11.5)	0.49	2.82; 70.4	89 (6.5)	92 (9.8)	0.55		

a. n=10

b. Relative to MTBE-d<sub>3</sub> as internal standard.

c. Calculated from multiplication of 3 times the standard deviation of relative recoveries with the low spike level.

d. Calculated from unspiked samples (n=5).

e. TBF recoveries and MDLs were determined as mass balances of TBA and TBF during a separate run with TBA-d<sub>10</sub> as an internal standard.

f. n=5.



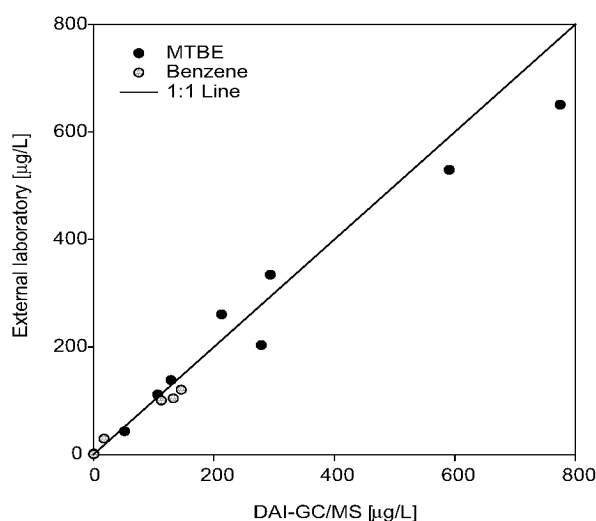


**Figure 2.2: Method Validation.** Correlation of MTBE and benzene concentrations determined in groundwater and lake water samples using DAI-GC/MS and headspace-GC/MS or P&T-GC/MS ( $n=16$ ). Headspace and P&T analyses were carried out by external laboratories

### 2.3.3 Optimization of Injection Volume and Injection Speed.

The increase of the injection volume allowed for lower MDLs for MTBE, ETBE, TAME, BENZ, and TOL. However, because of significant peak broadening of AC, MA, and TBA and an increase of the background signal in the second SIM window, the determination of these analytes, including TBF, was influenced by injection volumes exceeding 2  $\mu\text{L}$  (see Figure 2.3). A similar effect on the peak shape of TBA for 5  $\mu\text{L}$  injection volumes has been described previously.<sup>76</sup> The injection volume was therefore set to 1  $\mu\text{L}$ , which resulted in sufficiently low MDLs for most of our applications. If, however, very low MDLs were required for ethers, benzene, and toluene, these analytes were determined in a second chromatographic run with an injection volume of 10  $\mu\text{L}$ . High injection velocities (10  $\mu\text{L/s}$ ) led to phase soaking<sup>81</sup> and, as a consequence, to poorly reproducible shifts in the retention of the analytes. The optimum injection speed was 1  $\mu\text{L/s}$  in combination with a sufficiently long bake time after analysis.

### 2.3.4 Robustness of the Method.

Early work with DAI indicated the need of frequent system maintenance because of troublesome effects (active sites, peak tailing, reduced recovery, and sensitivity) caused by water and nonvolatile water constituents on the liner, analytical column, and ion source. To avoid problems with a liner, we used cold on column injection onto an 8-m deactivated precolumn. This precolumn was frequently shortened (down to a length of 5 m) and replaced thereafter. Lifetimes of the analytical columns

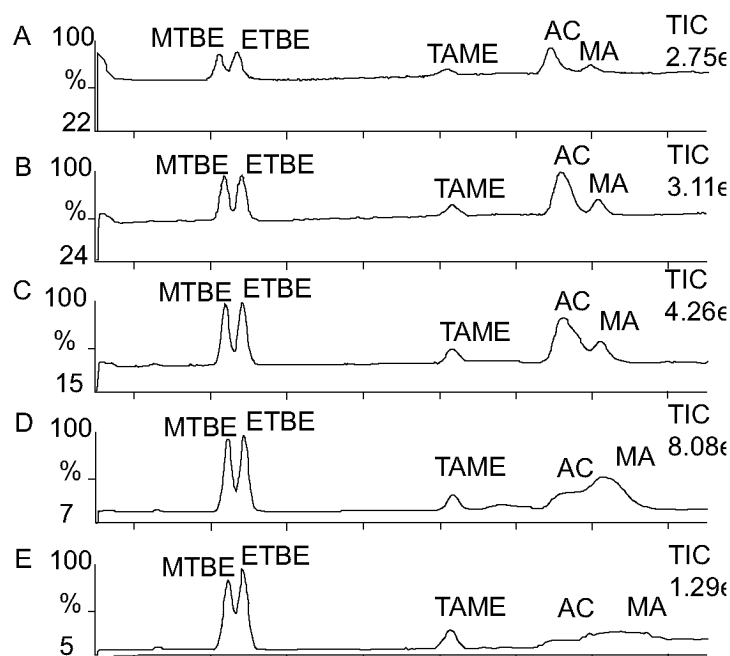


**Figure 2.3: Effect of Injection Volume.** Influence of injection volume on the peak shape of acetone and methyl acetate. Chromatograms derived from injections of (A) 0.5  $\mu\text{L}$ , (B) 1  $\mu\text{L}$ , (C) 2  $\mu\text{L}$ , (D) 5  $\mu\text{L}$ , and (E) 10  $\mu\text{L}$  of a standard containing 16 ppbv of each analyte. A similar effect can be observed for the TBA peak shape.

exceeded 1000 injections without a substantial loss of separation efficiency, although the injected samples contained high concentrations of organic compounds, nonvolatile buffers, or even residual reactive oxygen species. Bake cycles between sample injections were not necessary. After the first injections of water, the filament support in the ion source developed a blue surface without a notable effect on sensitivity. Neither the filament nor the other parts of the ion source had to be cleaned or replaced more frequently than in other GC/MS methods.

## 2.4 Applications to Environmental Samples.

The wide range of simultaneously detectable fuel components (from highly polar to nonpolar) as well as the simple and fast sample preparation contribute to the excellent robustness of the presented DAI method, make it a powerful tool for the rapid quantification of gasoline components at trace levels in water. The following applications of the DAI-GC/MS method exemplify its versatility. Detailed descriptions of these ongoing studies are, or will be presented in separate publications.

### 2.4.1 Application Example 1: Monitoring of Pollutant Degradation in a Gasoline-Contaminated Aquifer.

To assess natural attenuation of MTBE and other organic contaminants without ambiguities, the concentrations of both the parent compounds and their major metabolites need to be monitored in a large number of samples collected along the contaminant plume for several years. At an accidental gasoline spill site in Switzerland, about 70 t of gasoline including 5 t of MTBE were released to the environment in 1994.<sup>82</sup> Eight months after the spill, the monitoring of MTBE was started with HS-GC/MS, but TBA was never analyzed because of the lack of a suitable method. Using DAI-GC/MS, we were able to quantify MTBE and TBA concentrations with a single analysis as well as concentrations of other regulated organic contaminants (BTEX) simultaneously and with similar sensitivity (Figure 2.4). Several years after the spill, the concentrations of all of contaminants in the groundwater were still more than 1 order of magnitude higher than their respective MDLs. The advantages of DAI-GC/MS for this type of groundwater monitoring program are the simplicity and the speed of processing a large number of samples in combination with the simultaneous, sensitive, and accurate detection of MTBE and its major metabolite, TBA.

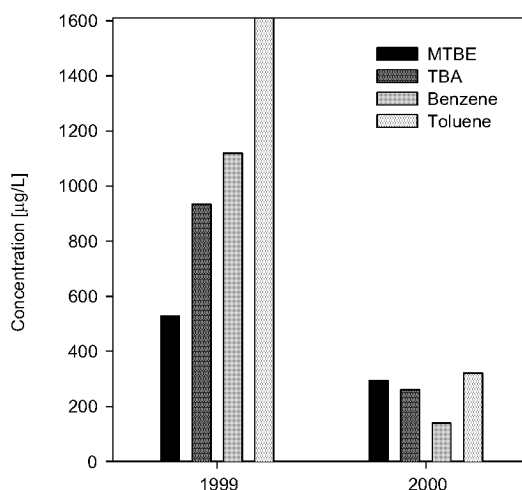


**Figure 2.4: Concentration Determination at a Contaminated Field Site.** MTBE, TBA, BENZ, and TOL concentrations measured in an observation well at 40 m distance from the gasoline spill site in the direction of groundwater flow in May 1999 and May 2000

### 2.4.2 Application Example 2: Advanced Oxidation Treatment of MTBE in Drinking Water.

The product formation of the oxidation of MTBE by conventional ozonation and advanced oxidation process (AOP) ozone/hydrogen peroxide was studied under drinking water treatment conditions.<sup>83</sup> This study

required an analytical method that allows the simultaneous and rapid determination of MTBE, TBF, TBA, AC, and MA in small sample volumes. These polar analytes are poorly extractable from water by conventional techniques (SPME, P&T). DAI-GC/MS enabled the sensitive and simultaneous determination of the target analytes, using TAME as the internal standard instead of the more expensive deuterated compounds. 2-Methoxy-2-methylpropionaldehyde (MMP), another degradation product of MTBE, could also be analyzed with this method. In this study, it was important to process the samples rapidly, to minimize loss of TBF by hydrolysis to TBA.<sup>79</sup> DAI-GC/MS was the only analytical method, which fulfilled all requirements necessary to conduct this study (i.e., fast and sensitive detection of polar analytes in small aqueous sample volumes).

### 2.4.3 Application Example 3: Characterization of Various Gasoline Brands.

Aqueous extracts of gasoline brands have been analyzed in order to identify water-soluble components of commercial fuels. Figure 2.5 shows a chromatogram of an aqueous extract of an unleaded regular gasoline measured in SIM mode. It is shown that, in addition to the analytes, for which the method validation has been carried out, numerous other compounds can be determined including sec-butanol (2BA), 2-propanol (IPA), 2-butanone (MEK), and 2-pentanone (MPK). In addition, ethanol, 1-butanol, and isobutanol could be quantified by the same procedure. Calculated concentration ratios of MTBE and TBA in seven different gasoline brands and their aqueous extracts are shown in Table 2.4. The technical specifications of all gasoline samples using direct gasoline analysis indicated TBA contents below the detection limit of 0.1 vol. %. In contrast to MTBE, TBA was thus not added intentionally as an oxygenate to the investigated fuels. Instead, the low concentrations of TBA in gasoline were presumably due to impurities of fuel-grade MTBE. Nevertheless, TBA was found in all investigated aqueous extracts at concentrations up to 340 mg/L because of the efficient extraction of TBA from gasoline by water. Thus, the rather selective extraction from a nonpolar matrix (fuel) allows for a much more sensitive analysis of the TBA content of gasoline using DAI-GC/MS than using the direct analysis of TBA in gasoline. Furthermore, TBA is expected to be present in gasoline-contaminated groundwater together with MTBE. Monitoring MTBE degradation at contaminated sites on the basis of analysis of its primary transformation product TBA, therefore, is only feasible if the TBA resulting from MTBE degradation can be distinguished from the TBA initially present in the spilled gasoline. .

**Table 2.4: MTBE/TBA Concentration Ratios in Gasoline and Its Aqueous Extracts**

gasoline sample	MTBE/TBA concentration ratio in gasoline <sup>a</sup>	MTBE/TBA concentration in aqueous extract
1	37	2.7
2	65	4.8
3	110	7.7
4	160	12
5	160	12
6	200	14
7	210	15

a. MTBE and TBA concentration in gasoline calculated using partitioning coefficients given in Table 2.1 for TBA, an average  $K_{fw}$  of 0.24 was used.

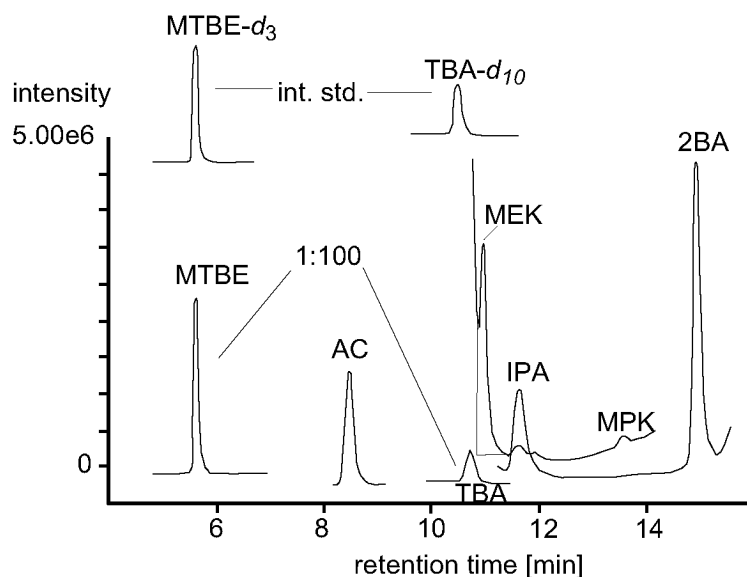


**Figure 2.5: DAI-Measurement of an Aqueous Gasoline Extract.** Chromatogram recorded in SIM mode. The mass traces shown are  $m/z$  43 (MEK, MPK), 45 (IPA, 2BA), 58 (AC), 59 (TBA), 65 (TBA- $d_{10}$ ), 73 (MTBE) and 76 (MTBE- $d_3$ ). The MTBE and TBA signals were reduced by a factor of 100 to allow for comparison with the other analytes

## 2.5 Conclusions

Our study demonstrates that DAI-GC/MS is a versatile, sensitive, and robust method that is well-suited to quantify trace levels of gasoline components in various aqueous matrixes. Accurate determinations of analyte concentrations in the low  $\mu\text{g/L}$  range are possible from very small sample volumes ( $\geq 50 \mu\text{L}$ ). The lack of preconcentration and cleanup steps and the very simple sample preparation (addition of internal standard) help to minimize losses of volatile analytes as well as a sample contamination and make the method an ideal monitoring tool. The achieved sensitivity, especially for polar compounds such as alcohols, is competitive with existing SPME or P&T methods. Thus, DAI-GC/MS has the potential to be used as a routine tool in monitoring groundwater, drinking water, and surface water quality, because it unites a large number of detectable analytes and has good sensitivity and accurate results as well as a high sample throughput without the need of large sample volumes or specialized equipment. The number of analytes detectable by DAI-GC/MS is currently expanded to other small chain alcohols, esters, aldehydes, and ketones in our laboratories.

# COMPOUND-SPECIFIC CARBON ISOTOPE ANALYSIS OF VOLATILE ORGANIC COMPOUNDS IN THE LOW-MICROGRAM PER LITER RANGE

Compound-specific carbon isotope analysis (CSIA) has become an important tool in biological, archeological, and geological studies as well as in forensics, food sciences, and organic chemistry. If sensitivity could be enhanced, CSIA would further have an improved potential for environmental applications such as, for example, in situ remediation studies to assess contaminated environments, identification of pollutant degradation pathways and kinetics, distinction between degradation/formation mechanisms, or, verification of contaminant sources. With this goal in mind, we have developed methods to determine  $\delta^{13}\text{C}$  values of commonly reported groundwater contaminants in low-microgram per liter concentrations. Several injection and preconcentration techniques were evaluated for this purpose, i.e., on-column injection, split/splitless injection, solid-phase microextraction (SPME), and purge and trap (P&T) in combination with gas chromatography-isotope ratio mass spectrometry. The  $\delta^{13}\text{C}$  values of the target compounds were determined by liquid injections of the analytes dissolved in diethyl ether or, in the case of P&T and SPME, by extraction from water spiked with the analytes. P&T extraction was the most efficient preconcentration technique reaching method detection limits (MDLs) from 0.25 to 5.0  $\mu\text{g/L}$ . These are the lowest MDLs reported so far for continuous-flow isotope ratio determinations, using a commercially available and fully automated system. Isotopic fractionation resulting from preconcentration and injection was investigated and quantified for the priority groundwater pollutants methyl tert-butyl ether (MTBE), chloroform, tetrachloromethane, chlorinated ethylenes, benzene, and toluene. The isotopic fractionations caused by the extraction techniques were small but highly reproducible and could therefore be corrected for. P&T was characterized by a higher reproducibility and smaller isotopic fractionations than SPME. Among the liquid injection techniques, cold on-column injection resulted in slightly better precision compared to split/splitless injection. However, the MDLs determined for liquid injections were 4-6 orders of magnitude higher (i.e., 9.5-2800  $\text{mg/L}$ ) than for P&T and SPME. Since both of the latter methods are solventless, a better chromatographic resolution was obtained than for the liquid injection techniques. The P&T and SPME methods described here are also applicable for CSIA of D/H ratios, which require 10-20 times higher analyte concentrations than  $^{13}\text{C}/^{12}\text{C}$  analysis. Finally, the applicability of the described methods is demonstrated for pollutant concentrations of only 5-60  $\mu\text{g/L}$  in environmental samples.

## 3.1 Introduction

In recent years, compound-specific stable isotope analysis (CSIA) of complex mixtures using gas chromatography-isotope ratio mass spectrometry (GC-IRMS) has become a powerful analytical tool to infer the origin and fate of organic compounds in various systems. Thus, CSIA is applied in many fields including archaeology, biomedical sciences, food science, forensic science, and organic geochemistry.<sup>84</sup> More recently, CSIA has been applied in contaminant hydrology for source apportionment of different groundwater contaminants<sup>85-87</sup> and the proof of in situ degradation of organic pollutants.<sup>10,24,32,37,51</sup>

CSIA is achieved by on-line coupling of a gas chromatograph (GC) to an isotope ratio mass spectrometer (IRMS). After the chromatographic separation on the GC column, the analytes are transferred to a combustion/pyrolysis interface where CO<sub>2</sub> or H<sub>2</sub> is formed for <sup>13</sup>C/<sup>12</sup>C or D/H measurements, respectively.<sup>88-90</sup> In many applications such as food analysis and biogeochemical applications, liquid injections via split/splitless injectors have been used. Evaporation of the analytes in the injector as well as gas chromatographic effects are known sources of isotopic fractionation.<sup>91,92</sup> The major drawback of GC-IRMS for trace analysis in environmental applications is its relatively poor sensitivity (i.e., 0.8 nmol of carbon of each individual compound). As a consequence, a concentration of, for example, 66 mg/L tetrachloroethylene (injection volume 1 μL), a common groundwater contaminant, would be needed for a reliable <sup>13</sup>C/<sup>12</sup>C ratio determination. Yet, the aqueous concentrations of such contaminants are regulated at the microgram per liter range in most OECD countries. To lower method detection limits in GC-IRMS applications, enrichment of the analytes prior to analysis without compromising accurate and precise isotope ratio determinations is therefore necessary.

Solid-phase microextraction (SPME) represents an increasingly used enrichment technique in combination with GC-IRMS. SPME utilizes a thin (0.4 mm) fused-silica fiber coated with a polymeric stationary phase for analyte extraction. This fiber is mounted in a syringelike device and is exposed to the headspace of the sample (headspace SPME) or directly into the liquid sample (direct immersion SPME). After analyte enrichment, the fiber is thermally desorbed in the split/splitless injector of the gas chromatograph.<sup>93,94</sup> Hunkeler and Aravena<sup>55</sup> achieved method detection limits (MDLs) of 130-290 μg/L for chlorinated ethylenes using direct immersion SPME as enrichment technique coupled to GC-IRMS. δ<sup>13</sup>C values determined for volatile compounds measured by headspace SPME or direct immersion SPME did not deviate significantly from those



of the pure phase analytes.<sup>27,36,55,95,96</sup> Dias and Freeman<sup>96</sup> determined the isotopic signature of toluene, methylcyclohexane, and hexanol using a 100- $\mu\text{m}$  PDMS fiber as well as acetic, propionic, and valeric acids in water using a 65- $\mu\text{m}$  Carbowax fiber. For toluene, they reported MDLs of 45  $\mu\text{g/L}$  for a precise isotopic measurement. MDLs for the organic acids were  $>2.5$   $\text{mg/L}$ .<sup>96</sup>

The application of SPME in GC-IRMS to analyze compound mixtures may be compromised by competition among the analytes for sorption sites on the extracting polymer phase, in particular when a phase is used that shows adsorption as well as partitioning. Black and Fine<sup>72</sup> reported a discrimination of the extraction of methyl tert-butyl ether (MTBE) by various SPME fibers in the presence of BTEX compounds, thereby obstructing the quantification of MTBE. So far the potential effects of sorption competition on the isotopic signatures of the analytes have not been evaluated.

Purge and trap (P&T) is a routinely used extraction method for the trace level quantification of volatile organic compounds.<sup>69,97,98</sup> Due to higher sample volumes as well as the higher sorption capacities of the traps, lower MDLs for volatile organic compounds can be obtained with P&T than with SPME. Nevertheless, the on-line coupling of P&T with GC-IRMS has rarely been reported.<sup>15,22,42,52,99,100</sup> Beneteau and co-workers<sup>22</sup> extracted tetrachloroethylene from water with a custom-made P&T unit and a purge time of 1.5 h. The analyte was subsequently processed off-line for  $\delta^{13}\text{C}$  and  $\delta^{37}\text{Cl}$  measurements. For these two elements, the P&T extraction did not cause detectable isotopic fractionation, most likely due to the high extraction efficiency of 80%. Whiticar and Snowdon<sup>99</sup> determined isotopic signatures of C5-C8 compounds in oils using a custom-made P&T apparatus. This method, however, was not developed for trace level analyses, but allowed reproducible determination of isotopic ratios for 26 different analytes. Smallwood et al.<sup>15</sup> determined carbon isotopic signatures of MTBE in aqueous samples using P&T coupled on-line to a GC-IRMS system. They determined MDLs of 15  $\mu\text{g/L}$  and a small isotopic fractionation caused by the P&T procedure leading to a significant but reproducible shift of  $\delta^{13}\text{C}$  values of +0.66‰. Kolhatkar et al.<sup>37</sup> reported a MDL of 5  $\mu\text{g/L}$  using short extraction times of 8 min. Recently, P&T has been applied as the extraction procedure for the determination of  $^{13}\text{C}/^{12}\text{C}$  ratios of chlorinated ethylenes, achieving MDLs of 5  $\mu\text{g/L}$ .<sup>52</sup> All these studies, however, do not provide a systematic evaluation of the P&T-GC-IRMS method with regard to its (potential) effects on the isotopic composition of the analytes. Since the

P&T procedure includes various phase transition steps that may shift the isotopic signature of the analytes (evaporation, sorption, condensation), it is important to evaluate the effects of the P&T method parameters such as purge time, desorption time, and injection temperature on the determination of the  $\delta^{13}\text{C}$  values of the analytes.

In this work, we developed methods for the simultaneous, compound-specific  $\delta^{13}\text{C}$  determination of volatile priority pollutants in aqueous samples. The major goals were to (i) improve the concentration techniques, (ii) lower the method detection limits of GC-IRMS to the low-microgram per liter level and, hence, (iii) make CSIA a more valuable tool for environmental applications such as contaminant hydrology. To this end, the carbon isotopic fractionation effect of common GC injection techniques and analyte concentration procedures (i.e., cold on-column injection, split and splitless injection, SPME, and P&T concentration) were thoroughly evaluated and a sensitive and precise P&T-GC-IRMS method was developed. Finally, the applicability of this method is demonstrated for the determination of  $\delta^{13}\text{C}$  values of trichloroethylene (TCE) and *cis*-1,2-dichloroethylene (*cis*-DCE) present at very low concentrations (20-60 and 5-12  $\mu\text{g/L}$ , respectively) in groundwater samples originating from a contaminated aquifer.

## 3.2 Experimental Section

### 3.2.1 Reagents and Materials.

Methanol (>99.9%) from Scharlau (Barcelona, Spain) and diethyl ether (>99.5%) from Merck (Dietikon, Switzerland) were used to prepare stock solutions. 1,1-Dichloroethylene (>99.9%), trichloroethylene (>99.9%), tetrachloroethylene (>99.9%), tetrachloromethane (>99.5%), chloroform (IR-grade), benzene (>99.9%), toluene (> 99.9%), and methyl *tert*-butyl ether (>99.5) were purchased from Fluka (Buchs, Switzerland). *cis*-1,2-Dichloroethylene (97%) and *trans*-1,2-dichloroethylene (98%) were obtained from Aldrich (Steinheim, Germany). Table 3.1 shows the names and abbreviations of the investigated analytes used in this work.

**Table 3.1: Investigated Compounds, Molecular Weights, Densities, Air-Water Partition Constants at 25 °C ( $K_{iaw}$ ), and Purge Times Necessary To Achieve 40% Extraction Efficiency**

compounds in order of GC elution	abbrevia-tion	MW <sup>a</sup>	density <sup>a</sup> [kg/L]	$K_{iaw}$ [25 °C]	purge time needed for 40% extraction	
					calculated for 25 °C [min]	measured [min]
1,1-dichloroethylene	1,1-DCE	96.9	1.22	1.26	0.4	n.d. <sup>b</sup>
<i>trans</i> -1,2-dichloroethylene	<i>trans</i> -DCE	96.9	1.27	0.26	2.2	1.7
methyl <i>tert</i> -butyl ether	MTBE	88.2	0.74	0.03	19.1	14.8
<i>cis</i> -1,2-dichloroethylene	<i>cis</i> -DCE	96.9	1.27	0.22	2.6	n.d. <sup>b</sup>
chloroform	CHCl <sub>3</sub>	119.4	1.48	0.14	4.1	2.3
tetrachloromethane	CCl <sub>4</sub>	153.8	1.59	0.91	0.6	0.8
benzene	Benz	78.1	0.88	0.22	2.6	1.9
trichloroethylene	TCE	131.4	1.46	0.49	1.2	1.7
toluene	Tol	92.2	0.87	0.25	2.3	n.d. <sup>b</sup>
tetrachloroethylene	PER	165.8	1.62	1.20	0.5	1.4

a. Reference (63)

b. Not determined.

### 3.2.2 Gas Chromatography-Combustion-Isotope Mass Spectrometry.

The compound-specific isotope ratios were determined using a Trace GC (Thermo Finnigan, San Jose, CA) coupled to an isotope ratio mass spectrometer (Delta<sup>PLUS</sup>XL, Thermo Finnigan MAT, Bremen, Germany) via a combustion interface (GC Combustion III, Thermo Finnigan MAT) maintained at 940 °C. The GC was equipped with a cold on-column injector, a split/splitless injector with a Merlin Microseal (Merlin Instrument Co., Half Moon Bay, CA), a deactivated precolumn (0.5 m × 0.53 mm; BGB, Anwil, Switzerland), and a Restek RTX-VMS capillary column (60 m × 0.32 mm, 1.8 mm film thickness; Restek Corp., Bellefonte, PA). Helium at a constant pressure of 100 kPa was used as carrier gas. In addition to the IRMS, the GC was equipped with a flame ionization detector (FID) that received ~10% of the eluting carrier gas. The temperature program used to obtain baseline separation of the target analytes was as follows: 2 min at 40 °C, then to 50 °C at 2 °C/min, 4 min at 50 °C, then to 100 °C at 8 °C/min, 2 min at 100 °C, then to 210 °C at 40 °C/min, 3.5 min at 210 °C. The GC was equipped with a CombiPAL Autosampler (CTC, Zwin-

gen, Switzerland), allowing liquid injections as well as solid-phase microextraction.

### 3.2.3 $\delta^{13}\text{C}$ Determination of the Pure Liquid Analytes.

The  $\delta^{13}\text{C}$  value is defined as:

$$\delta^{13}\text{C} = \left( \frac{R_{\text{sample}}}{R_{\text{reference}}} - 1 \right) \cdot 1000 \quad [\text{‰}] \quad (3-1)$$

where  $R_{\text{sample}}$  and  $R_{\text{reference}}$  are the  $^{13}\text{C}/^{12}\text{C}$  ratios of the sample and an international standard material, respectively. An aliquot of the pure liquid standards was introduced into the combustion chamber of an elemental analyzer (EA) (NC2500, Thermoquest, San Jose, CA) coupled to an IRMS (Isoprime, Micromass, Manchester, U.K.). The isotopic signatures of the analytes were corrected in order to obtain  $\delta^{13}\text{C}$  values relative to Vienna PeeDee Belemnite (VPDB). This correction was obtained using a linear regression derived from the  $\delta^{13}\text{C}$  determination of three different solid reference materials measured with the same instrumental setting and the same internal reference  $\text{CO}_2$ .

### 3.2.4 $\delta^{13}\text{C}$ Determination of the Analytes with GC-IRMS.

In the case of liquid injections, the standards were diluted in diethyl ether. The concentrations of the analytes were adjusted to obtain IRMS signals of similar intensities to avoid any linearity effects. In the case of preconcentration from aqueous samples (i.e., SPME and P&T), the analytes were diluted from methanolic stock solutions in tap water. Tap water consistently showed the lowest background contamination levels of volatile organic compounds and thus the least potential for interference with our analytes.<sup>101</sup> The isotopic signatures of all the compounds relative to VPDB were obtained using  $\text{CO}_2$  that was calibrated against referenced  $\text{CO}_2$ .

### 3.2.5 Influence of the Oxidation Capacity of the Combustion Unit.

Our experience shows that it is necessary to oxidize the NiO-CuO catalyst frequently in particular when  $\delta^{13}\text{C}$  values of halogenated compounds are measured. Significant deviations of the isotopic composition determined for the chlorinated compounds from the values of the pure phase compounds determined by EA-IRMS resulted when the combustion unit was not oxidized before the measurements. In a series of liquid

injections in split mode without prior oxidation, the following deviations from the original  $\delta^{13}\text{C}$  values were observed:  $-0.93 \pm 0.21\text{‰}$  for trans-DCE,  $-2.23 \pm 0.17\text{‰}$  for cis-DCE,  $-8.95 \pm 0.44\text{‰}$  for  $\text{CHCl}_3$ ,  $-6.64 \pm 0.37\text{‰}$  for  $\text{CCl}_4$ ,  $-2.94 \pm 0.13\text{‰}$  for TCE, and  $-3.03 \pm 0.3\text{‰}$  for PER. In the case of the nonchlorinated analytes, this effect was not observed. The oxidation capacity of the combustion unit was still sufficient to maintain the specified sensitivity, while the  $\delta^{13}\text{C}$  determinations of halogenated compounds were already strongly affected. After a reoxidation of the combustion unit, the GC-IRMS measurements again yielded isotopic signatures, which corresponded well to the  $\delta^{13}\text{C}$  signatures determined beforehand. As a consequence of this effect, we regularly oxidized the catalyst by flushing oxygen through the oven for at least 1 h after ~40 samples. After this oxidation phase, the oxygen background was typically elevated so that a conditioning period of 2 h was necessary to remove excess oxygen and to obtain reproducible isotopic measurements. The  $\delta^{13}\text{C}$  values presented in this paper have all been determined after a sufficient oxidation of the catalyst; hence, the deviations of the isotopic values from the elemental analyzer data are due to fractionations resulting from the sample preparation and the injection/concentration procedure(s).

### **3.2.6 Liquid Injections.**

For the on-column (OC) and splitless (SL) injections, 1.5  $\mu\text{L}$  of a diethyl ether standard solution (60-640 mg/L) was injected on the cold on-column injector (25 °C) or on the split/splitless injector, which was maintained at 250 °C. The split/splitless injector was equipped with a deactivated glass liner. The splitless time was set to 1 min. In the case of split injections (S), a deactivated split liner was used and the injection volume was increased to 5  $\mu\text{L}$ . The split ratio was set to 1:50, and the carrier gas was set to a constant flow of 2 mL/min.

### **3.2.7 SPME Measurements.**

In preliminary evaluations we found the Carboxen-PDMS (75  $\mu\text{m}$ ) extraction fiber (Supelco, Bellefonte, PA) to be best suited for the extraction of the target analytes investigated in this work. A 1.3-mL sample of the aqueous samples was filled into 2-mL vials containing 0.3 g of NaCl, and the vials were immediately closed with Teflon-sealed crimp caps. Subsequently, the samples were shaken on a Vortex shaker to completely dissolve the NaCl. The samples were equilibrated at 30 °C for 2 min followed by direct immersion SPME for 30 min. After the extraction, the

analytes were thermally desorbed for 1 min in the split/splitless injector (270 °C) equipped with a deactivated SPME liner. Following the injection, the fiber was introduced to a fiber conditioning unit maintained at 270 °C for 3 min to avoid carryover of less volatile compounds. The SPME fiber was also conditioned for 30 min at 270 °C in the conditioning unit after 20-30 samples and replaced after about 100 injections. In the case of the variation of extraction times, all other parameters were maintained constant. Duplicates were measured for each extraction time.

### 3.2.8 Purge and Trap Measurements.

A purge and trap concentrator Tekmar LSC3100 together with a liquid autosampler Tekmar AQUATEk 70 (Tekmar-Dohrmann, Mason, OH) was coupled online to the precolumn of the GC-IRMS system through a cryofocusing unit. The aqueous samples were filled into 40-mL vials without headspace. A 25-mL aliquot of the water samples was transferred by the autosampler into a fritted sparging glassware and purged for 30 min with N<sub>2</sub> (40 mL/min). The analytes were trapped on a VOCARB 3000 (Supelco) trap at room temperature. By heating the trap to 250 °C for 1 min, the analytes were thermodesorbed and transferred to the cryofocusing unit maintained at -120 °C using liquid nitrogen. The GC temperature program was started with the heating of the cryofocusing unit. These method parameters have been optimized in order to obtain sufficient extraction efficiencies for the different analytes. An example chromatogram is shown in Figure 3.1. For the evaluation of the effects of one parameter on the  $\delta^{13}\text{C}$  measurement, all other parameters were kept constant.

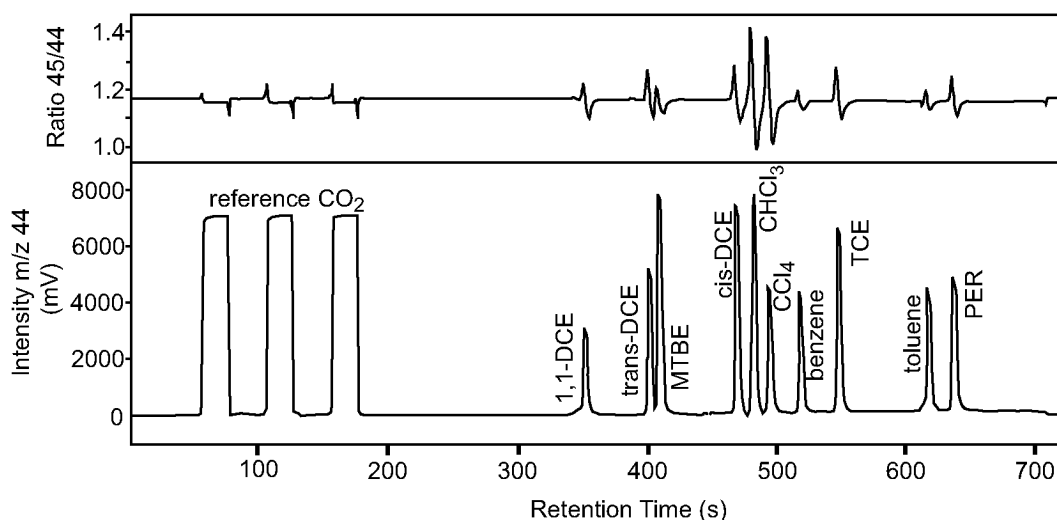


**Figure 3.1: Chromatogram of an On-line P&T-GC-IRMS Analysis.** The concentrations of the different analytes were adjusted to achieve similar signal intensities (1.7 (toluene)- 32  $\mu\text{g/L}$  ( $\text{CCl}_4$ )). The three first peaks correspond to the reference  $\text{CO}_2$  gas.

### 3.2.9 Determination of Method Detection Limits.

To obtain reproducible  $\delta^{13}\text{C}$  values, the GC-IRMS signals should reach an amplitude of about 0.5 V (m/z 44), according to the technical specifications of the mass spectrometer. Hence, the method detection limits reported in this paper correspond to the concentrations yielding peak amplitudes of 0.5 V. These concentrations were obtained based on a five-point calibration curve measured in duplicate using the peak height of the  $^{12}\text{CO}_2$  peak (m/z 44) measured on the IRMS. If not mentioned otherwise, the stated reproducibility corresponds to the single standard deviation of 10 replicate measurements.

### 3.2.10 Determination of Extraction Efficiencies.

The FID chromatograms were used to determine the absolute amount of the individual analytes injected on the GC column after the SPME and P&T extraction steps. The quantification was based on a fivepoint calibration curve obtained from on-column injection. The extraction efficiency corresponds to the ratio of the absolute amount of the analyte injected on-column to the total amount of analyte present in the aqueous sample.

### 3.2.11 Assumptions for Calculation of P&T Extraction Efficiency.

The volume of purge gas needed to transfer a given fraction of a dissolved compound from the aqueous sample to the trap could be predicted fairly well by assuming that the compound in the aqueous phase is permanently in equilibrium with the purge gas. The following equation has been used to determine extraction efficiency of the analyte:<sup>63</sup>

$$\frac{C_{iw}(t)}{C_{iw}(0)} = e^{-\left(\frac{K_{iaw} \cdot G}{V_w}\right) \cdot t} \quad (3-2)$$

where  $C_{iw}(0)$  and  $C_{iw}(t)$  are the concentrations in the aqueous phase before the extraction and after the purge time ( $t$ ), respectively.  $V_w$  stands for the volume of the aqueous sample (e.g., 25 mL) and  $G$  for the purge gas flow rate (e.g., 40 mL/min).  $K_{iaw}$  stands for the air-water partition constant that characterizes the partitioning of a compound  $i$  between the two phases.

### 3.3 Results and Discussion

The scope of the presented work was to develop and characterize on-line preconcentration and injection procedures allowing compound-specific isotope analysis in the low-microgram per liter concentration range. To evaluate isotopic fractionation caused by these techniques, volatile organic compounds with known isotopic composition were extracted under different conditions and their isotopic signature was determined with a GC-IRMS system.

#### 3.3.1 Liquid Injection.

Cold OC injections showed better reproducibilities than SL injections. Furthermore, the early-eluting analytes (e.g., *trans*-DCE and MTBE) showed relatively high standard deviations in split (S) as well as SL injections (see Table 3.2). Although these two analytes elute very closely, this

**Table 3.2: Precision and Reproducibility of  $\delta^{13}\text{C}$  Values Determined with the Evaluated Preconcentration and Injection Techniques (‰ vs VPDB)<sup>a</sup>**

com- pound	EA-IRMS	GC-IRMS				
	pure liquid compound (n=3)	on column (n=10)	splitless (n=10)	split 1:50 (n=9)	SPME (n=10)	P&T (n=10)
1,1-DCE	-29.25±0.14	n.d. <sup>b</sup>	n.d. <sup>b</sup>	n.d. <sup>b</sup>	-28.46±0.41	-29.07±0.08
<i>trans</i> -DCE	-26.42±0.17	-27.32±0.19 <sup>c</sup>	-27.84±0.91	-27.03±1.45	-25.99±0.16	-25.61±0.22
MTBE	-28.13±0.15	-27.91±0.06	-29.01±0.57	-27.89±0.76	-29.67±0.40 <sup>c</sup>	-27.75±0.09
<i>cis</i> -DCE	-26.61±0.06	-26.33±0.09	-25.81±0.26 <sup>c</sup>	-26.10±0.12 <sup>c</sup>	-25.76±0.17 <sup>c</sup>	-25.96±0.07 <sup>c</sup>
CHCl <sub>3</sub>	-45.30±0.19	-47.16±0.20 <sup>c</sup>	-44.73±0.45	-47.04±0.19 <sup>c</sup>	-44.31±0.41	-46.22±0.14 <sup>c</sup>
CCl <sub>4</sub>	-38.62±0.01	-41.93±0.34 <sup>c</sup>	-39.76±0.38 <sup>c</sup>	-40.19±0.17 <sup>c</sup>	-45.93±2.19 <sup>c</sup>	-38.37±0.27
benzene	-27.88±0.20	-27.56±0.07	-27.69±0.26	-27.35±0.11	-27.37±0.36	-27.27±0.20
TCE	-26.59±0.08	-27.37±0.12 <sup>c</sup>	-26.13±0.15	-26.71±0.15	-26.83±0.13	-26.11±0.20
toluene	-27.90±0.24 <sup>d</sup>	-28.07±0.15	-26.97±0.15 <sup>c</sup>	-26.81±0.11 <sup>c</sup>	-28.62±0.56	-27.16±0.35
PER	-27.32±0.14	-27.19±0.17	-27.33±0.34	-27.99±0.26	-28.16±1.31	-26.76±0.19

a. Uncertainties correspond to standard deviations of replicate measurements.

b. Not determined.

c. Significant deviation from  $\delta^{13}\text{C}$  value of pure liquid compound.

d. n=9.

effect does not result from insufficient chromatographic resolution because this would also affect the results of the on-column measurements. As the uncertainties of the  $\delta^{13}\text{C}$  values are much smaller for the early-eluting *trans*-DCE and MTBE in the on-column measurements, the observed effect might be due to an incomplete transfer of the analytes to



the GC column. A fraction of the highly volatile analytes is likely to be lost during evaporation in the GC- liner. Nevertheless, the  $\delta^{13}\text{C}$  values determined after OC, S, or SL injection and gas chromatographic separation generally showed small deviations from the reference values obtained with the elemental analyzer for the pure liquid compound (Table 3.2). The major advantage of the on-column injection lies in the overall superior precision compared with the other methods. A liquid-liquid extraction method could be used in order to improve MDLs for the analytes in aqueous solution. However, the risk of contamination of the solvents with volatile compounds is relatively high and the impurities have retention times similar to the target analytes used in this study. We therefore decided to further focus on the solvent-free extraction techniques (SPME, P&T) that can easily be automated and hence be used for a wide range of applications.

### **3.3.2 Solid-Phase Microextraction.**

The extraction efficiencies for all analytes exceeded 30%, indicating that the Carboxen-PDMS fiber used in this work extracted the investigated volatile organic compounds efficiently. Quantitative SPME analysis requires internal standards to correct for extraction efficiency deviations. However, in this work we did not use internal standards, since we attempted to minimize sample preparation and did not focus on quantitative measurements, hence, the high scatter of the extraction efficiency. As can be seen from Figure 3.2, the extraction efficiency did not affect the  $\delta^{13}\text{C}$  values, indicating that the sorption and desorption process caused no or only negligible fractionation.

Similarly, Dias and Freeman<sup>96</sup> measured a slight enrichment ( $\leq 0.2\text{‰}$ ) of toluene extracted by SPME. Considering the uncertainty in our measurements, such a small shift could not be observed. The significant scatter of extraction efficiencies of TCE was thus not found in the corresponding  $\delta^{13}\text{C}$  data. Desorption times (1-5 min) of the SPME fiber in the injector affected neither desorption efficiencies nor isotopic signatures of the analytes (results not shown). However, we found a large deviation of the  $\delta^{13}\text{C}$  values for  $\text{CCl}_4$  ( $-7.13 \pm 2.19 \text{‰}$ ) determined by SPME compared with the other methods employed here (see Table 3.2). This effect as well as the poor precision of  $\delta^{13}\text{C}$  values of PER determined with SPME-GC-IRMS could not be explained. A possible exhaustion of the combustion oven can be ruled out, since the catalyst was regularly oxidized, as mentioned before. Nevertheless, it is notable that the highest chlorinated compounds having no C-H bonds show the highest devia-

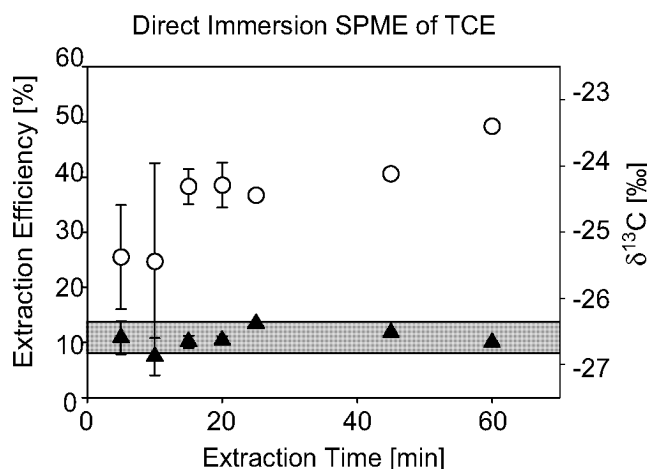


**Figure 3.2: Solid-phase Microextraction.** Influence of increasing extraction times on the extraction efficiency of TCE (open circles) and its isotopic signature (filled triangles). The horizontal bar corresponds to the isotopic signature ( $\pm$  triple standard deviation) of the pure phase liquid determined with an elemental analyzer-IRMS.

tions. As shown by Black and Fine<sup>72</sup> high concentrations of BTEX (>1 mg/L) hamper the use of the Carboxen-PDMS fiber for the quantification of MTBE in aqueous mixtures due to competition for sorption sites. Figure 3.3 shows the effect of competitive sorption of BTEX and MTBE on the isotopic signature of MTBE.

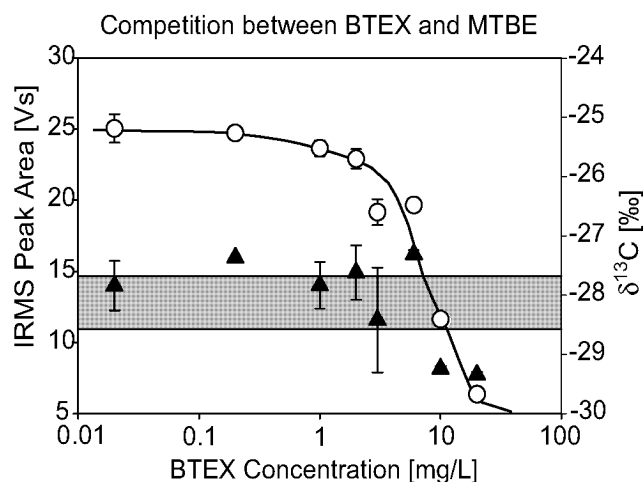


**Figure 3.3: Competition for Sorption Sites on SPME Fiber.** Concentrations of more than 1 mg/L BTEX compounds significantly affect the extraction efficiency of MTBE (open circles) from the aqueous solution. This competition also slightly influences the determination of the  $\delta^{13}\text{C}$  value of MTBE (filled triangles) in the case of BTEX concentrations of  $\geq 10$  mg/L. The horizontal bar corresponds to the isotopic signature ( $\pm$  triple standard deviation) of the pure phase liquid determined with an elemental analyzer-IRMS.

While concentrations above 1 mg/L BTEX significantly affect the extraction efficiency of MTBE, its isotopic signature is only slightly affected in the presence of very high BTEX concentration ( $\geq 10$  mg/L). This effect has to be considered in the case of field experiments where

MTBE contaminations often coexist with high BTEX concentrations. The fractionation ( $-1\text{‰}$ ) due to the competitive sorption is, however, small compared to fractionations due to biodegradation of MTBE.<sup>24,36,42,60</sup> Hence, SPME-GC-IRMS is indeed a valuable tool to identify and quantify in situ biodegradation of MTBE.

### 3.3.3 Purge and Trap.

Figure 3.4 shows typical results obtained by the variation of the purge

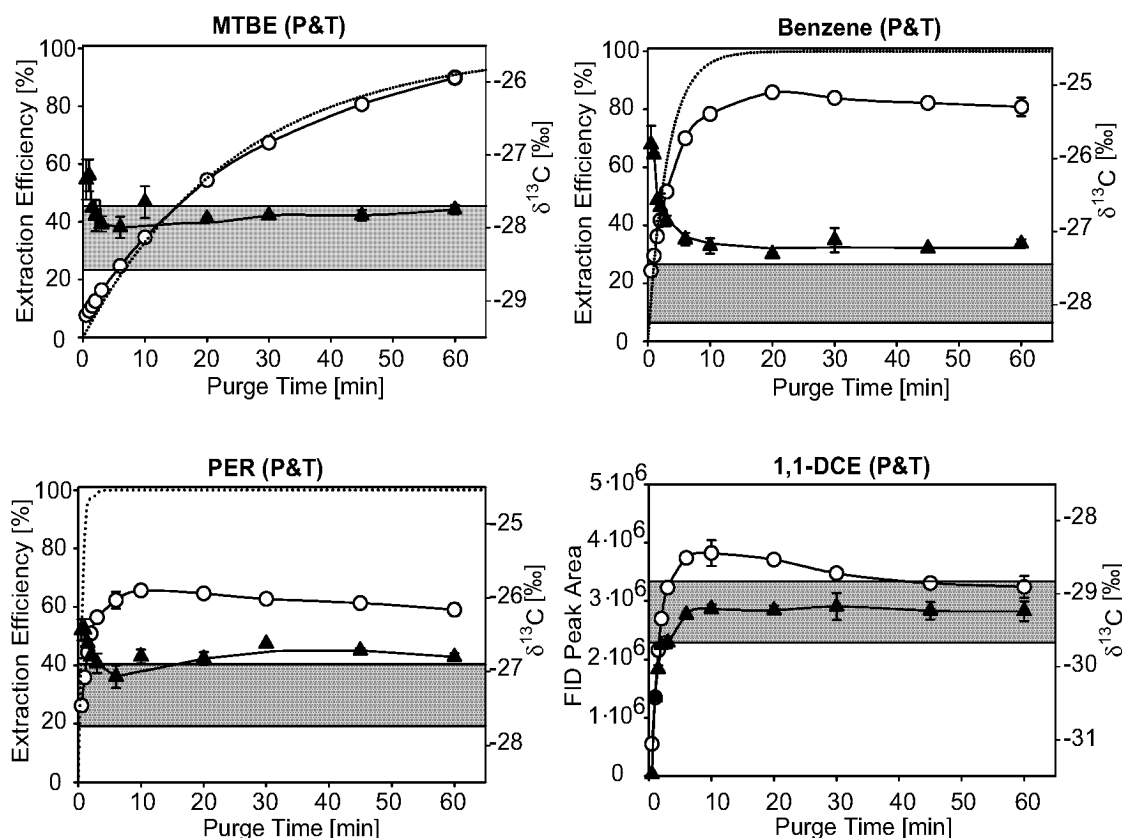


**Figure 3.4: Purge and Trap Extraction and Isotopic Fractionation with Increasing Purge Times.** Influence of increasing extraction times on the extraction efficiency (open circles) of different analytes and their isotopic signatures (filled triangles). The horizontal bar corresponds to the  $\delta^{13}\text{C}$  ( $\pm$  triple standard deviation) of the pure phase liquid determined with an elemental analyzer-IRMS. The dotted line corresponds to the predicted extraction efficiency using Equation (3-2) with  $K_{iaw}$  corrected for 23 °C. Because of coelution with the solvent peak, calibration of 1,1-DCE by OC injection was not possible. Hence, FID signal areas are plotted instead of extraction efficiencies for 1,1-DCE.

times for representative analytes of different compound classes. The measured extraction efficiency could be predicted quite well (see Table 3.1) by applying the dynamic phase equilibrium model (using Equation (3-2)); hence, the aqueous phase was in equilibrium with the gas phase throughout the purging process. Differences between measured and predicted extraction efficiencies for benzene and PER result from trap breakthrough. The  $\delta^{13}\text{C}$  values varied significantly for extraction efficiencies

below 40% but approached the pure phase compound isotopic signatures with increasing extraction efficiencies. MTBE, being the compound with the smallest air-water partition constant ( $K_{iaw}$ ) among the evaluated substances, showed the slowest increase of extraction efficiency with purge time. But also in this case, stable  $\delta^{13}\text{C}$  values were obtained for extraction efficiencies above 40%. A slight deviation toward heavier isotopic values remained for most analytes, even for relatively high extraction efficiencies (>60%). The extent of the observed fractionation due to P&T analysis was compound-specific, but the direction of the effect was the same for all the analytes except for 1,1-DCE. For short purge times (i.e., low extraction efficiencies) all analytes except 1,1-DCE were enriched with the heavier isotope. This is consistent with the “inverse isotope effect” commonly observed for evaporation processes of organic compounds.<sup>102-105</sup> It is not clear why an opposite effect occurred for 1,1-DCE, i.e., the preferential enrichment of the lighter isotope in the gas phase.

The most volatile analytes were partly lost from the trap with increasing purge times as can be seen for 1,1-DCE in Figure 3.4. At our experimental conditions, the loss of analytes due to trap breakthrough had only a limited effect on the extraction efficiency (-5 to -15%), and thus on the method detection limit. No significant isotopic fractionation associated with this breakthrough was observed. Longer trap desorption times ( $\geq 1$  min) showed no influence on the sensitivity or on the  $\delta^{13}\text{C}$  values, demonstrating that temperatures of 250 °C for 1 min were sufficient to completely desorb the analytes from the trap. However, for shorter desorption times (30 s), we observed a drop in sensitivity of ~1 order of magnitude accompanied with a significant deviation in the  $\delta^{13}\text{C}$  value of up to -10‰, demonstrating the necessity of complete thermal desorption. Hence, in the case of less volatile compounds, the desorption parameters need to be adjusted to ensure reproducible  $^{13}\text{C}/^{12}\text{C}$  measurements and sensitive detection of the analytes.

P&T allowed very reproducible isotope ratio measurements at concentrations in the low-microgram per liter range with no significant deviations from the elemental analyzer data (with the exception of cis-DCE and chloroform, which showed small deviations). To obtain highly reproducible  $\delta^{13}\text{C}$  data, it is important to ensure relatively high extraction efficiencies (>40%) and constant P&T parameters. For analytes that have not been validated in this work, the extraction efficiency can be estimated from their air-water partition constant (adjusted to the appropriate temperature) using Equation (3-2). This estimation does not account

for analyte losses related to a breakthrough from the trap (see differences between measured and predicted extraction efficiencies with increasing purge times for PER and benzene in Figure 3.4). It is however possible to use Equation (3-2) to obtain a good estimate of purge times needed to achieve the necessary 40% extraction efficiencies (see Table 3.1).

### **3.3.4 Comparison and Validation of Different Injection and Extraction Techniques.**

All injection and extraction techniques evaluated in this paper allow an accurate determination of the isotopic signature for the volatile compounds studied. The obtained precision (standard deviation) for most analytes and methods is better than 0.3‰, which is comparable to the instrument specifications of 0.5‰ usually reported by the IRMS manufacturer. As already mentioned, this precision could only be achieved if the combustion unit of the instrument was regularly (i.e., after ~40 samples) reoxidized.

The precision of the  $\delta^{13}\text{C}$  determination is dependent on the GC technique used (see Figure 3.5 and Table 3.2). As discussed earlier, S and SL injection techniques showed higher standard deviations as the OC injection, while SPME showed a poor precision for the highly chlorinated compounds (PER and  $\text{CCl}_4$ ). The design of the split/splitless injector used for S, SL, and SPME might cause evaporative losses of analytes, hence explaining slightly higher standard deviations compared to P&T and OC methods (see below). Schmitt et al. found that the split/splitless injector is a possible source of isotopic fractionation depending on the actual amount of injected analyte.<sup>92</sup> If the samples were directly introduced into the column without passing through a liner in the split/splitless injector (OC injection and P&T), the precision and reproducibility of the  $\delta^{13}\text{C}$  measurements were always better 0.5‰. An alternative explanation for the higher standard deviations for the  $\delta^{13}\text{C}$  values of MTBE and trans-DCE measured by S and SL could be the fact that the resolution of the chromatography was not as good as in on-column measurements. This effect might be related to the transfer processes from the liner to the column, which do not occur in the case of OC injections. The chromatography of the other analytes was not affected.

If very high accuracy is needed, it is advisable to validate the selected procedure by using external standards (i.e., aqueous reference samples containing all target analytes with known isotopic signatures) because the observed small fractionation effect due to the extraction is highly

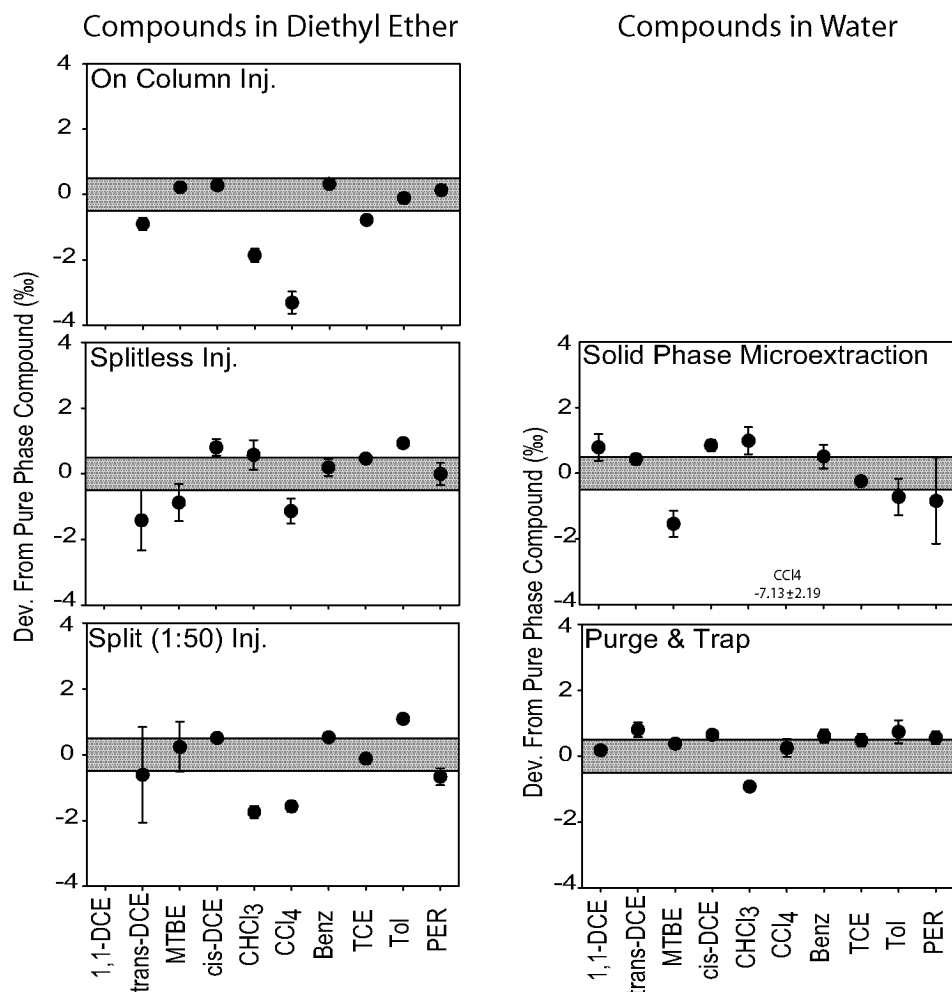


**Figure 3.5: Reproducibility of Different Injection and Extraction Techniques.**

Plotted are the differences from the pure liquid standards measured by EA-IRMS and the horizontal bars correspond to a  $\delta^{13}\text{C}$  measurement within a  $\pm 0.5\text{‰}$  interval of the EA-IRMS measurements allowing a direct comparison between the different compounds. Note that the  $\delta^{13}\text{C}$  value determined for  $\text{CCl}_4$  using SPME lies outside the scale of the y-axis.

compound-specific and thus cannot be accounted for by the use of an internal standard.

The MDLs of the five investigated techniques are shown in Table 3.3. The lowest MDLs (0.25-5.0  $\mu\text{g/L}$ ) were clearly achieved with the P&T concentration procedure, followed by SPME (9-280  $\mu\text{g/L}$ ). The liquid injection techniques resulted in  $10^4$ - $10^6$  times higher MDLs compared to P&T. Ideally, the MDLs in the splitless mode should not differ significantly from the ones in cold on-column mode. This has only been found for the later-eluting compounds (with the exception of toluene). Compared with SL injections, the MDLs are lower for the on-column measurements of trans-DCE (26%), MTBE (20%), and cis-DCE (16%). This is another indication for the supposed evaporative losses within the split/splitless injector. Using a pulsed splitless injection could possibly reduce these losses, but this has not been evaluated. Note that, for the split injections, the MDLs reported in Table 3.3 are not correlated to the

split ratio (1:50), since a higher injection volume (5  $\mu\text{L}$  rather than 1.5  $\mu\text{L}$ ) was used in S injections..

**Table 3.3: Method Detection Limits of the Various Injection and Pre-concentration Techniques Achieved with GC-IRMS**

compound	on column [ $\mu\text{g/L}$ in DEE <sup>a</sup> ]	splitless [ $\mu\text{g/L}$ in DEE <sup>a</sup> ]	split 1:50 [ $\mu\text{g/L}$ in DEE <sup>a</sup> ]	SPME [ $\mu\text{g/L}$ in water]	P&T [ $\mu\text{g/L}$ in water]
1,1-DCE	n.d. <sup>b</sup>	n.d. <sup>b</sup>	n.d. <sup>b</sup>	79	3.6
<i>trans</i> -DCE	75'000	94'000	860'000	130	1.5
MTBE	24'000	29'000	330'000	16	0.63
<i>cis</i> -DCE	71'000	83'000	840'000	92	1.1
$\text{CHCl}_3$	170'000	160'000	1'900'000	170	2.3
$\text{CCl}_4$	220'000	220'000	2'800'000	280	5.0
benzene	19'000	18'000	210'000	22	0.3
TCE	84'000	80'000	1'100'000	94	1.4
toluene	9'500	14'000	220'000	9.0	0.25
PER	74'000	74'000	1'200'000	66	2.2

a. Diethyl ether.

b. Not determined.

SPME lowered the method detection limits by 3-4 orders of magnitude compared with liquid injection. Thus, an enrichment factor of more than  $10^3$  is needed for liquid-liquid extraction to compete with SPME enrichment for CSIA. The reported MDLs using SPME for the chlorinated ethylenes are in the same range as reported by Hunkeler and Aravena<sup>55</sup> using a PDMS fiber. In the case of  $\text{CHCl}_3$ , however, the Carboxen-PDMS fiber used in this study lowered the MDL significantly (170 vs 630  $\mu\text{g/L}$ ). This fiber also yielded a 5 times lower MDL for toluene (9  $\mu\text{g/L}$ ) than noted by Dias and Freeman.<sup>96</sup> Since the extraction efficiencies were relatively high (20-40%), the concentrations in the sample solution significantly dropped during the extraction, limiting the uptake of the fiber. Hence, an increased sample volume could slightly improve the MDLs of SPME.

With the P&T method, both the sample volume (25 mL) and the extraction efficiency (up to 80%) were significantly larger compared with SPME, leading to MDLs below 5  $\mu\text{g/L}$ . Thus, P&T-GC-IRMS allows determination of compound-specific stable isotope signatures of contaminant concentrations frequently found in groundwater. The MDLs presented here for chlorinated ethylenes are a factor of 2 lower than reported by Song et al.<sup>52</sup> The better sensitivity for MTBE of the P&T method reported here (0.63  $\mu\text{g/L}$ ) as compared to the values reported by Smallwood et al.<sup>15</sup>

(15  $\mu\text{g/L}$ ) and Kolhatkar et al.<sup>42</sup> (5  $\mu\text{g/L}$ ) are probably due to (i) longer purge times (30 min compared to 11 and 8 min, respectively), resulting in higher extraction efficiencies and (ii) the use of larger sample volumes. As Figure 3.5 shows, P&T allowed highly reproducible CSIA measurements. However, the determined  $^{13}\text{C}/^{12}\text{C}$  ratios tend to show slight enrichments of the heavier isotope, similar to the observations made by Smallwood et al.<sup>15</sup> As can be seen from Figure 3.4, the MDL of MTBE could still be lowered by further increasing the purge times. Here, we have standardized the purge time to 30 min, to avoid significant losses of the more volatile analytes due to trap breakthrough.

Expressed as the absolute amount of carbon injected on-column, the averaged MDLs for compounds injected in diethyl ether solutions were  $1.9 \pm 0.4$  nmol of carbon on-column. This value is above the specified detection limit of the instrument of 0.8 nmol. However, taking into account the compound-specific extraction efficiencies of SPME and P&T, the method detection limits of these solventless techniques correspond to  $0.6 \pm 0.2$  (SPME) and  $0.4 \pm 0.1$  (P&T) nmol of C on-column. The absence of a solvent yields sharper peaks and hence lowers the detection limit (defined in this case as peaks of a minimal height, i.e., 0.5 V). In the case of the P&T method, this detection limit could even be slightly lowered, since the chromatograms are very clean and the peaks are very sharp due to cryofocusing (see Figure 3.1).

### 3.3.5 Environmental Application of CSIA at Trace Levels.

The applicability of the P&T method for the determination of  $\delta^{13}\text{C}$  values at low-microgram per liter levels was tested with an assessment of potential in situ degradation of TCE in groundwater contaminated by a leachate from a waste disposal site. The concentrations of TCE and of cis-DCE (a known degradation product of TCE) were 20-60 and 5-12  $\mu\text{g/L}$ , respectively. Due to the presence of cis-DCE, the local authorities concluded that TCE was degraded in the aquifer (see Figure 3.6).

Such a degradation reaction would, however, result in the  $^{13}\text{C}$  enrichment of the remaining TCE and hence the formation of an isotopically lighter cis-DCE.<sup>39</sup> Yet, the  $\delta^{13}\text{C}$  values determined with our described P&T-GC-IRMS method demonstrate that (i)  $\delta^{13}\text{C}$  values for TCE do not vary systematically with increasing distance from the contamination source and (ii) cis-DCE is enriched (not depleted) in  $^{13}\text{C}$  compared to TCE. These results shown in Figure 3.6 indicate that cis-DCE must originate from another source. This application example illustrates the potential of the P&T-GC-IRMS method in the field of contaminant hydrology,



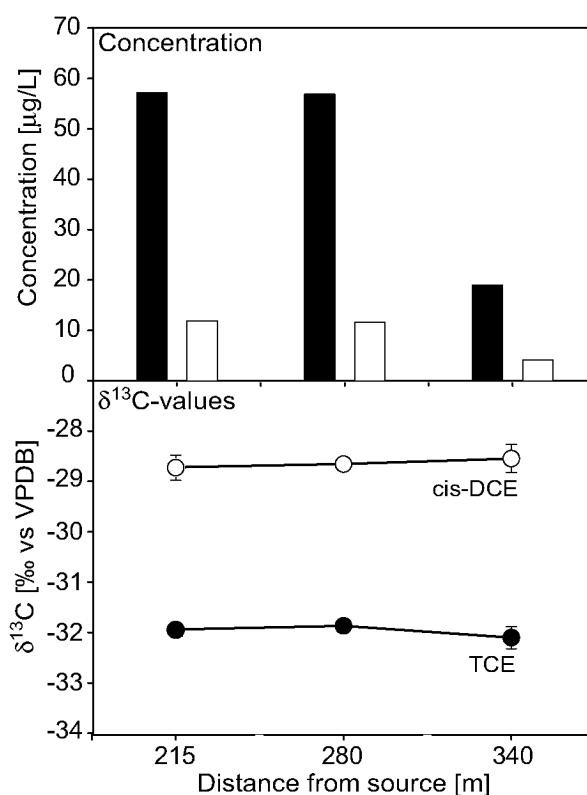


**Figure 3.6: Environmental Application of CSIA for Trace Level Contaminants.** Concentration of TCE (filled bars) and cis-DCE (open bars) as well as  $\delta^{13}\text{C}$  values of TCE (filled circles) and cis-DCE (open circles) measured in samples originating from three groundwater wells with increasing distance from the contamination source.

even for few available samples (three in this case). The achieved MDLs allow accurate analysis of  $^{13}\text{C}/^{12}\text{C}$  ratios from very low pollutant concentrations in groundwater sampled at moderately contaminated field sites.

### 3.4 Conclusions

In this paper, we present for the first time a complete evaluation of cold on-column injection, split/splitless injection, SPME and P&T for the determination of stable carbon isotope signatures of a variety of volatile organic compounds. The  $\delta^{13}\text{C}$  values of the pure phase liquids of the standards (Table 3.2) have been obtained by a fully independent method based on a different secondary standard compared to the values obtained on the GC-IRMS. The extraction and injection techniques could therefore be thoroughly investigated for their suitability in combination with GC-IRMS. Slight but highly reproducible deviations of the  $\delta^{13}\text{C}$  signatures compared to the pure phase compounds occur in all of the evaluated injection and preconcentration techniques. These effects are negligible compared to the fractionations occurring due to microbial or chemical transformation reactions<sup>27,29,32</sup> or compared to typical differences in isotopic signatures of compounds from different manufacturing

processes.<sup>86</sup> Hence, all the discussed techniques are suitable for environmental applications. The choice of the optimal technique depends mainly on the required method detection limits. To be able to compare  $^{13}\text{C}/^{12}\text{C}$  ratios obtained with different analytical techniques or from different laboratories, it is necessary to determine these ratios relative to an international standard (e.g., VPDB). This evaluation has shown that, due to possible compound-specific isotopic fractionations, it is not sufficient to use  $\text{CO}_2$  as a reference gas for the determination of these ratios. Instead, it is important to measure external standards of known isotopic composition in the same aqueous matrix and with the same analytical method than the samples.

P&T proved to be a very reproducible extraction method with the lowest MDLs reported in GC-IRMS applications so far. Since the validated extraction techniques show little if any carbon isotopic fractionations due to relatively high extraction efficiencies, they are also applicable for CSIA of D/H ratios, which require 10-20 times higher analyte concentrations than  $^{13}\text{C}/^{12}\text{C}$  analysis. P&T and SPME preconcentration methods could also be used to lower analyte concentrations needed for  $^{15}\text{N}/^{14}\text{N}$  and presumably for  $^{18}\text{O}/^{16}\text{O}$  analysis.

**VARIABILITY OF THE CARBON  
ISOTOPIC FRACTIONATION  
DURING THE REDUCTIVE  
DEHALOGENATION OF CARBON  
TETRACHLORIDE BY  
SURFACE-BOUND FERROUS IRON**

## 4.1 Introduction

Halogenated aliphatic compounds including tetrachloromethane are common groundwater contaminants<sup>106-108</sup> that may undergo reductive transformation reactions in anoxic environments. It has been shown that Fe(II) sorbed to mineral surfaces shows an increased reactivity compared to ferrous iron in solution towards the reduction of chlorinated aliphatic compounds.<sup>109-111</sup> Since, under iron reducing conditions, Fe(II) may be constantly regenerated by microbial Fe(III) reduction, such an abiotic reduction may be an important or even the predominant process responsible for an *in situ* degradation of reducible groundwater contaminants.<sup>112,113</sup>

The assessment of *in situ* degradation in the field is, however, often complicated by the fact that it is difficult to establish complete mass balances based on concentration data from a limited number of sampling wells. Recently, the use of compound-specific stable isotope analysis has been presented as a useful tool to gain additional information on the fate of groundwater contaminants.<sup>9,32,34,36,42,51,54,114</sup> This approach is based on the differences in reaction rates between molecules with heavy isotopes at the reacting bond and molecules with light isotopes. During the course of the reaction, this kinetic isotope effect may lead to an enrichment of the molecules with heavy isotopes in the remaining fraction of the parent compound. This effect can be quantified and may be used for the quantification of the extent of a given degradation reaction. However, such a quantification relies on the assumption that the enrichment factor of a given reaction does not vary significantly between different environmental conditions.<sup>30,47,48</sup> At first sight, this assumption seems to hold for the <sup>13</sup>C-enrichment associated with the reductive dehalogenation of CCl<sub>4</sub>, where it is assumed that the reaction starts with a dissociative electron transfer (e.g. the simultaneous transfer of one electron and the cleavage of one C-Cl bond) leading to the formation of a trichloromethyl radical.<sup>115</sup>

However, in the case of reactions with one-bond changes, one would expect the isotopic enrichment to increase with later positions of the transition state on the reaction coordinate.<sup>116</sup> According to the Hammond Postulate, slow and endergonic reactions have a late (product-like) transition state and fast and exergonic reactions have an early (parent compound-like) transition state, and hence, different reaction rates may cause different isotopic enrichments due to differing rate-limiting steps. It has been shown that the reactivity of Fe(II) sorbed to the surfaces of a range of iron containing minerals (siderite, hematite, lepidocrocite, goet-

hite, magnetite, pyrite, mackinawite and green rust) towards the reduction of 4-chloronitrobenzene, 4-chlorophenylhydroxylamine and hexachloroethane spans several orders of magnitude.<sup>117</sup> This effect has been attributed to large differences in the sorption densities of Fe(II) on the different minerals, and should, therefore, not influence the isotopic enrichment. If, however, the different reaction rates are due to different positions of the transition state on the reaction coordinate, different isotopic enrichments would be expected. While inconsistent enrichment factors for the abiotic dehalogenation would certainly complicate the application of compound-specific stable isotope analysis (CSIA) in the quantification of *in situ* degradation, they could possibly yield important information on the degradation mechanism. Differing reactivities but stable enrichment factors would be indicative of a different abundance but a similar reactivity of reactive sites. In the case of changes in the stabilization of the transition states, one would expect, as postulated above, enrichment factors to increase with decreasing reaction rate constants.

The isotopic enrichments could, secondly, be influenced by the presence of several concurring reactions.<sup>118</sup> The degradation pathway proposed for the dehalogenation of CCl<sub>4</sub> comprises a first “branching” between the initial formation of a trichloromethyl radical on the one hand and a path leading to the formation of formate on the other hand.<sup>119</sup> A

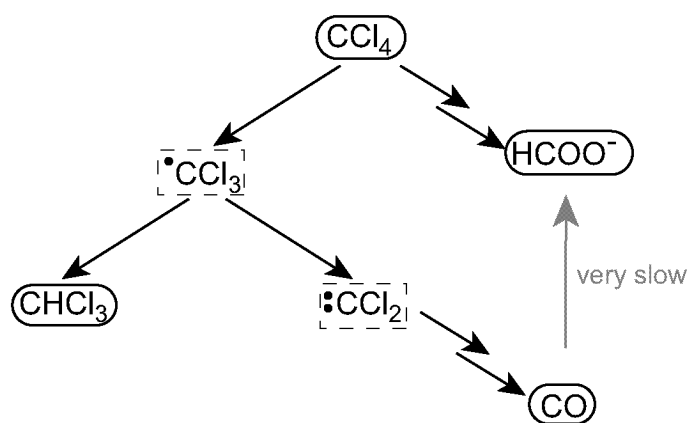


**Figure 4.1: Proposed Degradation Pathway for the Surface-Mediated Reductive Dehalogenation of CCl<sub>4</sub> by Fe(II) on Goethite.**<sup>119</sup> Products in rounded boxes were determined analytically. Molecules in dashed boxes represent proposed intermediates.

second “branching” occurs after the formation of the trichloromethyl radical. Either chloroform is formed by hydrogen (H<sup>·</sup>) abstraction or a second electron is transferred leading to trichloromethyl carbanion which reacts further to form carbon monoxide. Depending on different factors such as pH, presence of radical scavengers and surface stabiliza-

tion of reaction intermediates, the yields of the identified products have been found to vary significantly.<sup>119</sup> Thus, the relative importance of the different reaction pathways can shift, supposedly producing shifts in isotopic enrichments. Whereas the isotopic enrichment of  $\text{CCl}_4$  is only influenced by the initial reaction pathway(s), isotopic signatures of the resulting products are influenced by the successive branches.

In this study we evaluated the isotopic enrichment caused by the abiotic reductive dehalogenation of  $\text{CCl}_4$  by surface-bound Fe(II) species. In order to address the influence of the location of the transition state, the reaction was studied using Fe(II) sorbed to different iron minerals (siderite, hematite, lepidocrocite, magnetite, goethite and mackinawite), that have shown different intrinsic reactivities in the dehalogenation of hexachloroethane. Furthermore, the concentrations as well as the isotopic signatures of chloroform were determined, to get an estimate of the importance of the different branches in the degradation pathway on the observed isotopic signatures.

## 4.2 Experimental Section

### 4.2.1 Reagents and Materials

Methanol (>99.9%) used for the preparation of stock solutions was obtained from Scharlau S. A. (Barcelona, Spain). Tetrachloromethane ( $\text{CCl}_4$ , >99.5%), chloroform ( $\text{CHCl}_3$ , >99.5%), tetrachloroethene (PER, >99.9%), kanamycinsulfate and ampiciline were purchased from Fluka (Buchs, Switzerland). Bromoform (>99%) was obtained from Aldrich (Steinheim, Germany). The carbon isotopic signatures of  $\text{CCl}_4$  ( $-38.62 \pm 0.01\text{‰}$ ),  $\text{CHCl}_3$  ( $-45.30 \pm 0.19\text{‰}$ ) and PER ( $-27.32 \pm 0.14\text{‰}$ ) were determined using an elemental analyzer (NC2500, Thermoquest, San Jose, CA) coupled to an isotope ratio mass spectrometer (Isoprime, VG Instruments, Manchester, U.K.).

Goethite, hematite and lepidocrocite were purchased from Bayer (Leverkusen, Germany). The synthesis of magnetite, siderite and mackinawite has been described in a previous study.<sup>120</sup> The crystal structures of the minerals were characterized using X-ray diffraction (Siemens D 5000 and XDS 2000 with a  $\text{Cu K}\alpha$  source, scan rate:  $1^\circ/\text{min}$ ), the specific mineral surfaces were determined by  $\text{N}_2$  adsorption (Sorptomatic 1990,

Fisons Instruments). Table 4.1 gives the surface areas of the investigated minerals.

**Table 4.1: Specific Surfaces of the Investigated Minerals**

Mineral	Abbreviation	Specific Surface Area [m <sup>2</sup> /g]
Mackinawite 1 <sup>a</sup>	FeS 1	12.6
Mackinawite 2 <sup>a</sup>	FeS 2	77
Goethite	α-FeOOH	16.2
Hematite	α-Fe <sub>2</sub> O <sub>3</sub>	13.7
Lepidocrocite	γ-FeOOH	17.6
Magnetite	Fe <sub>3</sub> O <sub>4</sub>	19.2
Siderite	FeCO <sub>3</sub>	38.3

a. Both mackinawite batches were prepared analogously. Mackinawite batch 1 was washed, centrifuged, freeze-dried and stored for 2 years in an oxygen-free glovebox. Mackinawite batch 2 was washed, filtered using an ultrafiltration cell, freeze dried and stored for 3 months in an oxygen-free glovebox.

Fe(II)-solutions were prepared by adding 28 g (0.5 mol) iron powder (Merck,) to 1 L of 1M deoxygenated HCl. The suspension was brought to 70 °C under gentle stirring until the release of H<sub>2</sub> ceased (2 - 2.5 h). The solution was taken into an oxygen free glovebox and filtered through a 0.2 μL PTFE filter to remove the excess iron powder. The Fe(II) concentration was determined photometrically using to the phenantroline method.<sup>121</sup>

#### 4.2.2 Preparation of Solutions for Transformation Experiments

Stock solutions of CCl<sub>4</sub> and PER (as internal standard) were prepared in degassed deionized water or anoxic methanol. The concentrations of CCl<sub>4</sub> and PER in the aqueous solution were 0.24 mM and 0.12 mM, respectively. In order to reduce the spike volume in the case of experiments carried out in ampules, concentrated methanolic spike solutions were prepared (3 mM of CCl<sub>4</sub> and 1.5 mM of PER). PER was chosen as internal standard to correct for losses during the spiking of the reaction vials as well as for diffusion into the Viton stopper. PER has been selected, because its physico-chemical properties are similar to CCl<sub>4</sub> but can be regarded as persistent under the given experimental conditions.

### 4.2.3 Preparation of Mineral Suspensions.

Aliquots of iron oxides as well as iron hydroxides were resuspended in 500 mL deionized water to yield a surface concentration of 50 m<sup>2</sup>/L. The suspensions were agitated for 24 hours and, after sedimentation, the minerals were rinsed several times with deionized water. The suspensions were then degassed with argon and introduced into an oxygen free glovebox. Suspensions of oxygen sensitive minerals (siderite, FeS) were prepared and rinsed in the glovebox with anoxic deionized water. Aliquots of the 0.5 M FeCl<sub>2</sub> solution were added to the suspensions and the pH was adjusted to 7.2 (1M NaOH, HCl). Suspensions, with the exception of goethite suspensions (where the intrinsic buffer capacity was shown to be sufficient<sup>120</sup>) were buffered by 1 mM 4-morpholinopropane-sulfonic acid (MOPS). After equilibration ( $\geq 12$  h), the concentration of the dissolved Fe(II) was determined using the phenantroline method.<sup>121</sup> If necessary, the Fe(II) concentration was increased by successive additions of FeCl<sub>2</sub> and pH adjustments until a concentration of  $\sim 1$  mM was obtained. The characteristics of the mineral suspensions used for the experiments are summarized in Table 4.2.

**Table 4.2: Characteristics of Investigated Mineral Suspensions**

Mineral	Added	Measured		Calculated	
	MOPS [mM]	Fe(II) [mM]	pH	Fe(II) <sub>ads</sub> [mM]	Fe(II) <sub>ads</sub> [ $\mu\text{mol}/\text{m}^2$ ]
Mackinawite 1	0.76	1.06	7.22	1.26	25.2
Mackinawite 2	0.76	0.881	7.18	0.526	10.52
Goethite	-	n.d. <sup>a</sup>	7.30		
Magnetite	1.52	1.05	7.30	0.784	15.68
Lepidocrocite	1.00	0.98	7.23	0.827	16.54
Hematite	1.00	0.95	7.20	0.529	10.58
Siderite	1.2	0.93	7.10	0.045	0.9

a. Not determined.

### 4.2.4 Preparation of Transformation Experiments.

The reaction kinetics of the different suspensions were screened in preliminary experiments. 21 mL of the equilibrated suspension were filled into a 25 mL serum vial, 3 mL of the aqueous spike solution were added, and the solution was then immediately transferred into 0.8 mL autosampler vials. The vials were subsequently closed without headspace with Viton®-sealed crimp-caps (BGB Analytik, Anwil, Switzerland) taken out of the glovebox and agitated on an reciprocating shaker at 23 °C. For each data point one vial was sacrificed. The analytes were extracted by



transferring 0.4 mL of the suspension into a second autosampler vial and adding 0.35 mL n-hexane containing 10  $\mu$ M bromoform as internal standard to both vials. The extracts were then stored at -30 °C until analysis.

The main transformation experiments of CCl<sub>4</sub> in the presence of FeS, goethite, magnetite and lepidocrocite were carried out in 25 mL serum vials. 12-18 replicates were prepared for each experiment by adding 3 mL of an aqueous spike solution to 21 mL of the equilibrated suspension, yielding initial concentrations of ~10  $\mu$ M. The vials were sealed with Viton stoppers and crimped. Experiments with slower reaction kinetics ( $t_{1/2} \geq 200$  h), such as hematite and siderite were prepared in 20 mL glass ampules. In the glovebox 100  $\mu$ L of the methanolic spike solution were added to 20 mL of the suspensions, yielding concentrations of ~10  $\mu$ M. To keep the suspensions anoxic, the ampules were closed with Viton stoppers before they were taken out of the glovebox. To avoid evaporative losses during the sealing, the liquid in the ampules was then rapidly frozen in acetone cooled with liquid nitrogen and flame sealed. The bursting of the ampules was avoided by piercing the viton stopper with a needle kept in an argon-flushed hose. The ampules as well as the serum vials were agitated on a reciprocating shaker at 23 °C. Control samples in deionized water were prepared for each experiment in serum vials or glass ampules, respectively.

#### **4.2.5 Sampling and Analytical Procedures**

Reaction vials were sacrificed at appropriate time intervals. In a first step, samples of 2.5 mL were taken for concentration determination. The samples were extracted with 5 mL n-hexane containing 10  $\mu$ M bromoform as internal standard. The extraction was carried out in 8 mL glass vials closed with PTFE-sealed screw caps on a Vortex shaker for 3 min. The extract was filled in 0.8 mL autosampler vials and stored at -30°C until analysis. For the determination of the isotopic signatures of the analytes, the remaining of the suspensions was centrifuged for 10 minutes (Heraeus Megafuge 1.0R, Kendro, Asheville, NC). The supernatant was transferred to 8 mL glass vials, closed with PTFE-lined screw caps and stored without headspace at 4°C until analysis.

The concentrations of the halogenated compounds were determined on a gas chromatograph (Carlo Erba HRGC 5160) equipped with a liquid autosampler AS200 (Thermo Finnigan, San José, CA) and an electron capture detector (ECD 400 with <sup>63</sup>Ni-source, Carlo Erba) maintained at 250 °C. Separation of the analytes was achieved on a DB-624 capillary column (30m  $\times$  0.32 mm I.D., 1.8  $\mu$ m film thickness) obtained from J&W

Scientific. 1.5  $\mu\text{L}$  of the hexane extracts were injected on a split/splitless injector maintained at 250  $^{\circ}\text{C}$ . The temperature program was as follows: 2 min at 50  $^{\circ}\text{C}$  then to 175  $^{\circ}\text{C}$  with 10  $^{\circ}\text{C}/\text{min}$ , then to 250  $^{\circ}\text{C}$  with 30  $^{\circ}\text{C}/\text{min}$  and 5 min at 250 $^{\circ}\text{C}$ . The quantification was based on an 8 point calibration (0 to 10  $\mu\text{M}$ ).

The  $^{13}\text{C}$ -isotopic composition of the analytes was determined on a GC-C-IRMS system (Trace GC, coupled to a GC Combustion III interface and a Delta<sup>PLUS</sup>XL isotope ratio mass spectrometer, ThermoFinnigan MAT, Bremen, Germany) coupled to a purge and trap concentrator (LSC 3100, Tekmar Dohrmann, Mason, OH) and a liquid autosampler (AquaTek 70, Tekmar Dohrmann). In the initial phase of the study the GC was equipped with a RTX-VMS capillary column (60m  $\times$  0.32 mm I.D., 1.8  $\mu\text{m}$  film thickness, Restek). In order to enhance the separation of  $\text{CCl}_4$  and  $\text{CHCl}_3$ , especially when one of the 2 analytes was highly concentrated compared to the second (e.g. in the beginning or at the end of the reaction, respectively), a more polar capillary column was used (Stabilwax, 60 m  $\times$  0.32 mm I.D., 1.0  $\mu\text{m}$  film thickness, Restek). The purge and trap method parameters were thoroughly investigated in order to achieve optimal extraction efficiencies and reproducible isotopic measurements (Chapter 3). The carrier gas was helium at a constant pressure of 1.9 bar. The temperature program was as follows: 2 min at 45 $^{\circ}\text{C}$ , then to 100  $^{\circ}\text{C}$  with 14 $^{\circ}\text{C}/\text{min}$ , then to 210  $^{\circ}\text{C}$  with 20  $^{\circ}\text{C}/\text{min}$  and 4 min at 210  $^{\circ}\text{C}$ . The analytes were oxidized within the combustion interface maintained at 940  $^{\circ}\text{C}$ . The catalyst was regularly reoxidized after  $\sim$ 40 samples. External standards with known isotopic signatures were measured under the same conditions as the unknown samples to allow to correct for potential isotopic fractionation due to the extraction process.

Isotopic enrichment factors ( $\epsilon$ ) were determined using the linearized Rayleigh equation (Equation (4-1)).

$$\ln\left(\frac{\delta^{13}\text{C}_t + 1000}{\delta^{13}\text{C}_0 + 1000}\right) = \frac{\epsilon}{1000} \cdot \ln\frac{[\text{CCl}_4]_t}{[\text{CCl}_4]_0} \quad (4-1)$$

The subscripts  $t$  and  $0$  stand for the concentration and the isotopic signature of  $\text{CCl}_4$  at time  $t$  and at the beginning of the reaction, respectively.  $\epsilon$ -values were determined using the DOS software Lin2D<sup>122</sup> that allows to consider the uncertainties in the x and y coordinates for the calculation of the linear regression.

## 4.3 Results and Discussion

### 4.3.1 Reaction Kinetics and Isotopic Enrichment.

As illustrated by Figure 4.2, generally the reaction of CCl<sub>4</sub> with Fe(II) sorbed on the surface of different iron minerals followed a pseudo first order behavior.

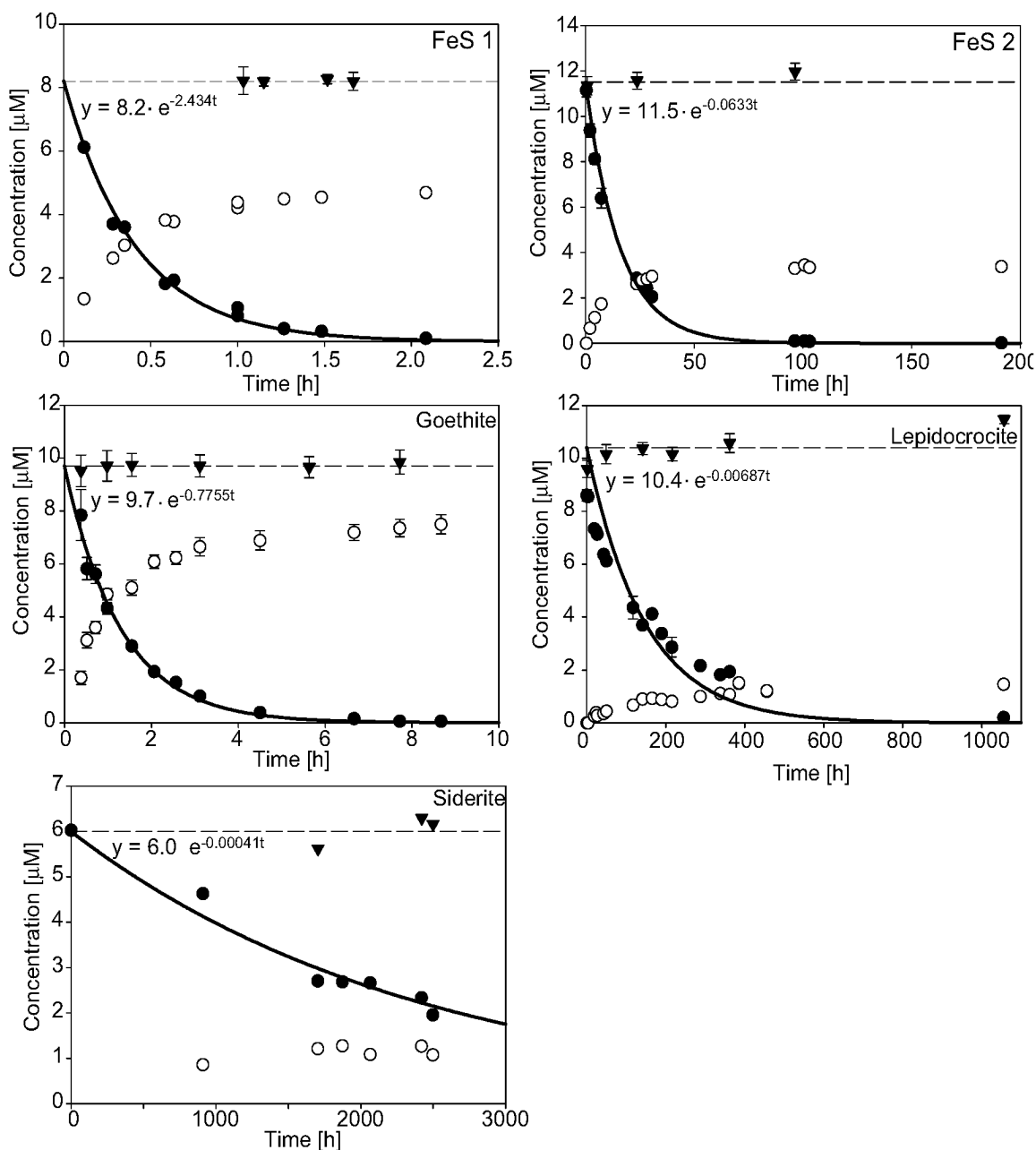


**Figure 4.2: Reaction of CCl<sub>4</sub> with Surface-Bound Fe(II) on Different Minerals.** Evolution of carbon tetrachloride concentrations (filled circles), the pseudo first order fit (continuous line) and chloroform concentrations (open circles). The dashed line corresponds to the average concentration of CCl<sub>4</sub> blanks (filled triangles) sampled during the course of the reaction and used as  $y(0)$ -values for the calculation of the reaction rate constants. Note the different scales of the x-axes.

The pseudo first order rate constants were determined by an exponential fit of the  $\text{CCl}_4$  concentration vs time data (Figure 4.2) and are resumed in Table 4.3. As expected from hexachlorethane data,<sup>117</sup> the determined first order rate constants spanned several orders of magnitude depending on the investigated mineral. The reactivities increased in the following order; siderite < hematite < lepidocrocite < mackinawite 2 < magnetite < goethite < mackinawite 1. With the exception of the mackinawite 2 batch the observed reactivities increased from Fe(II)-carbonates to Fe(II)-(hydr)oxides to iron sulfide.

**Table 4.3: Pseudo First Order Rate Constants and Surface Area Normalized Rate Constants and Isotopic Enrichment Factors for the Degradation of  $\text{CCl}_4$  by Different Iron Minerals and Polysulfide.**

Reductant	$k_{\text{obs}}$ [ $\text{h}^{-1}$ ]	$\log k'_{\text{obs}}^{\text{a}}$ ( $\text{CCl}_4$ )	$\log k'_{\text{obs}}$ ( $\text{C}_2\text{Cl}_6$ ) <sup>b</sup>	$\varepsilon_{\text{Rayleigh}}^{\text{c}}$ [‰]	KIE	$\varepsilon_{\text{CHCl}_3}$ [‰] <sup>d</sup>
Mackinawite 1	$2.434 \pm 0.13$	-1.31	-1.79	$-15.9 \pm 0.3$	1.016	$-17.2 \pm 0.3$
Mackinawite 2	$0.0633 \pm 4.6 \cdot 10^{-3}$	-2.90	n.d. <sup>e</sup>	$-15.9 \pm 0.2$	1.016	$-22.1 \pm 1.1$
Goethite	$0.776 \pm 0.054$	-1.81	n.d. <sup>e</sup>	$-19.3 \pm 1.2$	1.020	$-19.3 \pm 1.0$
Goethite <sup>f</sup>	$0.019 \pm 0.002$	-3.72	-3.04	$-26.5 \pm 2.79$	1.027	n.d. <sup>e</sup>
Magnetite (start)	$0.39 \pm 0.022$	-2.11	n.d. <sup>e</sup>	$-24.0 \pm 1.6$	1.033	n.d. <sup>e</sup>
Magnetite (end)	$0.198 \pm 0.027$	-2.40	n.d. <sup>e</sup>	$-31.6 \pm 2.9$	1.025	n.d. <sup>e</sup>
Magnetite (overall)	$0.245 \pm 0.013$	-2.31	-3.12	$-25.8 \pm 1.0$	1.026	$-25.8 \pm 0.9$
Lepidocrocite	$6.9 \cdot 10^{-3} \pm 9 \cdot 10^{-4}$	-3.86	-3.74	$-32.0 \pm 0.5$	1.033	$-31.9 \pm 0.4$
Hematite (start)	$6.2 \cdot 10^{-4}$	-4.91	n.d. <sup>e</sup>	$-49.7 \pm 4.9$	1.026	n.d. <sup>e</sup>
Hematite (end)	$1.1 \cdot 10^{-3}$	-4.66	n.d. <sup>e</sup>	$-25.8 \pm 0.8$	1.052	n.d. <sup>e</sup>
Hematite (overall)	$1 \cdot 10^{-3} \pm 5 \cdot 10^{-5}$	-4.69	-3.82	$-29.5 \pm 1.0$	1.030	$-29.4 \pm 1.0$
Iron(II) porphyrin <sup>f</sup>	$0.042 \pm 0.002$	- <sup>g</sup>	n.d. <sup>e</sup>	$-26.2 \pm 0.3$	1.027	n.d. <sup>e</sup>
Polysulfide <sup>f</sup>	$0.145 \pm 0.003$	- <sup>g</sup>	n.d. <sup>e</sup>	$-21.6 \pm 0.4$	1.022	n.d. <sup>e</sup>
Siderite	$4 \cdot 10^{-4} \pm 3 \cdot 10^{-5}$	-5.09	-4.76	$-26.7 \pm 2.9$	1.027	$-22.0 \pm 3.2$

a. Surface normalized pseudo first order rate constants.

b. Surface normalized pseudo first order rate constants of the dehalogenation reaction of hexachloroethane with the investigated iron minerals<sup>117</sup>.

c. Determined based on the Rayleigh Equation (Equation (4-1)).

d. Determined based on the differences in  $\delta^{13}\text{C}$ -values of  $\text{CCl}_4$  and  $\text{CHCl}_3$  in the beginning of the reaction.

e. Not determined

f. Reaction studied by Elsner et al.<sup>119</sup>

g. No surface reaction.

In two experiments the apparent reaction kinetics changed during the course of the experiment (Figure 4.3). The reaction of  $\text{CCl}_4$  with Fe(II) sorbed to magnetite slowed down at the end of the investigated time span. The reaction rate during the first 3 half life periods was  $k_{\text{obs}} = 0.39 \text{ h}^{-1}$ , compared to a  $k_{\text{obs}}$  of  $0.198 \text{ h}^{-1}$  for the rest of the reaction (overall reaction rate  $0.245 \pm 0.013 \text{ h}^{-1}$ ). In the case of the hematite experiment, the

opposite observation could be made, the reaction rate increased during the experiment, doubling from  $6.2 \cdot 10^{-4} \text{ h}^{-1}$  in the first half life period to  $1.14 \cdot 10^{-3} \text{ h}^{-1}$  in the second half life period (overall reaction rate  $1.03 \cdot 10^{-3} \pm 0.05 \cdot 10^{-3} \text{ h}^{-1}$ ).

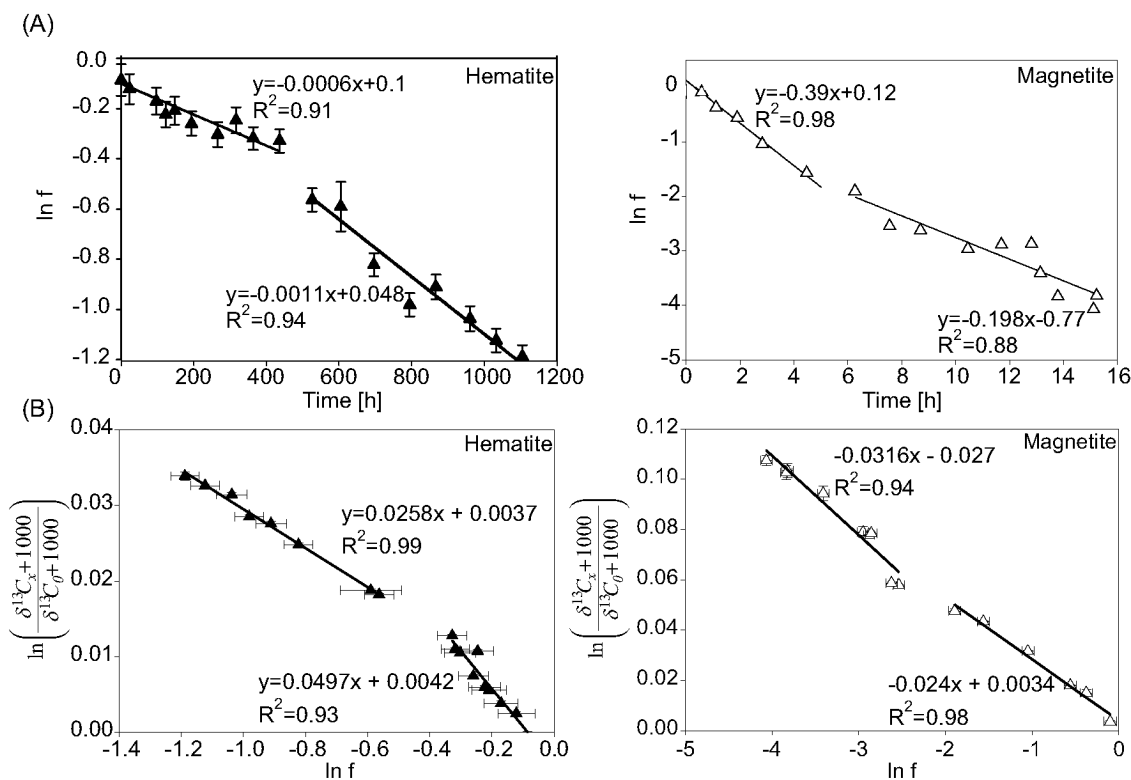


**Figure 4.3: Shifting Reaction Rates and Isotopic Fractionations during the Reaction.** (A) During the course of the reaction the reaction rates shifted in the case of the magnetite (open triangles) and hematite (filled triangles) experiments. (B) In the case of the hematite experiment this shift was correlated with a significant change in the isotopic enrichment. A similar but less pronounced observation was made in the case of the magnetite experiment.

The relative reactivities of the investigated iron minerals matched more or less with the trend observed with hexachloroethane.<sup>117</sup> The absolute reactivities differed, however, significantly.

The reaction of  $\text{CCl}_4$  with goethite was much faster in the present study than previously described,<sup>111,119</sup> showing that the reactivities within the same mineral can differ significantly. Experiments at different temperatures and in the presence of antibiotics were carried out to exclude temperature effects or microbial activity as reasons for this observation. Slight shifts in the pH may strongly affect the Fe(II) adsorption on the surface and hence affecting the quantity of the reactive sites.<sup>123-126</sup> Since we relied on the intrinsic buffer capacity of the goethite mineral, small but relevant pH variations could not be ruled out and may contribute to the different reactivities. Similarly, the kinetic data for the

two different mackinawite experiments varied by more than an order of magnitude.

As expected from earlier studies using hexachloroethane, the rates of the investigated reactions varied largely. Furthermore, high variations between different batches of the same mineral were observed. As shown in Table 4.3 the determined isotopic enrichment factors ( $\varepsilon$ ) did also spread over a large range (-15.9‰ to -32.0‰). This finding hampers the use of isotopic enrichment factors for quantifying *in situ* degradation of abiotic dehalogenation reactions, since this approach relies on the assumption of one given isotopic enrichment for one given transformation reaction.<sup>13,46-48</sup> All reaction systems showed a Rayleigh type behavior (Figure 4.4) with the exception of the hematite and magnetite experiments (Figure 4.3 (B)). Note that the isotopic enrichment shifted during the latter experiments, analogously to the observed shift of the reaction rate in these systems. While the reactivity increased in the hematite system the isotopic enrichment decreased during the reaction, consistent with a shift in the position of the transition state on the reaction coordinate. Conversely, a slightly increasing isotopic fractionation occurred as the reaction rate decreased in the magnetite system. The change in the latter reaction was not very pronounced and could not be unambiguously determined (a regression considering all data points still yielded a correlation  $R^2 \geq 0.98$ ), however, the direction of the change in  $\varepsilon$  was as expected. Hence, in the case of hematite, the observed increase in reaction rates was supposedly due to a change of the position of the transition state on the reaction coordinate. This might be due to a difference in the reactive Fe(II)-sites, leading to a different surface-stabilized intermediate. In the case of the magnetite experiment, it was not clear whether such a stabilization was the reason for the decrease in reactivity or if it was due to a decrease in the number reactive sites.

An inverse correlation between  $k_{\text{obs}}$  and  $\varepsilon$  could also be observed for the different experiments (Figure 4.5). In the case of replicate experiments with the same mineral, two different observations could be made. In the case of the goethite experiments, the differences in the reactivity appeared also in the isotopic enrichment, indicating that a change of the intrinsic reactivities of the sorbed Fe(II)-sites occurred. At the investigated pH,  $\equiv\text{FeOFeOH}$ -sites and  $\equiv\text{FeOFe}^+$ -sites are believed to coexist.<sup>125</sup> Since no additional buffer was used in these systems, small changes in pH could not be excluded. Such changes vary the relative quantities of the different sites and may hence influence the stabilization of the transition states during the reaction, leading to varying isotopic enrichments.

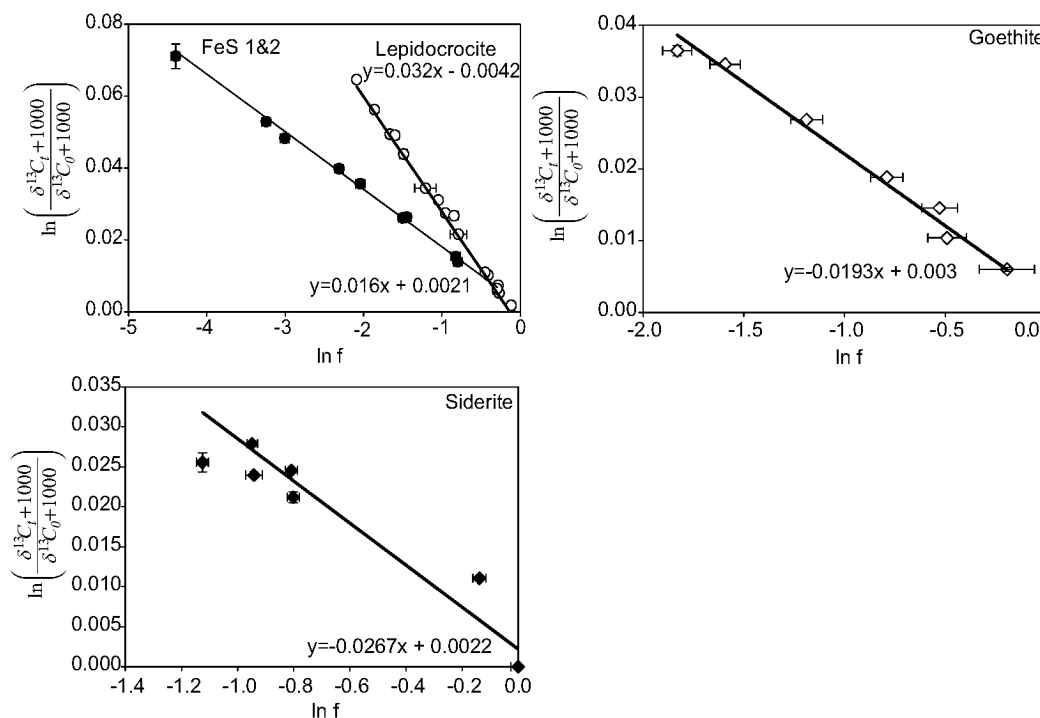


**Figure 4.4: Rayleigh Plots for 4 Different Reaction Systems.** (The plots show that the isotopic fractionation of CCl<sub>4</sub> during the reduction by Fe(II) sorbed to FeS (filled circles), lepidocrocite (open circles), goethite (open diamonds) and siderite (filled circles) followed a Rayleigh type behaviour.

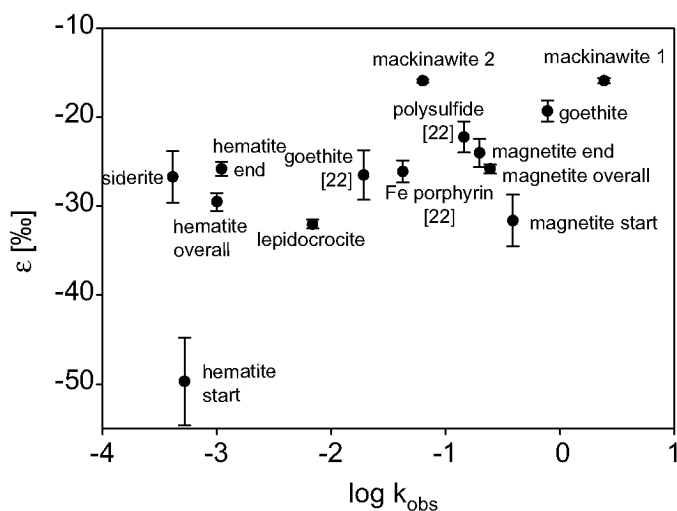


**Figure 4.5: Plot of Isotopic Enrichment versus log k<sub>obs</sub>.**

In the case of the two FeS batches, a different behaviour could be observed. While the transformation reaction was much faster for FeS 1 than for FeS 2 ( $\log k'_{\text{obs}}$  -1.31 vs -2.90), the isotopic enrichment factor was the same. Identical isotopic fractionation factors but differing reactivities were also observed for different types of minerals (siderite, magnetite and one goethite batch<sup>119</sup>), suggesting similar positions of the transition states but differences in the sorption density of the reactive Fe(II)-sites.

### 4.3.2 Product Yields and Isotopic Enrichments - Mechanistic Considerations.

Among the different potential transformation products of  $\text{CCl}_4$  that may be formed under the experimental conditions, only  $\text{CHCl}_3$  could be quantified and isotopically characterized. The average isotopic composition of the sum of all other products was, however, calculated based on a mass balance of the heavy and light isotopes, respectively. The yields and isotopic signatures of chloroform, and the average isotopic compositions of the other compounds are summarized in Table 4.4.

**Table 4.4: Chloroform Yields and  $\delta^{13}\text{C}$  Isotopic Signatures of Chloroform**

Mineral	Chloroform Yield <sup>a</sup> [%]	$\delta^{13}\text{C}$ $\text{CCl}_4$ , start [‰]	$\delta^{13}\text{C}$ $\text{CHCl}_3$ , end [‰]	$\Delta\delta^{13}\text{C}^{\text{b}}$ $\text{CHCl}_3$ [‰]	$\delta^{13}\text{C}^{\text{c}}$ other [‰]
Mackinawite 1	55.3 ± 1.3	-38.3 ± 0.1	-40.7 ± 0.2	-2.4 ± 0.3	-35.3 ± 0.3
Mackinawite 2	29.1 ± 1.0	-38.3 ± 0.1	-49.6 ± 0.2	-11.3 ± 0.2	-20.7 ± 4.2
Goethite	77.3 ± 4.7	-38.7 ± 0.2	-43.9 ± 0.3	-5.2 ± 0.4	-25.8 ± 3.0
Magnetite	80.7 ± 4.3	-39.1 ± 0.1	-42.2 ± 0.2	-3.1 ± 0.2	-34.5 ± 0.2
Lepidocrocite	14.2 ± 0.4	-38.6 ± 0.1	-62.7 ± 0.8	-24.1 ± 0.9	-34.6 ± 0.2
Hematite	17.5 ± 7.3 <sup>d</sup>		n.d. <sup>e</sup>	n.d. <sup>e</sup>	n.d. <sup>e</sup>
Siderite	33.5 ± 4.6 <sup>d</sup>		n.d. <sup>e</sup>	n.d. <sup>e</sup>	n.d. <sup>e</sup>

a. Corresponds to the  $\text{CHCl}_3$ -yield at 99% degradation of  $\text{CCl}_4$ , if not stated otherwise.

b. Calculated as  $\delta^{13}\text{C}$  of  $\text{CHCl}_3$  at the end of the reaction minus  $\delta^{13}\text{C}$  of  $\text{CCl}_4$  at the beginning.

c. Calculated as  $\delta^{13}\text{C}_{\text{other}} = \delta^{13}\text{C}_{\text{CCl}_4} + \Delta\delta^{13}\text{C}_{\text{other}} = \delta^{13}\text{C}_{\text{CCl}_4} - \frac{f(\text{CHCl}_3) \cdot \Delta\delta^{13}\text{C}_{\text{CHCl}_3}}{f(\text{other})}$  where  $f(\text{CHCl}_3)$  and  $f(\text{other})$  stand for the fraction of formed chloroform and other products, respectively.

d. Corresponds to the average  $\text{CHCl}_3$  for all data points. The determination of the chloroform yield at 99% degradation was not possible since the reactions have not been followed to completion.

e. Not determined, since reaction was not monitored to completion.

While almost 80% of the initial tetrachloromethane was transformed to chloroform in the goethite and magnetite experiments, the lowest  $\text{CHCl}_3$ -yields were found in the lepidocrocite and hematite experiments. The chloroform yield in the goethite experiment, as well as in all preliminary goethite experiments, was higher as previously reported<sup>111,119</sup> (Figure 4.6).

With a simplified mechanistic model of the degradation reaction assuming two parallel ways leading from  $\text{CCl}_4$  to chloroform on the one hand and all the other products on the other hand (Figure 4.7) the data shown in Table 4.4 can be used to calculate the relative isotopic fractionation caused by the way leading to  $\text{CHCl}_3$  compared to the one leading to the other products ( $\text{KIE}_{\text{CHCl}_3}/\text{KIE}_{\text{CCl}_4}$ ) using Equation (4-4),

As can be seen in Table 4.5 the reaction leading to the production of  $\text{CHCl}_3$  is associated with a higher fractionation, than the effect leading to



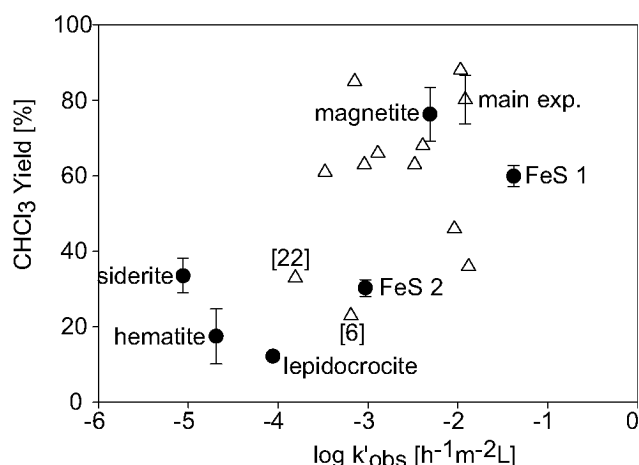
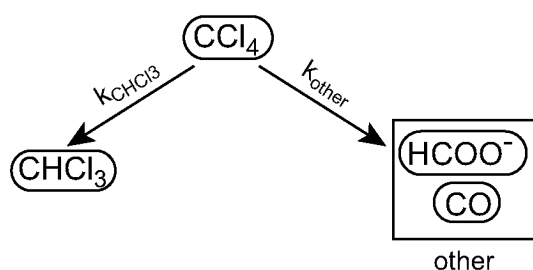


**Figure 4.6: Plot of Chloroform Production versus Surface Normalized Reaction Rate.** Filled circles correspond to results found for the main experiments of the different investigated minerals. Open triangles correspond to results for goethite experiments (preliminary experiments and main experiment of this study as well as two systems reported by Elsner et al.<sup>119</sup> and Pecher et al.<sup>111</sup>)



$$\frac{{}^{12}C_{CHCl_3}}{{}^{12}C_{other}} = \frac{{}^{12}k_{CHCl_3}}{{}^{12}k_{other}} \quad (4-2)$$

$$\frac{{}^{13}C_{CHCl_3}}{{}^{13}C_{other}} = \frac{{}^{13}k_{CHCl_3}}{{}^{13}k_{other}} \quad (4-3)$$

Dividing Equation (4-2) by Equation (4-3) yields:

$$\frac{\zeta IE_{CHCl_3}}{KIE_{other}} = \frac{\left(\frac{{}^{12}k}{{}^{13}k}\right)_{CHCl_3}}{\left(\frac{{}^{12}k}{{}^{13}k}\right)_{other_3}} = \frac{\left(\frac{{}^{13}C_{other}}{{}^{12}C_{other}}\right)}{\left(\frac{{}^{13}C_{CHCl_3}}{{}^{12}C_{CHCl_3}}\right)} = \frac{R_{other}}{R_{CHCl_3}} = \frac{(1000 + \delta^{13}C_{other})}{(1000 + \delta^{13}C_{CHCl_3})} \quad (4-4)$$

**Figure 4.7: Simplified Reaction Model.** For both pathways a specific reaction rate constant can be postulated for the heavy isotopes <sup>13</sup>k<sub>CHCl<sub>3</sub></sub> and <sup>13</sup>k<sub>other</sub> as well as for the light isotopes <sup>12</sup>k<sub>CHCl<sub>3</sub></sub> and <sup>12</sup>k<sub>other</sub>

the other products, which is consistent with the observation of isotopic compositions of CHCl<sub>3</sub> that are systematically depleted in <sup>13</sup>C compared to the initial tetrachloromethane at the end of the reaction. However, the inconsistency of the results shows that the simplified 2-way reaction scheme does not apply supporting the reaction scheme proposed by Elsner et al.<sup>119</sup> (Figure 4.1). The absolute KIE's were also calculated but,

due to the error propagation, the results were afflicted with large errors, preventing the determination of significant differences.

**Table 4.5: Kinetic Isotope Effects (KIE) for the Degradation of  $\text{CCl}_4$  and Relative Importance of Fractionation towards  $\text{CHCl}_3$  Compared to the Production of Other Products.**

Mineral	$\frac{KIE_{\text{CHCl}_3}}{KIE_{\text{other}}}$	$KIE_{\text{CCl}_4}$
Mackinawite 1	$1.006 \pm 5 \cdot 10^{-4}$	$1.016 \pm 10^{-4}$
Mackinawite 2	$1.017 \pm 3 \cdot 10^{-4}$	$1.016 \pm 10^{-3}$
Goethite	$1.024 \pm 5 \cdot 10^{-3}$	$1.020 \pm 3 \cdot 10^{-4}$
Magnetite	$1.017 \pm 3 \cdot 10^{-3}$	$1.026 \pm 10^{-3}$
Lepidocrocite	$1.030 \pm 9 \cdot 10^{-4}$	$1.033 \pm 2 \cdot 10^{-3}$

The two different mackinawite batches represent a special case. They did not only show significant differences in their reactivities but also in the product formation, indicating a change of the importance of the different branches of the reaction. At first sight, this observation is in contradiction with the observation of identical isotopic enrichments supporting the hypothesis, that both batches differ only by the amount of Fe(II)-sites, made above. These effects may, however, be explained by assuming that in the case of  $\text{CCl}_4$  reduction by FeS, the entire reaction proceeds via the trichloromethyl radical and that a branching of the reaction mechanism only occurs after this first step (Figure 4.8). This would also mean that no significant concentrations of  $\text{HCOOH}$  would be expected. Kriegman-King and Reinhard found that during the degradation of  $\text{CCl}_4$  on pyrite under different anaerobic conditions the  $\text{HCOOH}$  formed only accounted for 4-5% .<sup>127</sup>

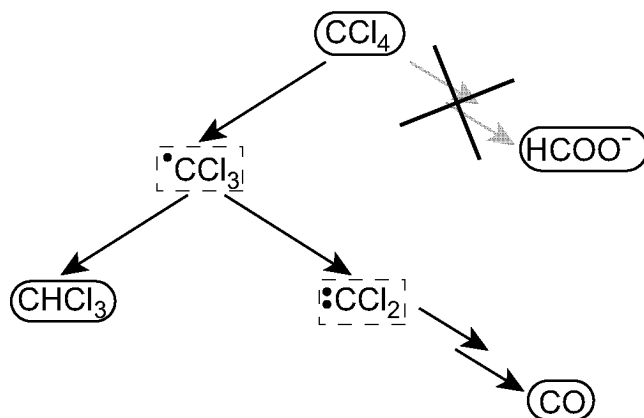


**Figure 4.8: Simplified Reaction Model for the Reaction with Iron Sulfides.** In the presence of  $\text{HS}^-$  the production of  $\text{CS}_2$  from the trichloromethyl radical has also been shown<sup>127</sup>.

## 4.4 Conclusions

In environmental studies, the potential of the use of isotopic enrichments to determine the nature of observed *in situ* transformations has often been addressed. This study shows, that, as expected, not only microbially mediated reactions but also abiotic dehalogenation of polyhalogenated compounds, this case tetrachloromethane, is accompanied by a significant isotopic enrichment. A distinction between abiotic and microbial dehalogenation of tetrachloromethane based on isotopic enrichments is, however, hampered by the fact that enrichment factors for the abiotic reductive degradation with Fe(II) sorbed on the surface of different iron minerals span a wide range. Hence, an identification of the nature of an *in situ* degradation (e.g. abiotic versus microbially mediated reaction) would only be possible if the microbially mediated reaction is associated with isotopic enrichments that are significantly different from the range of factors observed in the present study. Furthermore, the finding of a variable isotopic fractionation associated with abiotic dehalogenation of CCl<sub>4</sub> implicates that the quantification of abiotic dehalogenation reaction at field sites based on the determination of the isotopic composition of the contaminants will not yield unequivocal results, because this approach would necessitate one robust and specific fractionation factor for one given reaction.

While the use of isotopic fractionation of the reductive dehalogenation of CCl<sub>4</sub> at contaminated field sites may be limited, the results of this study may be used to gain further mechanistic insights on factors governing the abiotic dehalogenation of CCl<sub>4</sub> by surface-bound Fe(II)-species. Changes in reactivities that are correlated with different isotopic enrichments (increasing fractionation for slower reactions) may be explained by shifts in the position of the transition state on the reaction coordinate. Constant isotopic signatures for reactions with varying reaction kinetics might, however, indicate that the different reaction rates are caused by changes in the quantity of reactive sites at the surface.

To confirm the hypothesis that isotopic fractionation is not influenced by the quantity of reactive sites, multiple experiments with the same mineral and different Fe(II) sorption densities should be carried out. Furthermore the determination of isotopic enrichments during the microbial reductive dehalogenation of tetrachloromethane would yield additional information on the variability of carbon isotopic enrichments that can be found for such a "simple" molecule.



**DIFFERENTIATION BETWEEN  
ABIOTIC AND MICROBIALLY  
MEDIATED REDUCTIVE  
DEHALOGENATION OF  
CHLORINATED ETHENES BASED  
ON STABLE CARBON AND  
HYDROGEN ISOTOPIC ANALYSIS**

## 5.1 Introduction

Chlorinated ethenes such as tetrachloroethylene (PER) and trichloroethene (TCE) are widely used in dry cleaning and for metal degreasing in manufacturing processes. Their widespread use makes them ubiquitous groundwater pollutants in industrialized countries. Due to their prevalent occurrence and potential human cancerogenicity, the fate of these compounds has been thoroughly investigated under different environmental conditions. Reductive dehalogenation is the major degradation process leading to the remediation of these highly oxidized organic compounds in contaminated aquifers. Abiotic reductive dehalogenation can occur in the presence of zero valent metals [Fe(0)<sup>128-130</sup> and Zn(0)<sup>128</sup>], or iron(II)-containing soil minerals (e.g., magnetite<sup>131</sup>, green rust<sup>132</sup> and iron sulfides<sup>131,133,134</sup>). Microbially, the chlorinated ethenes may be reduced either cometabolically or by halorespiration.<sup>135-137</sup>

Typically, oxygen is rapidly consumed in contaminated groundwater, leading to environmental conditions in which both reactions, abiotic and microbial reductive dehalogenation may occur. While the abiotic reaction is often thought to be slower than the microbially mediated one, under certain environmental conditions, the relative importance of these concurrent processes may reverse. This is expected for sulfate-reducing conditions, where poorly crystalline iron sulfides with high surface areas may be formed.<sup>138</sup> Such iron sulfides have been shown to reduce chlorinated as well as nitroaromatic compounds<sup>120,139,140</sup> (see also Chapter 4). Surface normalized pseudo first order rate constants for the reduction of PER and TCE were determined to be in the order of  $2 \cdot 10^{-2} \pm 1 \cdot 10^{-2} \text{ d}^{-1}$ .<sup>133,141</sup>

Recently, compound-specific isotope analysis has been used for the identification and quantification of *in situ* degradation of chlorinated ethenes at contaminated field sites.<sup>32,34,39,51,52,54</sup> The extent of the observed isotopic enrichment has been reported for various processes such as microbial reductive dehalogenation<sup>29,34,39,41,44</sup>, aerobic biodegradation<sup>40</sup>, abiotic reduction<sup>27,35,45</sup> and oxidation with permanganate.<sup>54,142</sup> The reported enrichment factors vary over a wide range (Appendix A2), but they do significantly differ from isotope effects observed for volatilization<sup>31,49</sup> or sorption processes.<sup>50</sup> Hence, it should be possible to distinguish between concentration declines of the contaminants in the plume due to degradation reactions on the one hand and dilution or phase transfer processes on the other hand.

Based on isotopic enrichment factors, it is in principle even possible to quantify *in situ* degradation assuming one single and constant  $\epsilon$ .<sup>46-48,143</sup> Hence, in remediation scenarios, it is important to know the nature of the degradation reaction to allow an isotope based quantification of the reaction. While in the case of engineered remediation techniques the nature of the degradation is known, (e.g. abiotic reductive dehalogenation with Fe(0) in reactive walls, oxidation by permanganate in push and pull experiments) and, hence, an adapted  $\epsilon$  can be chosen for quantification, the monitoring of *in situ* remediation is hampered by the fact that a distinction between abiotic and microbial processes may be difficult. The isotopic enrichments reported for microbially mediated reductions depended on the number of chlorine atoms but varied also for one given compound (-2‰<sup>10</sup> to -5.5‰<sup>39</sup> for PER, -2.5‰<sup>34</sup> to -13.8‰<sup>39</sup> for TCE, -12‰<sup>10</sup> to -20.4‰<sup>39</sup> for *cis*-DCE, -30.3‰<sup>41</sup> and -21.5‰<sup>34</sup> to -26‰<sup>10</sup>). In the case of PER, the isotopic enrichment for abiotic dehalogenation was found to be significantly higher (-25.3‰ for the reduction by Fe(0)<sup>27</sup> and -15.8 to -16.5‰ for the abiotic reduction by vitamin B<sub>12</sub><sup>45</sup>), potentially allowing a distinction between abiotic and microbially mediated processes. In the case of TCE this differentiation seems no longer possible, since enrichment factors for the abiotic reduction by Fe(0) range from -7.6‰<sup>35</sup> to -16‰<sup>27</sup>, hence, partly overlapping with the range of reported microbial enrichments. TCE reduction by vitamin B<sub>12</sub> shows an enrichment factor (-16.6‰ to -17.2‰<sup>45</sup>) comparable to the one of PER for the same reaction. Since the enzyme responsible for the reductive dehalogenation is supposed to contain a vitamin B<sub>12</sub>-like corrinoid<sup>144</sup>, it is interesting that the isotopic enrichments found for PER and TCE in microbial degradation experiments are significantly different, while they are identical for the reaction at the reactive centre of the enzyme. This may (partially) be rationalized by the fact that different affinities of the enzyme for the different substrates exist, an effect often referred to as "commitment to catalysis".<sup>145</sup> This effect has been explained in the case of the aerobic mineralization of 1,2-dichloroethane by the well studied haloalkane dehalogenase.<sup>146</sup> In the first step of an enzymatic reaction, an enzyme-substrate complex forms in a reversible reaction. Commitment to catalysis (C) represents the tendency of the enzyme-substrate complex to go forward through catalysis rather than to break down to free enzyme and substrate ( $C = k_2/k_{-1}$ )(Figure 5.1). The intrinsic fractionation

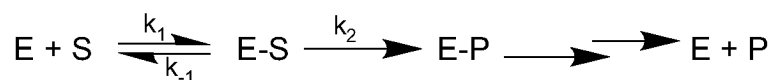


**Figure 5.1: Reaction Scheme for Haloalkane Dehalogenase.** *This reaction scheme was modified from Hunkeler & Aravena<sup>146</sup>, see also Appendix A1.3.*

factor is defined as the relative reaction rates of the substrates containing the heavy isotopes compared to the ones with the light isotopes in the first irreversible step of the reaction ( $^{13}k_2/^{12}k_2$ ). As is evident from Equa-

$$\frac{1}{\alpha} = \frac{^{12}k_2/^{13}k_2 + C}{1 + C} \quad (5-1)$$

tion (5-1) the magnitude of the isotopic fractionation depends on the commitment of catalysis. The derivation of Equation (5-1) is explained in Appendix A1.3. The larger the rate of catalysis ( $k_2$ ) compared to  $k_{-1}$  (e.g., the larger C) the smaller is the measured isotopic fractionation for a given intrinsic isotope effect. Hence, depending on this affinity of the enzyme for different substrates, differences between microbial and abiotic reactions can be more or less pronounced, complicating the differentiation between abiotic and microbial reactions at field sites.

A further challenge in the assessment of *in situ* remediation of chlorinated ethenes, lies in the identification of the sources of contamination (see Chapter 3.3.5). Since TCE is used as solvent and is the first degradation of product of PER, the cooccurrence of TCE and PER in a contaminant plume is not an unambiguous evidence for the existence of *in situ* degradation, but may also be explained by a second contamination source of TCE. It has been shown that the hydrogen isotopic signature of chemically manufactured TCE is significantly enriched in deuterium as compared to TCE formed during the abiotic degradation of PER.<sup>19</sup> Hence, the determination of  $^1\text{H}/^2\text{H}$ -isotopic ratios of TCE, *cis*-1,2-dichloroethene and *trans*-1,2-dichloroethene may be a promising approach to distinguish a degradation-linked source of these compounds from a multiple contamination source scenario.

In this study we investigated the kinetics as well as the isotopic enrichment of the abiotic and microbial reductive dehalogenation under sulfate-reducing conditions in order to evaluate prospects and limitations of this approach for distinguishing between two reactions that may occur under the same environmental conditions. The microbial degradation experiments were carried out with a pure culture of *dehalospirillum multi-*



*multivorans*, a halo-respiring microorganism that is able to use PER as well as TCE as terminal electron acceptor.<sup>147</sup> In the preliminary abiotic experiments, FeS (mackinawite), that is formed under sulfate-reducing conditions in the presence of Fe(II) and that exhibits a high reactivity towards the reduction of chlorinated hydrocarbons (see also Chapter 4), was used as reductant. In addition, the hydrogen isotopic signatures of the degradation products TCE and *cis*-DCE have been determined and have been compared to the <sup>2</sup>H/<sup>1</sup>H-ratios of chemically manufactured compounds.

## 5.2 Experimental Section

### 5.2.1 Reagents and Materials

Stock solutions of tetrachloroethene (PER, >99.9%), trichloroethene (TCE, >99.9%), both obtained from Fluka (Buchs, Switzerland) and *cis*-1,2-dichloroethene (*cis*-DCE, 97%) from Aldrich (Steinheim, Germany) were prepared in methanol (>99.9%) purchased from Scharlau (Barcelona, Spain). Aqueous samples were extracted with *n*-hexane (pro analysi) obtained from Merck (Darmstadt, Germany) containing chloroform (IR grade, from Fluka, Buchs, Switzerland) as internal standard (10 μM).

### 5.2.2 Microbial Degradation Experiment

A pure culture of *dehalospirillum multivorans* was grown in anaerobic medium, which was composed of 1L basal medium, 0.5 mL vitamin solution, 1 mL trace element solution SL10, 1 mL vitamin B<sub>12</sub> solution (cyanocobalamin 50 mg/L), 0.1 mL selenite solution (Na<sub>2</sub>SeO<sub>3</sub>·5H<sub>2</sub>O 3 mg/L), 40 mL NaHCO<sub>3</sub> solution (84 g/L, flushed with CO<sub>2</sub> and autoclaved with CO<sub>2</sub> in the headspace), 1 mL cysteine solution (cysteine hydrochloride, 50 g/L), 20 mL yeast extract (10%) and 2.5 mL of FeSO<sub>4</sub> solution. 1L of basal medium contained 70 mg Na<sub>2</sub>SO<sub>4</sub>, 200 mg KH<sub>2</sub>PO<sub>4</sub>, 250 mg NH<sub>4</sub>Cl, 1 g NaCl, 400 mg MgCl<sub>2</sub> · 6 H<sub>2</sub>O, 500 mg KCl, 150 mg CaCl<sub>2</sub> · 2 H<sub>2</sub>O and 1 mL resazurin. The vitamin solution contained per liter 50 mg *p*-aminobenzoic acid, 10 mg D(+)-biotin, 100 mg nicotinic acid, 25 mg Ca-D(+)-pantothenat, 250 mg pyridoxamine hydrochloride and 50 mg/L thiamine hydrochloride. The pH of the medium was between 7.3 and 7.7. After inoculation the serum vials were gently shaken on an horizontal shaker at room temperature.

The reaction was carried out in 4 replicates for PER and TCE, respectively. Aliquots of the pure chlorinated ethene were added to 55 mL of

anoxic medium contained in 100 mL serum vials and closed with Viton® stoppers. After equilibration, the reaction was started by inoculating the serum vials with 5 mL of the previously grown culture to each vial. The vials were placed in the dark on a horizontal shaker at 23°C. At each sampling point, 4 mL samples were taken, the reaction was stopped by adding NaOH to a final concentration of 0.1 M and stored at 4°C until analysis. Samples for concentration determination were immediately extracted with n-hexane containing chloroform (10 µM) as internal standards. The hexane extracts were stored at -30°C until analysis. The concentrations were corrected for the losses of the analytes to the headspace of the reaction vial. With this objective, the vials were weighed before each sampling point for the calculation of the volume of the aqueous phase ( $V_w$ ) and the gas phase ( $V_a$ ). The air-water partition coefficients (at 25 °C) used for the correction were 1.2, 0.49 and 0.22 for PER, TCE and *cis*-DCE, respectively.<sup>63</sup>

### 5.2.3 FeS Experiments

The FeS was freshly prepared following a procedure modified from Rickard et al.<sup>148</sup> by adding an FeCl<sub>2</sub> solution to a solution of Na<sub>2</sub>S under stirring in an oxygen free glovebox. The FeCl<sub>2</sub> solution (0.8 M) was prepared by adding 27.9 g of iron (> 99.5%, Merck, Darmstadt, Germany) to 0.4 L of degassed HCl (2 M). The solution was heated and gently stirred until hydrogen production stopped. The solution was transferred into the glovebox and filtered to eliminate the excess Fe(0) and added to the Na<sub>2</sub>S solution. The resulting FeS suspension was stirred for 2 days, after settling the supernatant was replaced with anoxic deionized water.

After an equilibration time of >48 hours, aliquots of an FeCl<sub>2</sub> solution were added and the pH of the suspension was adjusted to 7.3. The final concentration of Fe(II) in solution was 4 mM as determined by the phenantroline method.<sup>121</sup> Two different sets of 20 mL glass ampules were prepared by adding 19 mL of the iron sulfide suspension to the ampules and subsequently adding 1 mL of an aqueous anoxic solution of PER and TCE, respectively, yielding a concentration of ~10 µM. Blank controls for the TCE and PER experiment were also prepared in glass ampules, by adding 1 mL of the PER and TCE aqueous solution to 18 mL of anoxic, deionized water. Subsequently, the ampules were closed with Viton® stoppers and taken out of the glovebox. The ampules were then rapidly frozen, by placing them in acetone cooled with liquid nitrogen, to avoid evaporative losses during the flame sealing. The bursting of the ampules during flame-sealing was avoided, by piercing the Viton® stopper with a

needle kept in an argon-flushed hose. The ampules were then placed on a reciprocating shaker at 23 °C until sampling. At each sampling point, one glass ampule was sacrificed, 2 mL of the suspension were transferred to 8 mL vials, and extracted with 5 mL of n-hexane, containing chloroform (10 µM) as internal standard for concentration determination. The extracts were stored at -30°C until analysis. The remaining of the suspension was transferred to 20 mL serum vials, and centrifuged for 15 minutes at 4000 rpm (Heraeus Megafuge 1.0R, Kendro, Asheville, NC) to stop the reaction. The supernatant was withdrawn and transferred into 8 mL glass vials closed with teflon-lined screw caps and stored at 4 °C until the determination of the isotopic signature.

#### **5.2.4 Sampling and Analytical Procedures**

The concentrations of the chlorinated hydrocarbons were determined using a gas chromatograph (GC 8000, Fisons, Manchester, U.K.) coupled to a mass spectrometric detector (single quadrupole MD 800, Fisons, Manchester, U.K.) and equipped with an autosampler (AS 800, Fisons, Manchester, U.K.). The GC was equipped with a guard-column (2 m × 0.53 mm I.D.) deactivated with OV-1701-04 (BGB, Anwil, Switzerland) and an analytical capillary column (Stabilwax, 60 m × 0.32 mm ID, 1.0 µm film thickness purchased from Restek, Bellefonte, PA). The temperature program used was as follows: 4 min at 65 °C, then with 8 °C/min to 90 °C, then with 20 °C/min to 155 °C, 1 min at 155 °C then with 20 °C/min to 210 °C and 4 min at 210 °C. Detection and quantification of the analytes was performed in the electron impact positive ion mode and selected ion monitoring (SIM). Concentrations were calculated based on an 8 point calibration curve.

The  $^{13}\text{C}/^{12}\text{C}$  and  $^2\text{H}/^1\text{H}$  isotopic composition of the analytes was determined on a GC-C-IRMS system (Trace GC, coupled to a GC Combustion III interface and a Delta<sup>PLUS</sup>XL isotope-ratio mass spectrometer, ThermoFinnigan MAT, Bremen, Germany) coupled to a purge and trap concentrator (LSC 3100, Tekmar Dohrmann, Mason, OH) and a liquid autosampler (Aquatek 70, Tekmar Dohrmann, Mason, OH). The samples were diluted by adding aliquots of the samples to 40 mL of tap water in autosampler vials, that were closed without headspace with teflon-lined septa and screw caps. Tap water was used since it consistently showed the lowest background contamination levels of volatile organic compounds and thus the least potential for interference with our analytes.<sup>101</sup> 25 mL of a given sample were transferred by the autosampler to the purge vessel and purged for 11 minutes with N<sub>2</sub> (40 mL/min), yielding

sufficient extraction efficiencies for a reproducible measurement of carbon isotopic signatures (Chapter 3). After extraction the analytes were transferred via the cryofocussing unit kept at  $-120\text{ }^{\circ}\text{C}$  to a deactivated GC guard-column ( $1\text{ m} \times 0.32\text{ mm}$  I.D., BGB, Anwil, Switzerland). The chromatographic separation of the analytes was achieved on a RTX-VMS capillary column ( $60\text{ m} \times 0.32\text{ mm}$  I.D.,  $1.8\text{ }\mu\text{m}$  film thickness, Restek, Bellefonte PA) using the following temperature program: 2 min at  $45\text{ }^{\circ}\text{C}$ , then to  $100\text{ }^{\circ}\text{C}$  with  $14\text{ }^{\circ}\text{C}/\text{min}$ , then to  $210\text{ }^{\circ}\text{C}$  with  $20\text{ }^{\circ}\text{C}/\text{min}$  and 4 min at  $210\text{ }^{\circ}\text{C}$ . After chromatographic separation, the analytes were combusted at  $940\text{ }^{\circ}\text{C}$  in the presence of a Cu/Ni catalyst to  $\text{CO}_2$  for the determination of carbon isotope ratios. In order to guarantee reproducible carbon isotopic signatures, the catalyst was reoxidized after  $\sim 40$  samples (Chapter 3). External standards of known carbon isotopic composition were stored and measured under the same conditions as the unknown samples, to allow to correct for potential isotopic fractionation due to the handling and extraction of the samples. Hydrogen isotopic determination was achieved by pyrolyzing the analytes at  $1400\text{ }^{\circ}\text{C}$  after chromatographic separation.

## 5.3 Results and Discussion

### 5.3.1 Microbial Reductive Dehalogenation

As can be seen from Figure 5.2, *dehalospirillum multivorans* completely degraded PER to *cis*-DCE via TCE in less than 48 hours. No other chlorinated degradation products were observed during the reaction. The dehalogenation of TCE was slightly faster than the one of PER. After a short lag phase ( $\sim 5\text{ h}$ ) the reaction started and first degradation products could be observed. The low concentrations of initially present *cis*-DCE are due to the fact, that the microorganism was grown on PER prior to this experiment and hence produced *cis*-DCE which was transferred to the reaction vials by inoculating the reaction vials. The isotopic data corroborate the source of this "contamination", because the isotopic signature of *cis*-DCE corresponds to the one of PER used in the culture of the organism as well as for the start of the reaction. The isotopic fractionation of PER and TCE differed strongly. While the isotopic signatures of PER varied only slightly, TCE was subject to a large fractionation which also explains the depletion in  $^{13}\text{C}$  of *cis*-DCE during both experiments. At the end of the reaction the  $\delta^{13}\text{C}$  of *cis*-DCE corresponded to the one of the initially spiked PER ( $-26.96 \pm 0.07\text{‰}$ ) and TCE ( $-31.72 \pm 0.14\text{‰}$ ), respectively. The slight isotopic fractionation of PER on the one hand and the important

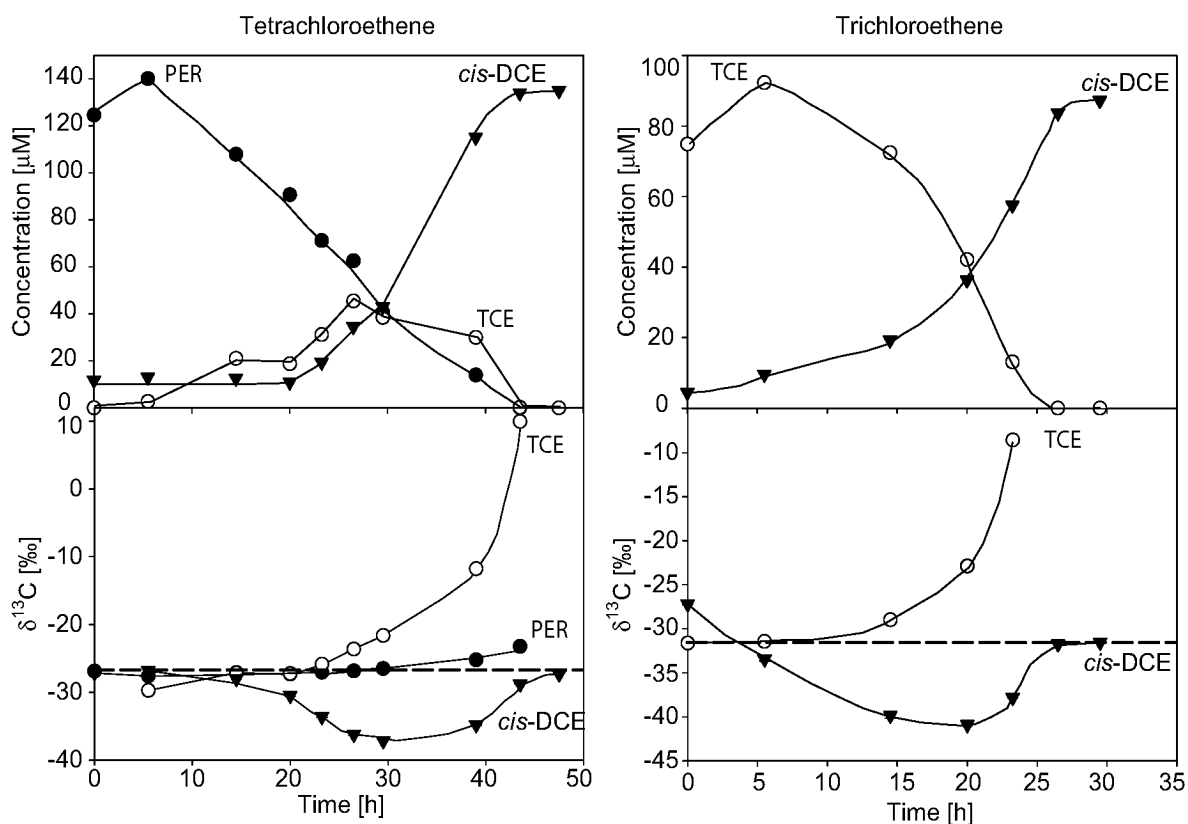


**Figure 5.2: Time Courses of Concentrations and Isotopic Signatures during the Microbial Dehalogenation of PER and TCE.** On the left hand side the concentrations and isotopic signatures of PER (filled circles), TCE (open circles) and *cis*-DCE (filled triangles) from a PER-experiment are plotted. On the right hand side data for TCE (open circles) and *cis*-DCE of a vial initially spiked with TCE are shown. The dashed line in the lower graphs represents the initial  $\delta^{13}\text{C}$ -value of the spiked PER and TCE, respectively.

isotopic enrichment of TCE on the other hand, resulted in an enrichment in  $^{13}\text{C}$  of TCE compared to its parent compound PER. Hence, the argument raised in Chapter 3.3.5, in favor of the absence of *in situ* degradation of TCE to *cis*-DCE, is only valuable in conjunction with the absence of isotopic fractionation with increasing distance from the contamination source and the fact that no degradation product of *cis*-DCE could be detected.

In order to determine the isotopic fractionation of PER and TCE, respectively observed in the replicate experiments, the natural logarithm of the remaining fraction (e.g.,  $f = [\text{PER}]_t / [\text{PER}]_0$ ) was plotted against  $\ln((\delta^{13}\text{C}_t + 1000) / (\delta^{13}\text{C}_0 + 1000))$ . Since the determined fractionation is so low, causing only changes of 1 to 2‰ during the course of the reaction, and the precision of the isotopic determination ( $\sim 0.3\text{‰}$ ), a significant fractionation was found in three out of four PER replicates. The Rayleigh plots for the TCE and PER data are shown in Figure 5.3. The reported  $\epsilon$  correspond to the slope of the regression of these plots. In the case of PER data from the three replicates that showed significant fractionation were used, for TCE two  $\epsilon$ -factors are reported, the lowest one corresponds to

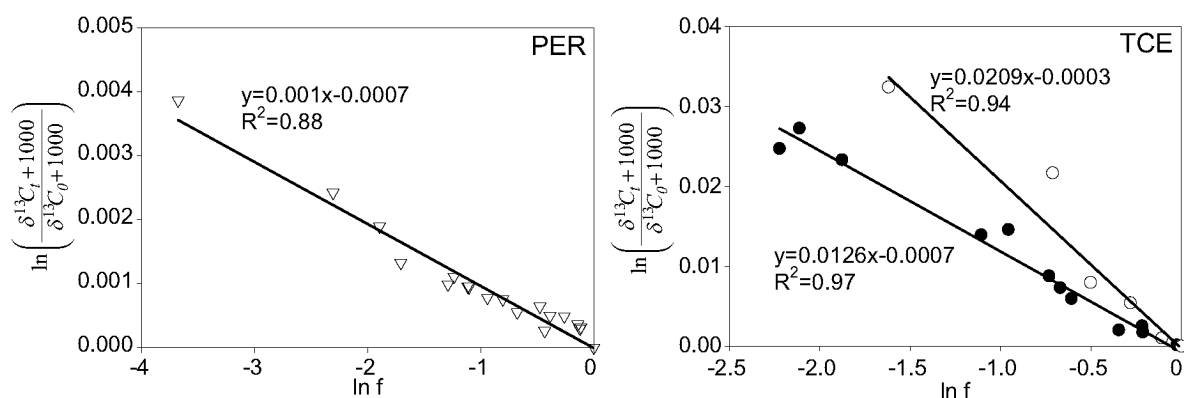


**Figure 5.3: Rayleigh Plots for PER and TCE Microbial Dehalogenation.** The Rayleigh plot of the three PER replicates that showed measurable fractionation is shown in the left graph. The right graph shows the results from the TCE experiment, three replicates (filled circles) showed a significantly lower fractionation than the fourth one (open circles).

the results of three out of four replicates, whereas the higher one corresponds to the replicate which showed a significantly higher fractionation.

The isotopic signatures during the reactions followed a Rayleigh-type behavior. The enrichment factor ( $\epsilon$ ) for PER was  $-1.02 \pm 0.06\text{‰}$  or even not detectable in one replicate. Compared to reported PER isotopic enrichment factors ( $-2\text{‰}^{10}$  to  $-5.5\text{‰}^{39}$ ), this  $\epsilon$  is very low. Conversely, the observed TCE isotopic enrichment ( $-12.6 \pm 0.5\text{‰}$ ) lies in the upper range of reported TCE isotopic enrichment factors for microbial reactions ( $-2.5\text{‰}^{34}$  to  $-13.8\text{‰}^{39}$ ). One TCE replicate experiment showed an even a larger isotopic enrichment ( $-20.9 \pm 2.4\text{‰}$ ).

The kinetics of the microbial reaction did not follow a pseudo-first order model, indicating that the microorganisms were able to grow during the experiment, leading to an increase in observed substrate consumption over time. Due to this fact, the observed course of concentrations and isotopic signatures could not be predicted by the model proposed by Hunkeler et al.<sup>41</sup>

### 5.3.2 Abiotic Reductive Dehalogenation in the Presence of FeS

As can be seen from Figure 5.4, the abiotic reaction of the chlorinated ethenes was much slower as compared to the dehalogenation by *dehalospirillum multivorans* under the chosen environmental conditions. However, a significant concentration decrease as well as an enrichment in  $^{13}\text{C}$  in the remaining fraction of the parent compound compared to the control samples was observed. The reaction kinetics of PER ( $1.04 \cdot 10^{-3} \text{ h}^{-1}$ ) were slightly higher than the ones for TCE ( $7.5 \cdot 10^{-4} \text{ h}^{-1}$ ), whereas the

pseudo-first order rate constants reported in the literature are higher for TCE ( $1.49 \cdot 10^{-3} \text{ h}^{-1}$ ) than for PER ( $5.7 \cdot 10^{-4} \text{ h}^{-1}$ )<sup>133</sup>..

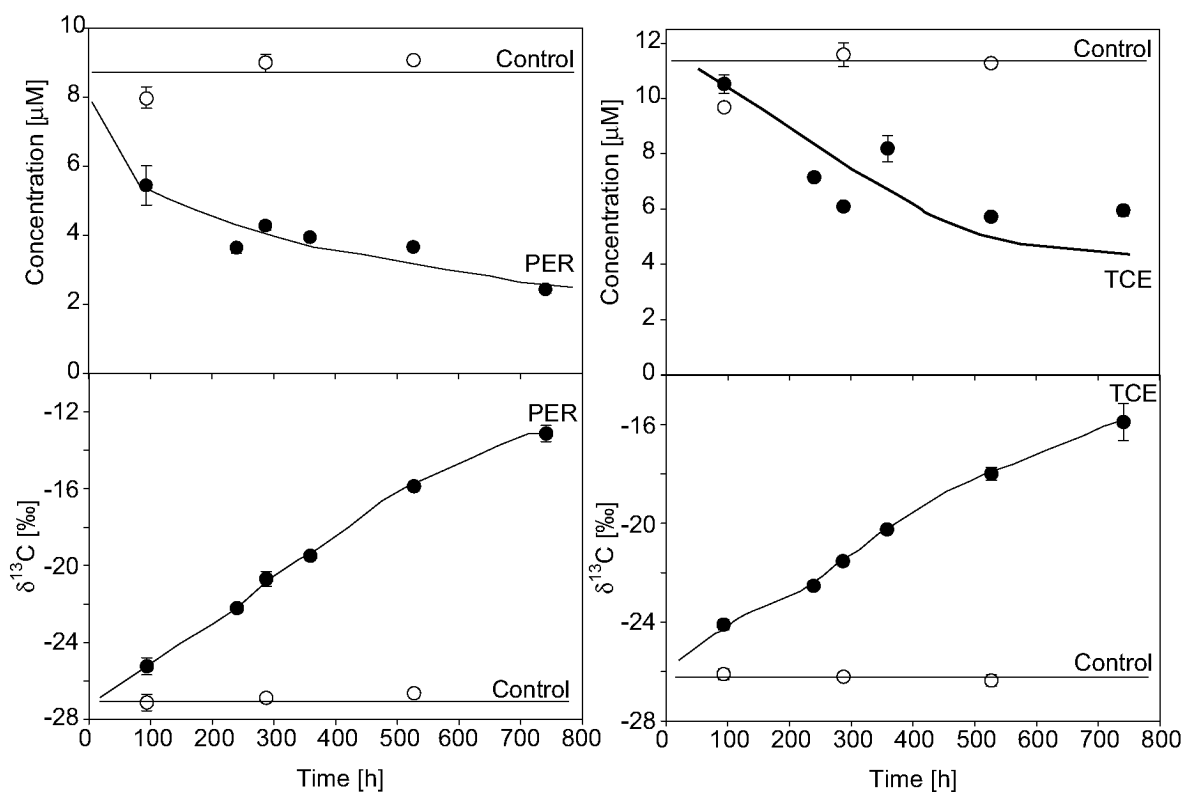


**Figure 5.4: Course of Concentrations and Isotopic Signatures during the Abiotic Dehalogenation of PER and TCE.** On the left side, the results of the PER degradation in the presence of FeS (filled circles) and of the control experiment (open circles) are shown. The course of concentrations and isotopic compositions in the TCE experiment are shown on the right side. No degradation products could be found by the used analytical methods, during both experiments.

The isotopic fractionations during these preliminary experiments also followed a Rayleigh-type behavior. The abiotic reductive dehalogenation of PER was linked to a significantly stronger isotopic enrichment ( $\epsilon = -14.7\text{‰}$ ) as compared to the microbial degradation. The fractionation of TCE ( $\epsilon = -9.6\text{‰}$ ) was less pronounced than for PER and slightly lower than  $\epsilon$  for the dehalogenation by *dehalospirillum multivorans*, but within the range of other enrichment factors reported for microbial reductive dehalogenation. Different isotopic enrichments of TCE during the reductive dehalogenation ( $\epsilon = -4.8\text{‰}$ <sup>35</sup>;  $\epsilon = -8.6\text{‰}$ <sup>27</sup>;  $\epsilon = -16.7\text{‰}$ <sup>149</sup>) have been reported. Hence, it seems possible to differentiate between abiotic and microbial reduction of PER based only on  $^{13}\text{C}$ -isotopic fractionation, while this distinction is not possible for TCE using  $^{13}\text{C}$ -data. One would expect that the dehalogenation step is associated with the same intrinsic kinetic isotope effect, hence, the difference between the isotopic enrichment observed during the microbial degradation of TCE and PER, might be due to a different “commitment to catalysis” of the corrinoid-like

enzyme for the different substrates. Differences observed during the abiotic degradation, however, must be linked to differing positions of the transition states on the reaction coordinate (see also Chapter 4)

Reported degradation products of PER as well as TCE in presence of FeS are acetylene and *cis*-1,2-dichloroethene.<sup>133,141</sup> During this experiment, *cis*-DCE was not found at significant extent and acetylene could not be detected due to the employed analytical methods. Hence, a further interpretation of the differences in isotopic enrichment based on <sup>13</sup>C-analysis could not be made. In the case of the TCE experiment, the reaction slowed down, which might indicate a loss of reductive sites or a change in reaction mechanism, similar to the observations made during the reductive dehalogenation of CCl<sub>4</sub> by Fe(0) sorbed to different iron-containing minerals (see Chapter 4).

### 5.3.3 Hydrogen Isotopic Data of Dehalogenation Products

In a preliminary degradation experiment with *dehalospirillum multivorans* as well as in the replicates spiked with PER, hydrogen isotopic data were collected in addition to stable carbon isotopic signatures of the analytes. The preliminary results of this investigation are shown in Table 5.1.<sup>1</sup>

**Table 5.1: Compound-Specific Hydrogen Isotopic Data of Degradation Products and Bulk H<sub>2</sub>O**

Experiment	$\delta^2\text{H}$		
	TCE [‰ vs VSMOW]	<i>cis</i> -DCE [‰ vs VSMOW]	H <sub>2</sub> O [‰ vs VSMOW]
Microbial 1	n.d. <sup>a</sup>	-203 ± 19	-72.2 ± 2.4
Microbial 2	-111 ± 11	-183 ± 23	-68.5 ± 4.4
Microbial 3	-119 ± 33	-165 ± 43	-72.8 ± 4.2
Microbial 4	-118 ± 6	-168 ± 16	-62.5 ± 7.3
Microbial 5	n.d. <sup>a</sup>	n.d. <sup>a</sup>	-71.3 ± 2.5
Microbial 6	-123 <sup>b</sup>	-160 ± 37	-68.3 ± 4.8
Standard	+596 ± 91	+314 ± 34	n.d. <sup>a</sup>

a. Not determined.

b. n=1

The high standard deviations are most probably due to the high chlorine content of the analytes, potentially producing HCl in the pyrolysis

1. Additional hydrogen isotopic data collected during a second experiment with replicates spiked either with PER or TCE can be found in Appendix A3.



step. This effect may lead to high deviations, due to an unreproducible yield of HCl formation in the reactor. This effect did, however, not produce a drop in sensitivity nor did it influence the determination of hydrogen isotopic signatures of not chlorinated compounds. This could be verified, because the mixtures of the chlorinated standards also contained benzene and toluene. The determined isotopic signatures of the latter two compounds presented a standard deviation of less than 5‰, which corresponds to the specified reproducibility of the mass spectrometer. Despite this variability in the hydrogen isotopic data determination, the isotopic signatures of the standards deviated significantly from the ones of TCE and *cis*-DCE produced during the degradation of PER. This shows that hydrogen isotopic measurements are an appropriate tool to distinguish between TCE and *cis*-DCE produced during *in situ* degradation of PER and additional contamination sources of the lower chlorinated ethenes. In all microbial batches, TCE and *cis*-DCE were depleted in <sup>2</sup>H compared to the bulk H<sub>2</sub>O in the reaction vial. This depletion further increased in the dechlorination step from TCE to *cis*-DCE. TCE was depleted by  $50 \pm 6\%$  compared to the bulk water, whereas the depletion of *cis*-DCE was  $-107 \pm 16\%$ . The observed depletion of deuterium relative to the bulk was in the same order of magnitude, as previously observed for the depletion occurring during the biosynthesis of lipids (113 - 376‰).<sup>150</sup> The authors conclude in the latter study, that high variability of hydrogen isotopic compositions of lipids from different compound classes, may be due to isotopically distinct pools of NADPH used in hydrogenation during biosynthesis.

## 5.4 Conclusions

This investigation addressed two major issues concerning the use of compound-specific isotope analysis in contaminant hydrology: (i) prospects and limitations in the identification of the type of reaction responsible for *in situ* degradation of chlorinated ethenes based on carbon isotopic fractionation and (ii) use of hydrogen isotopic data to infer the source of TCE found in a contaminated aquifer.

Under sulfate-reducing conditions, tetrachloroethene and trichloroethene may undergo abiotic as well as microbial reductive dehalogenation. In the case of PER these two different degradation mechanisms could be differentiated based on the observed fractionation of stable carbon isotopes during the reaction. The <sup>13</sup>C-isotopic fractionation of TCE, however, did not show a difference that would allow a distinction between abiotic and microbially mediated reactions at a contaminated field site

under the given environmental conditions. However, it is important to note, that in this investigation a pure culture of a dehalogenating microorganism was used. At a contaminated field site it is more likely that a microbial community would be involved in the reductive dehalogenation. Since the enrichment factor determined in this study is rather high compared to others reported for the microbial reductive dehalogenation of TCE, the identification of the nature of the process leading to TCE dehalogenation might still be possible.

It has been shown that the degradation products of the reductive dehalogenation are typically depleted in  $^2\text{H}$  compared to the surrounding  $\text{H}_2\text{O}$ . Since chemically manufactured chlorinated ethenes are generally strongly enriched in  $^2\text{H}$ , the determination of stable hydrogen isotope signatures is a promising tool for the identification of the sources of TCE (e.g. initially present contaminant or degradation product of PER dehalogenation) found in a contaminated aquifer.

# **DETECTION OF ANAEROBIC MTBE DEGRADATION AND HINTS ON REACTION MECHANISM USING COMPOUND-SPECIFIC STABLE ISOTOPE ANALYSIS.**

*Compound-specific stable isotope analysis was used to assess the fate of the gasoline additive methyl tert-butyl ether (MTBE) and its major degradation product tert-butanol (TBA) in a groundwater plume originating from an industrial disposal site. Due to the widespread contaminant plume, the existence of multiple MTBE sources, the presence of numerous other organic pollutants, and the complex hydrological regime at the site, the extent of MTBE degradation could not be assessed by a classical mass balance approach. However, fractionation factors reported for carbon and hydrogen isotopes during biodegradation of MTBE under oxic and anoxic conditions, respectively, could be used to determine both the nature and the extent of in situ biodegradation along the contaminant plume(s). The isotopic signatures of MTBE increased from -26.4‰ (carbon) and -73.1‰ (hydrogen) near the source regions to +40.0‰ (carbon) and +60.3‰ (hydrogen) downgradient of the major source indicating significant biodegradation. In contrast, carbon isotopic signatures of TBA remained almost invariant throughout the plume, suggesting the absence of TBA-degradation. The isotopic data suggest that additional removal process(es) such as evaporation occurred to match the measured MTBE-concentrations. A reevaluation of isotopic fractionation data reported for anaerobic and aerobic biodegradation of MTBE in terms of intrinsic kinetic isotope effects ( $^{12}\text{k}/^{13}\text{k}$  and  $^{\text{H}}\text{k}/^{\text{D}}\text{k}$ , respectively) rather than isotopic enrichments suggests that anaerobic biodegradation occurs most likely via an  $\text{S}_{\text{N}}2$ -type reaction mechanism.*

## 6.1 Introduction

With an annual production of 21 million tons in 1999,<sup>151</sup> MTBE is among the organic chemicals with the highest production volume worldwide. Among the various applications, the use as gasoline additive is by far the most important (>98%).<sup>152</sup> In contrast to the United States where oxygenates are used to improve the combustion processes, MTBE is used in Europe mainly as octane enhancer as a replacement of the banned alkyl lead compounds. Despite its relatively recent introduction, MTBE has become one of the most frequently detected groundwater contaminants.<sup>59</sup> Sources of contamination include point sources such as leaking underground storage tanks or accidental spills as well as diffuse inputs (e.g. precipitation and runoff water).<sup>60,153,154</sup> Whereas diffuse inputs can lead to background concentrations of MTBE in groundwater in the low  $\mu\text{g/L}$  range, local spills cause MTBE concentrations of up to several hundreds of  $\text{mg/L}$ .<sup>155</sup>

Because of its limited sorption to the aquifer material ( $K_{\text{ioc}} \sim 11$ )<sup>56,154</sup> and its limited biodegradability<sup>58,156,157</sup>, MTBE tends to form widespread contaminant plumes in the groundwater. Under oxic conditions, the biodegradation of MTBE has been observed with pure cultures.<sup>57,158-161</sup> Some microorganisms are only capable to degrade MTBE cometabolically in presence of short chain-alkanes.<sup>162-164</sup> It has, however, also been shown that the presence of other gasoline components such as BTEX may slow down or even completely inhibit the degradation of MTBE.<sup>165</sup> In the absence of oxygen, MTBE degradation has been observed in several microcosms under denitrifying conditions,<sup>166,167</sup> sulfate reducing conditions,<sup>166,168</sup> iron reducing conditions<sup>77,166,169</sup> and methanogenic conditions.<sup>167,170,171</sup> In laboratory experiments, these microcosms often showed significant lag phases (several 100 days) before MTBE degradation occurred.<sup>168,169</sup> The degradation rates determined under methanogenic conditions were very low ( $2.2 - 5.0 \text{ y}^{-1}$  in the field,  $3.5 \text{ y}^{-1}$  in microcosms with added alkylbenzenes, and  $3 \text{ y}^{-1}$  in unamended microcosms).<sup>172</sup> However, the reaction mechanisms prevailing under anoxic conditions have not been identified so far. O'Reilly et al.<sup>173</sup> have shown that MTBE may be hydrolyzed by diluted aqueous acid (HCl at pH 1 to 3), and speculated that MTBE may be susceptible to enzyme-catalyzed hydrolysis.

*Tert*-butanol (TBA) is considered as the major degradation product of MTBE under oxic as well as anoxic conditions. Compared to MTBE, little is known about the fate of TBA.<sup>174</sup> TBA has frequently been found to accumulate and is therefore generally used in field studies to verify in-situ degradation of MTBE. A few studies, however, reported degrada-

tion of MTBE without significant accumulation of TBA.<sup>36,175,176</sup> Bradley et al.<sup>176</sup> have shown that under oxic conditions, TBA was degraded more rapidly than MTBE, and that under denitrifying and sulfate-reducing conditions the extent of TBA mineralization was comparable to the one of MTBE.

The potential lack of TBA accumulation and the fact that TBA may be present as an impurity in the spilled gasoline<sup>77,101</sup> together with extended plumes complicate the assessment of the *in-situ* degradation of MTBE, even in cases in which the conditions are well known and in which a high resolution of sampling wells across the contaminated aquifer is available.<sup>6,177</sup> Hence in addition to concentration monitoring, alternative methods are needed to assess the source and fate of MTBE and TBA at a given field site. Compound-specific isotope analysis (CSIA) has been used at contaminated field sites to better understand the behaviour of different organic compounds such as chlorinated solvents,<sup>26,29,51,52,178,179</sup> BTEX<sup>47,48</sup> and recently also MTBE<sup>42,53</sup> in contaminant plumes and has proven to be a promising tool. Due to the kinetic isotope effect (KIE) which may occur during chemical reactions as well as during biodegradation, the isotopic signature of the parent compound may change during the reaction. Because molecules containing light isotopes in the reacting chemical bond, react faster than the molecules with heavy isotopes, the remaining fraction of the parent compounds becomes more and more enriched in molecules containing the heavy isotopes.

In the past years the isotopic fractionation during the degradation of MTBE and TBA has been studied by different groups. For the *aerobic* degradation of MTBE, Hunkeler et al.<sup>36</sup> determined carbon isotopic enrichment factors  $\epsilon$  between  $-1.5 \pm 0.1\text{‰}$  and  $-2.0 \pm 0.1\text{‰}$ . The enrichment factors did not significantly vary between different microcosms using MTBE as sole carbon source and cometabolically with 3-methylpentane as substrate. Similar carbon fractionation factors for the aerobic biodegradation of MTBE in microcosms enriched from contaminated sites as well as for a pure culture (strain PM1) have been observed by Gray et al.<sup>24</sup> In microcosm experiments Gray et al. found enrichment factors between  $-1.5 \pm 0.1\text{‰}$  and  $-1.8 \pm 0.1\text{‰}$  and in experiments with the pure strain  $\epsilon$  values ranged from  $-2.0 \pm 0.1\text{‰}$  to  $-2.4 \pm 0.3\text{‰}$ . Although these isotopic fractionations are relatively small, they differ significantly from those caused by physical processes such as organic phase/gas phase partitioning ( $0.50 \pm 0.15\text{‰}$ ), aqueous phase/gas phase partitioning ( $0.17 \pm 0.05\text{‰}$ ) and organic phase/aqueous phase partitioning ( $0.18 \pm 0.24\text{‰}$ ).<sup>36</sup> Gray et al. also determined hydrogen enrichment factors ranging from

$-29 \pm 4\text{‰}$  to  $-66 \pm 3\text{‰}$  in the microcosm experiments but only from  $-33 \pm 5\text{‰}$  to  $-37 \pm 4\text{‰}$  in the experiments with strain PM1.<sup>24</sup> The larger but less reproducible hydrogen isotopic fractionation was proposed a sensitive qualitative indicator of *in situ* degradation whereas the more reproducible carbon isotopic fractionation is best suited for the quantification of the observed biodegradation. During cometabolic degradation of TBA, a carbon isotopic enrichment ( $\epsilon$ ) of  $-4.21 \pm 0.07\text{‰}$  was observed.<sup>36</sup> TBA degradation in the field was monitored using carbon isotopes in a study by Day et al.<sup>180</sup> In this study the  $\delta^{13}\text{C}$  values of TBA changed from  $-28.6\text{‰}$  in the source zone to  $-22\text{‰}$  with decreasing TBA concentrations in a mainly anoxic plume.

Under *anoxic* conditions it has recently been shown that carbon isotopic enrichments during MTBE degradation were more pronounced ( $\epsilon = -8.1 \pm 0.85\text{‰}$  in the field and  $\epsilon = -9.2 \pm 5.0\text{‰}$  in microcosms)<sup>42</sup> as compared to aerobic biodegradation. If representative, this difference could be used to identify the nature of biodegradation in the field, and may point to different reaction mechanisms involved. Furthermore, in a field investigation, it has been shown that the hydrogen isotopic fractionation under anaerobic conditions is less pronounced than under aerobic conditions ( $\epsilon = -11.4\text{‰}$ ).<sup>53</sup> In both studies the  $\delta^{13}\text{C}$  values of TBA have also been determined but no significant fractionation was observed. In the latter field study by Kuder et al. the TBA isotopic signature did even show a slight enrichment with heavy isotopes compared to the initial MTBE.<sup>53</sup> A similar observation was made by Hunkeler et al. in laboratory experiments.<sup>36</sup> The authors explain this effect by the fact that TBA actually reflects the isotopic composition of the *tert*-butyl group. Since, under oxic conditions, the initial reaction involves the methoxy methyl group which is eliminated in the step from MTBE to TBA (see Figure 6.1) one can not expect to see a carbon isotopic fractionation between parent compound and product.

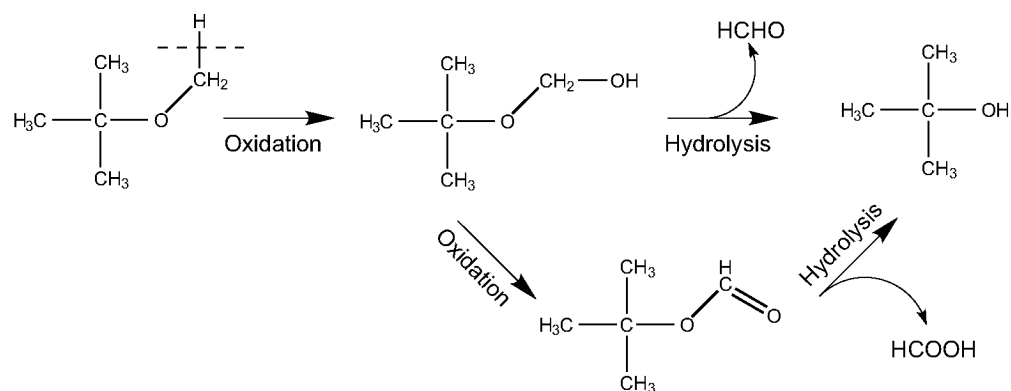


**Figure 6.1: Oxidation of MTBE by Monooxygenases.** In presence of oxygen the supposed degradation pathway from MTBE to TBA starts with an oxidation of the methyl group by a monooxygenase.<sup>160,162,181</sup> Tert-butoxy methanol has been proposed as intermediate, that either reacts directly to TBA and formaldehyde or is further oxidized to tert-butyl formate. The dashed line indicates the chemical bond that is broken during the first step of the reaction. Hence an isotopic fractionation would only be expected for the carbon and hydrogen atoms of the methoxy methyl group, whereas the isotopic composition of the tert-butyl group remains unchanged.

In this study, the use of compound-specific stable carbon and hydrogen analysis of MTBE and TBA was used to assess biodegradation at an industrial disposal site. In this particular case the “traditional” mass balance approach for the assessment of biodegradation was hampered by the widespread contamination plume, the existence of multiple contamination sources as well as a complex hydrological regime. The specific carbon and hydrogen isotopic fractionations under oxic and anoxic conditions, that have been reported for the biodegradation of MTBE, were used to assess the nature and the extent of the observed *in situ* biodegradation and to obtain further indications about the reaction mechanisms involved in the anaerobic MTBE degradation.

## 6.2 Experimental Section

### 6.2.1 Site Description

The investigated field site (Figure 6.2) is a former industrial landfill in South America where phenol and MTBE have been disposed in open ponds (mainly PM 01, PM 04 and PM 10). Phenol had been disposed for over 20 years until 1989. Over a span of several years MTBE was used as solvent in chemical synthesis and was also disposed. The major ponds are located on a shallow hill, leading to a radial groundwater flow pattern (Figure 6.2).

The water table varies between 10 and 20 meters below the top soil, the aquifer is shallow (10 - 15 meters), and has a low hydraulic conductivity

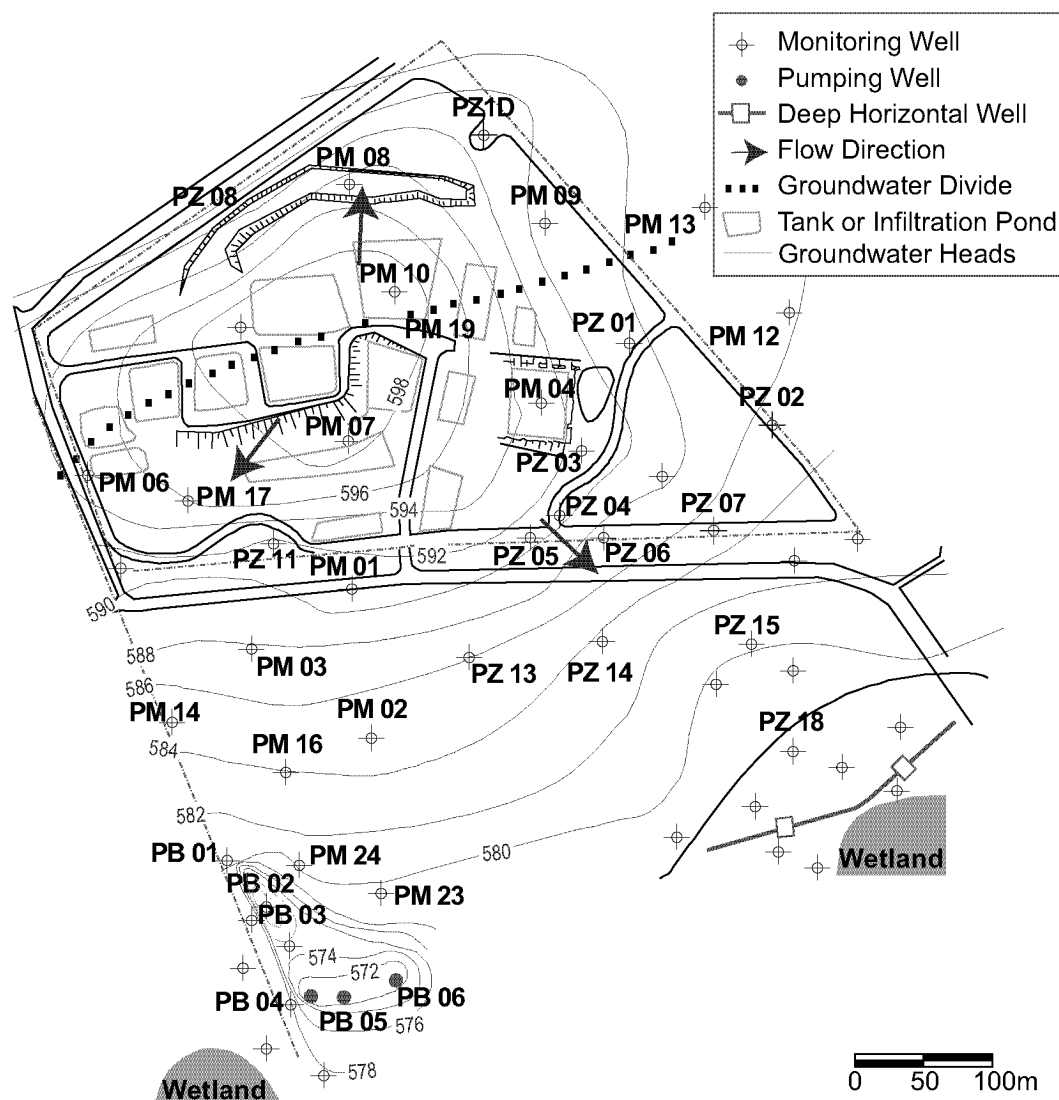


**Figure 6.2: Site Characterization.** Major MTBE sources are located at wells PM 04, PM 10, PM 01 and PM 24. In addition to the known MTBE sources, several other infiltration ponds exist at the site, where phenol among other organic compounds was disposed.

( $10^{-5}$  cm/s). It is confined by an underlying zone of basaltic rock from volcanic origin. This impermeable zone is fractured and, therefore, higher groundwater flows due to preferential flow along these fissures can not be ruled out. The average annual groundwater temperature is between 25 and 30 °C. The assessment of the biodegradation of MTBE is difficult at this particular site, because of the large number of different contamination sources of MTBE, BTEX, phenol and *isopropyl-benzene*. Two wetlands are situated 400 - 600 m downstream of the disposal site. In order to protect these wetlands from contamination, 5 pumping wells and a deep horizontal pumping well have been installed as hydraulic barriers. The installation of these wells has changed the hydrological regime at the site, leading to potentially higher transport velocities of the contaminants. 47 permanent monitoring wells have been installed at the site and are sampled semi-annually. The monitoring wells are not all reaching to



the bottom of the aquifer, hence varying dilution effects during sampling can not be excluded.

### 6.2.2 Sample Collection and Storage

The samples used for this study were taken during two sampling campaigns. Before sampling, the different wells had been prepumped for several hours. Water temperature and pH data were determined on site. Measurements with an oxygen-sensitive electrode on selected samples indicated an oxygen depletion ( $< 1$  mg/L) of the groundwater. The samples for the determination of inorganic parameters were collected in polyethylene flasks, acidified and kept at 4 °C until analysis. Samples for the determination of concentrations and isotopic signatures of MTBE and TBA were filled without headspace into 40 mL glass vials. The vials were closed with teflon-sealed screw caps and stored at 4 °C until analysis.

### 6.2.3 Analytical Methods

Concentrations of MTBE and of its major degradation products TBA and acetone as well as BTEX were determined using direct aqueous injection gas chromatography mass spectrometry (DAI-GC/MS) using the procedure described by Zwank et al.,<sup>101</sup> on a gas chromatograph (GC 8000, Fisons, Manchester, U.K.) coupled to a mass spectrometric detector (single quadrupole MD 800, Fisons, Manchester, U.K.).

In order to achieve a sufficient sensitivity for carbon and hydrogen isotopic analysis, the samples were extracted using a solid-phase microextraction (SPME) procedure.<sup>182</sup> The analytes were extracted for 30 minutes from the samples (to which 4M NaCl was previously added) by directly immersing a Carboxen-PDMS fiber (75  $\mu$ m, Supelco, Bellefonte, PA) into the sample. The fractionation of the carbon isotopic signature caused by this extraction step is very small and highly reproducible ( $-1.5 \pm 0.4\%$ ).<sup>182</sup> During a similar evaluation concerning the influence of the extraction procedure on the hydrogen isotopic signatures of MTBE and TBA, it was found that the  $\delta^2\text{H}$  measurements were also highly reproducible (e.g., the standard deviation of 19 replicate measurements was 7.4%). After extraction the analytes were thermally desorbed for 1 min in the split-splitless injector (270°C) equipped with a deactivated SPME liner. To reduce the peak tailing of the polar analytes, the splitless time was reduced to 0.75 min compared to the SPME extraction procedure described in Chapter 3. The chromatographic separation of the analytes for IRMS was achieved on a gas chromatograph (Trace GC, Thermo Finnigan) equipped with a 60 m  $\times$  0.32 mm Stabilwax fused sil-

ica column (1  $\mu\text{m}$  film crossbonded Carbowax-poly(ethylene glycol) film) purchased from Restek (Bellefonte, PA) with the following temperature program: 2 min at 45°C, then to 90°C at 7.5 °C/min, 2 min at 90 °C, then to 200 °C at 30 °C/min and 6 min at 200 °C. For carbon isotopic measurements the analytes were combusted after separation in a combustion interface (GC Combustion III, Thermo Finnigan MAT, Bremen, Germany) maintained at 940 °C and the resulting CO<sub>2</sub> was analyzed in an isotope ratio mass spectrometer (Delta<sup>PLUS</sup>XL, Thermo Finnigan MAT, Bremen, Germany). The catalyst in the combustion interface was oxidized regularly after ~40 samples. For hydrogen isotopic analysis, the analytes were pyrolyzed at 1400 °C and the resulting H<sub>2</sub> was analyzed in the isotope ratio mass spectrometer. H<sub>3</sub><sup>+</sup> is formed in the ion source of the mass spectrometer, and hence the precise detection at  $m/z = 3$  of HD<sup>+</sup> is hampered. The production of H<sub>3</sub><sup>+</sup> is correlated to the amount of H<sub>2</sub> entering the source and can be corrected with the H<sub>3</sub>-factor. In order to allow a good DH/H<sub>2</sub> determination, a low and stable H<sub>3</sub>-factor is a prerequisite. This factor was determined daily by measuring a set of 9 reference gas peaks of increasing amplitudes. This factor was constant ( $3.21 \pm 0.14$  ppm/nA). In order to verify the reproducibility of the isotopic measurements during one sequence of samples as well as throughout the measurement campaign, external standards of known carbon isotopic signature were measured after 3-5 samples. If not stated otherwise, the isotopic signatures correspond to the average of at least 3 replicate measurements.

#### 6.2.4 Quantification of Biodegradation

For the evaluation of field data, isotopic enrichment factors ( $\epsilon$ ) in permil are determined using the linearized Rayleigh equation (Equation (6-1)). For a more detailed derivation of Equation (6-1) see Appendix A1.1.

$$\ln\left(\frac{\delta^{13}C_x + 1000}{\delta^{13}C_0 + 1000}\right) = \frac{\epsilon}{1000} \cdot \ln f \quad (6-1)$$

where, in this case,  $\delta^{13}C_x$  and  $\delta^{13}C_0$  refer to the carbon isotopic signatures of the MTBE at well  $x$  and in the contamination source, respectively. The average carbon isotopic signature of MTBE from wells PM 01, PM 04 and PM 10 is used as  $\delta^{13}C_0$ .  $f$  is the remaining fraction of the reacting

compound and is defined as the ratio of the MTBE concentration at well  $x$  compared to the source concentration of MTBE:

$$f = \frac{[MTBE]_x}{[MTBE]_0} \quad (6-2)$$

Solving Equation (6-1) for  $f$  yields;

$$f = \left( \frac{\delta^{13}C_x + 1000}{\delta^{13}C_0 + 1000} \right)^{\frac{1000}{\epsilon}} \quad (6-3)$$

which allows to calculate the expected concentration ratio using the determined isotopic signatures, assuming that the difference between  $C_0$  and  $C_x$  is only due to a transformation reaction with a given  $\epsilon$ . Based on this ratio the extent of (bio)degradation ( $B$ ) can be estimated:<sup>46,143</sup>

$$B = (1 - f) \cdot 100 \quad [\%] \quad (6-4)$$

Assuming (i) identical transport processes for TBA and MTBE, (ii) MTBE degradation as the only source of TBA, and (iii) the absence of TBA (bio)transformation, the expected TBA concentration in well  $x$  can be calculated using  $B$  and the MTBE concentration found at this well using Equation (6-5).

$$[TBA]_x = \frac{B}{1 - B} \cdot [MTBE]_x \quad [\mu\text{M}] \quad (6-5)$$

### 6.2.5 Determination of $^{12}\text{k}/^{13}\text{k}$ and $^1\text{k}/^2\text{k}$ Values from Enrichment Factors

Isotopic signatures determined in degradation studies reflect the average isotopic composition over the entire molecule and not only of the atom(s) involved in the reaction. It is, however, the isotopic fractionation of the atom(s) at the reactive position that has to be known (i.e., the intrinsic kinetic isotope effects (KIE)) in order to use this information for mechanistic interpretations. Hence, if molecules contain more than one atom of the element for which isotope fractionation is studied, two different effects must be taken into account. One effect is the “dilution” of the measured isotopic shift due to the presence of atoms of the studied element at non-reacting positions in a molecule. In the case of MTBE oxidation (Scheme 6.1), for example,  $^{13}\text{C}$  and  $^2\text{H}$  isotope fractionation will

occur solely at the methoxy methyl group, whereas the isotopic composition of the *tert*-butyl group will remain unchanged. The elements of that group will, however, contribute to a great extent to the average isotopic signature of the whole molecule, and hence the observed effect will be much smaller than the intrinsic isotope effect occurring at the reactive bond. In a critical review by Elsner et al.<sup>183</sup> these effects are discussed in detail (see also Appendix A1.2). It is proposed to multiply average  $\delta^{13}C_x - \delta^{13}C_0$  values (and  $\delta^2H_x - \delta^2H_0$  values, respectively) with an appropriate factor  $n/x$ , where  $n$  corresponds to the number of atoms of one element present in the molecule and  $x$  corresponds to the number of atoms that are positioned at reactive sites in the molecule. The Rayleigh equation (Equation (6-1)) can then be rewritten:

$$\frac{1000 + \delta^{13}C_0 + \frac{n}{x} \cdot (\delta^{13}C_x - \delta^{13}C_0)}{1000 + \delta^{13}C_0} = f^\varepsilon \quad (6-6)$$

Second, intramolecular competition has to be taken into account. Depending on the symmetry of the molecule, it is possible that the investigated element is present at  $z$  chemically equivalent positions in the molecule. In the case of the oxidation of MTBE, this is the case for the 3 hydrogen atoms of the methoxy methyl group. The intrinsic kinetic isotope effect KIE is defined by the ratio between the reaction rate of the light isotope and the heavy isotope (e.g.,  $^Hk/^Dk$  and  $^{12}k/^{13}k$  for hydrogen and carbon KIEs, respectively) and can be obtained by solving Equation (6-6) for  $\varepsilon$  and using Equation (6-7) (see Elsner et al.).<sup>183</sup>:

$$\frac{1}{KIE} = \frac{^{13}k}{^{12}k} = z \cdot \frac{\varepsilon}{1000} + 1 \quad (6-7)$$

Hence, using the corrections proposed by equations (6) and (7), it becomes possible to obtain intrinsic kinetic isotope effects from previously published data of  $f$ ,  $\delta^{13}C$  and  $\delta^2H$ . This allows for comparing isotopic effects for different substrates in a given reaction mechanism and use the broad collection of data on isotopic enrichments from recent environmental studies together with the knowledge about intrinsic isotope

effects from chemical and biochemical studies. In the case of an enzymatic reaction, Equation (6-7) corresponds to:

$$\frac{1}{KIE} = \frac{{}^{13}(V/K_m)}{{}^{12}(V/K_m)} = z \cdot \frac{\varepsilon}{1000} + 1 \quad (6-8)$$

where  $V$  and  $K_m$  correspond to the maximum velocity and the Michaelis-Menten constant, respectively. For the reevaluation of literature data the corresponding datasets were obtained from illustrations found in the cited publications using an Excel™-based digitizing software (GrabIt! XP, Datatrend Software, Raleigh, NC).

### 6.2.6 Complete MTBE-Hydrolysis under Acidic Conditions

In order to evaluate whether the isotopic signature of the *tert*-butyl group of MTBE is significantly different from the isotopic composition of the methoxy methyl group, MTBE of known isotopic composition was hydrolyzed to TBA under acidic conditions. O'Reilly et al. postulated that the acid catalyzed hydrolysis of MTBE proceeds via the reaction mechanism, depicted in Figure 6.3.<sup>173</sup>

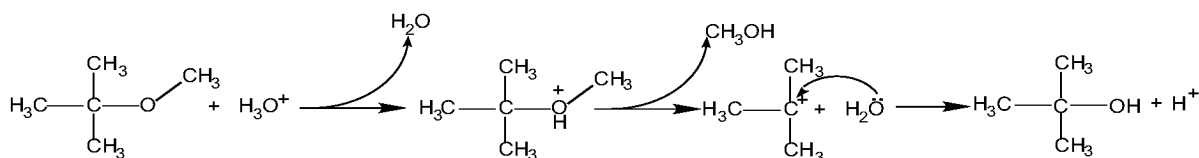


Figure 6.3: Postulated Reaction Mechanism of the Acid Catalyzed MTBE Hydrolysis.

Provided that MTBE is completely transformed into TBA as unique product, the carbon isotopic signature of TBA corresponds to the one of the *tert*-butyl group of MTBE. Preliminary experiments have been carried out to (i) determine the kinetics of the reaction and (ii) to verify that MTBE is completely transformed to TBA and that TBA stays stable under the given conditions.

The hydrolysis reaction was carried out in 20 mL headspace vials sealed with teflon lined crimp caps. The vials were filled with 17 mL deionized water and 1.7 mL of concentrated HCl were added. The vials were placed in the agitator of a CombiPAL Autosampler (CTC, Zwingen, Switzerland) heated at 60 °C, after an equilibration time of 1 hour 0.5  $\mu$ L of a pure MTBE standard were spiked into the reaction vials. To determine the reaction kinetics of this reaction, 75  $\mu$ L of sample were taken at appropriate time intervals from the reaction vials and neutralized with

NaOH. A control reaction at neutral pH was sampled in the same way. Instead of adding NaOH, the control samples were diluted accordingly with distilled water. The concentrations of MTBE and TBA were measured using DAI-GC/MS. The mass spectrometer was acquiring in the scan mode ( $m/z$  40-250) in order to verify that no additional products formed during hydrolysis. The high methanol concentrations produced during the reaction, led to an overestimation of the TBA concentrations, due to peak broadening, but since no additional products were formed, complete MTBE hydrolysis can be expected. During this preliminary experiment it was shown that (i) MTBE was hydrolyzed with an observed pseudo-first order constant of  $-0.0233 \text{ min}^{-1}$  ( $R^2=0.98$ ) corresponding to a half life of 30 min (at pH 0 and 60 °C), (ii) that MTBE was completely transformed to TBA and MeOH, and that (iii) TBA was stable under the experimental conditions. The reaction was slightly faster as would be expected from the rates and activation energies determined by O'Reilly et al. ( $t_{1/2} = 41 \text{ min}$ ) (29). For the isotopic determination of the MTBE *tert*-butyl group, one vial was spiked with 1  $\mu\text{L}$  of pure MTBE of known isotopic signature and one vial was spiked with 200  $\mu\text{L}$  of a methanolic solution (1:10) of a field sample from the MTBE source that contained no TBA. In order to assure complete hydrolysis, the vials were kept at 60 °C for 5 hours. After hydrolysis the samples were neutralized using NaOH (1M) and kept at 4°C until analysis. Carbon isotopic compositions were determined using purge and trap extraction coupled on-line to a GC-IRMS system following a method described in Chapter 3.

## 6.3 Results and Discussion

### 6.3.1 Qualitative Assessment of *In Situ* Biodegradation of MTBE

As can be seen from Figure 6.4, the MTBE plume at the contaminated site was very widespread (over a length of >500 m) with a maximum concentration of 1.7 g/L (aqueous solubility of MTBE = 48 g/L)<sup>56</sup> at the major source zone. In this region TBA concentrations were small but increased with further distance from the source, suggesting that TBA was originally not present as contaminant but was formed by biodegradation of MTBE. Since the site was contaminated as a result of a MTBE disposal from chemical manufacturing and not as a result of a gasoline spill, the absence of TBA as “impurity” of the MTBE might be explained by the fact that the MTBE used as solvent in organic synthesis had a higher purity than the MTBE used for gasoline blending. The highest TBA con-

centrations (>22.6 mg/L) were found downstream of the highest MTBE concentrations. The distribution of MTBE as well as of TBA concentrations (i.e., steep increases of MTBE concentrations with further distance from the main source area) can only be explained by assuming a multiple source contamination. This assumption is supported by the isotopic signatures of MTBE. An average source signature for MTBE of  $-26.37 \pm 0.12\text{‰}$  for carbon and  $-73.1 \pm 7.1\text{‰}$  for hydrogen was found in wells PM 01, PM 04 and PM 10 (see Figure 6.2 for the location of the wells), supporting the hypothesis based on concentration data that at least 3 different contamination sources of MTBE were present.

Table 6.1 shows the determined concentrations and carbon as well as hydrogen isotopic signatures of MTBE and TBA. A significant shift in the carbon and hydrogen isotopic composition of MTBE with increasing distance from the 3 distinct sources can be identified, leading to  $\delta^{13}\text{C}$  values of up to  $+40.04\text{‰}$  vs VPDB and  $\delta^2\text{H}$  of up to  $+60.3\text{‰}$  vs VSMOW. Based on concentration data, an additional source at well PM 24 seemed likely, the isotope data, however, are significantly different from the average isotopic signature found at the source wells. Furthermore, while the MTBE concentrations were highest at well PM 24, it was significantly enriched in  $^{13}\text{C}$  compared to the wells downstream that show lower concentrations. These observations might be due to preferential flow patterns linked to the important change in the hydrological regime due to the intense pumping (in wells PB 04, PB 05 and PB 06). As opposed to MTBE, the carbon isotopic signature of TBA was more or less invariable between the different sampling wells ( $-25.02 \pm 0.75\text{‰}$ ) with the exception of well PM 09 ( $-20.98 \pm 0.09\text{‰}$ ) but slightly enriched in  $^{13}\text{C}$  compared to the source MTBE. This effect has already been observed in laboratory as well as in field studies,<sup>36,53</sup> indicating that the *tert*-butyl group of MTBE is *not* directly involved in the reaction.

In order to verify this hypothesis, first experiments were carried out to determine the isotopic composition of the *tert*-butyl group. As described in the experimental section, an MTBE standard ( $\delta^{13}\text{C} = -28.13 \pm 0.15\text{‰}$ ) was *completely* hydrolysed to TBA, and the isotopic signature of the produced TBA i.e. of the *tert*-butyl group of the parent MTBE, was measured yielding a  $\delta^{13}\text{C}$  of  $-25.49 \pm 0.10\text{‰}$ . As a consequence the  $\delta^{13}\text{C}$  of the methyl group can be calculated based on an "isotopic mass balance" ( $\delta^{13}\text{C} = -36.35 \pm 1.11\text{‰}$ ). An identical transformation experiment was carried out with a diluted sample from the MTBE source at the investigated field site to enable an interpretation of the isotopic signature of TBA found and to test the assumption that TBA is recalcitrant at this site.

Unfortunately, due to chromatographic coelution of the formed TBA with other contaminants in the highly polluted sample and/or their hydrolysis products, the isotopic signature of TBA and hence of the *tert*-butyl group could not yet be determined.

The hydrogen isotopic signature of TBA did not show a consistent trend. This might be due to a variable hydrogen isotopic signature of the *tert*-butyl group of the MTBE disposed over the years. Alternatively, hydrogen exchange at the hydroxyl group of TBA might be significant.



**Table 6.1: Concentrations and Isotopic Signatures of MTBE and TBA.**

Sampling Well	MTBE			TBA		
	Conc. [μg/L]	$\delta^{13}\text{C}$ [‰ vs VPDB]	$\delta^2\text{H}$ [‰ vs VSMOW]	Conc. [μg/L]	$\delta^{13}\text{C}$ [‰ vs VPDB]	$\delta^2\text{H}$ [‰ vs VSMOW]
PM 04 <sup>a</sup>	1700000	-26.35 ± 0.73	-71.3 ± 1.9	n.f. <sup>b</sup>		
PM 09	58	+3.52 ± 0.05	-16.6 ± 1.3	1820	-21.98 ± 0.09	-75.5 ± 9.7
PM 10 <sup>a</sup>	3900	-26.26 ± 0.44	-67 ± 3.1	6140	-24.75 ± 1.00	n.d. <sup>c</sup>
PM 19	2690	-25.18 ± 0.54	-66.8 ± 9.5	10300	-25.26 <sup>d</sup>	n.d. <sup>c</sup>
PZ 01	23700	-26.47 ± 0.25	-61.6 ± 3.3	6610	-25.37 ± 0.63	n.d. <sup>c</sup>
PZ 02	3870	-21.07 ± 0.07	-48.6 ± 1.6	2120	-24.57 ± 0.16	-60.0 ± 17.8
PZ 03	4690	-26.64 ± 0.17	-76.2 ± 3.8	5190	-27.63 <sup>d</sup>	n.d. <sup>c</sup>
PZ 04	10800	-25.92 ± 0.19	-42.5 ± 5.4	8790	-24.42 ± 0.34	n.d. <sup>c</sup>
PZ 05	265	-25.83 ± 0.06	n.d. <sup>c</sup>	1780	-25.31 ± 1.33	n.d. <sup>c</sup>
PZ 06	5740	-21.11 ± 0.06	-56.5 ± 1.18	22600	-24.61 ± 0.2	-61.3 ± 7.0
PZ 07	4590	-18.12 ± .02	-56.7 <sup>d</sup>	8740	-24.76 ± 0.02	-68.8 ± 0.6
PZ 14	278	+40.04 ± 1.15	+60.3 ± 11.4	2270	-24.62 ± 0.07	-82.0 ± 3.1
PZ 15	318	-19.81 ± 0.07	-51.1 ± 1.8	746	-23.37 ± 0.13	-48.3 ± 4.4
PM 01 <sup>a</sup>	6060	-26.49 ± 0.02	-80.9 ± 1.4	10200	-25.44 ± 0.13	-116.2 ± 11.1
PM 02	270	-16.21 ± 0.15	-54.2 ± 1.9	1540	-24.61 ± 0.11	-63.3 ± 3.6
PM 03	506	-6.54 ± 0.07	-37.6 ± 10.4	7130	-24.69 ± 0.08	-76.7 ± 10.0
PM 14	401	-25.98 ± 0.44	-61.3 ± 2.2	309	-25.90 ± 0.34	-104.5 ± 14.1
PM 16	204	-20.97 ± 0.18	-57.9 ± 4.5	363	-24.99 ± 0.52	-63.4 ± 21.2
PZ 11	575	-22.25 ± 0.17	n.d. <sup>c</sup>	2030	-26.15 <sup>d</sup>	n.d. <sup>c</sup>
PZ 13	46	-13.2 ± 0.83	-109.6 ± 10.9	1520	-24.56 ± 0.17	-95.4 ± 12.6
PB 01	626	-22.57 ± 0.38	-58.2 ± 4.3	1270	-24.64 ± 0.17	-98.2 ± 4.3
PB 02	493	-23.03 ± 0.33	-74.0 ± 6.3	1730	-24.91 ± 0.13	-100.9 ± 6.3
PB 03	348	-25.12 ± 0.09	-63.8 ± 1.2	296	-24.69 ± 0.12	-95.8 ± 7.6
PB 05	88	-22.53 ± 0.06	-61.3 ± 10.3	43	-24.92 ± 1.39	n.d. <sup>c</sup>
PB 06	198	-22.77 ± 0.05	-59.3 ± 2.5	183	-24.95 ± 0.13	-92.0 ± 10.6
PM 23	726	-23.35 ± 0.08	-66.0 ± 3.0	459	-25.29 ± 0.11	-78.0 ± 1.1
PM 24	1420	-13.63 ± 0.07	-61.8 ± 2.8	4440	-25.1 ± 0.08	-102.2 ± 3.8

- a. Source well.  
b. Not found.  
c. Not determined  
d. n=1

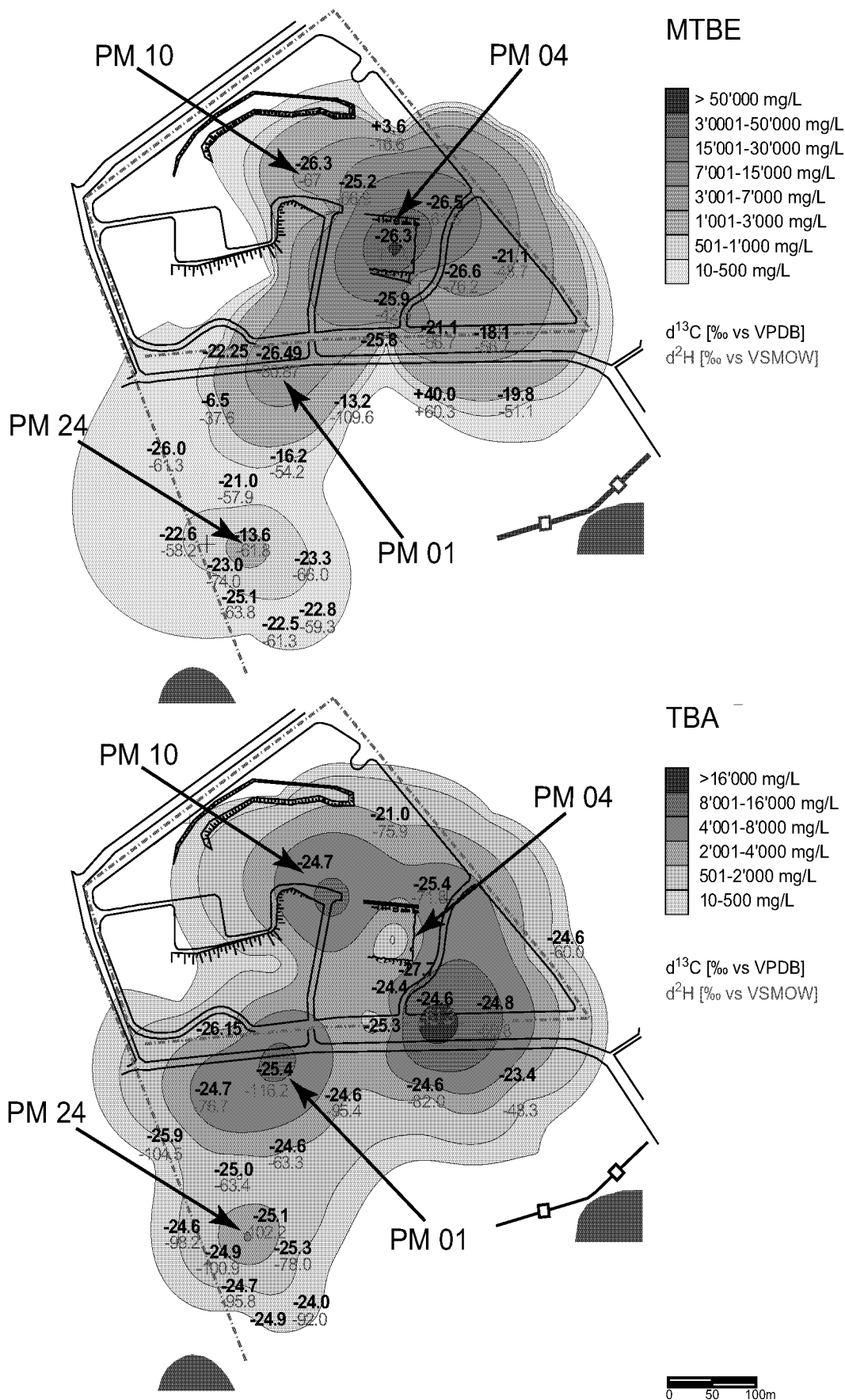


**Figure 6.4: Concentrations and Isotopic Composition of MTBE and TBA.** The maps show the extension of the MTBE (upper part) and TBA (lower part) plume as well as the carbon and hydrogen isotopic signatures of these two compounds. The upper isotopic value corresponds to  $\delta^{13}\text{C}$  vs VPDB and the lower value to  $\delta^2\text{H}$  vs VSMOW.

### 6.3.2 Quantification of Biodegradation

To minimize effects caused by the above mentioned variable hydrological conditions as well as pumping, the evaluation of the data mainly focuses on the wells that are located around the major contamination sources (PM 01, PM 04 and PM 10). The enrichment factor  $\epsilon$  at the investigated sampling wells can be determined and compared to laboratory experiments which have been carried out under controlled conditions.  $\epsilon$  factors are usually determined using the Rayleigh equation (Equation (6-1)) by plotting the logarithm of the change of  $\delta^{13}\text{C}$  values versus the logarithm of the change of concentrations. As can be seen from Figure 6.5 there is no apparent simple correlation between the MTBE concentration and the carbon isotopic enrichment patterns ( $R^2 = 0.25$ ).

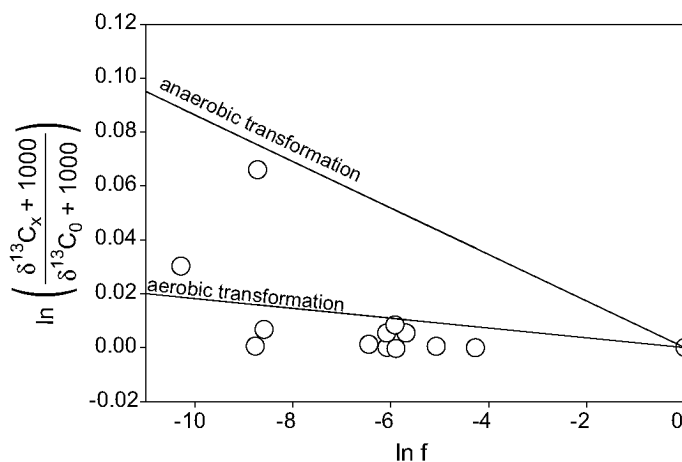


**Figure 6.5: Rayleigh Plot of  $\delta^{13}\text{C}$ -Data for MTBE.** The open circles represent data from the major plume (resulting from contamination from PM 10 and PM 04). The observed concentration decline does not correlate with the shift in isotopic signatures. The lines indicate the expected correlation between concentrations and carbon isotopic signatures assuming constant isotopic fractionation factors of  $\epsilon = -8.62\%$  for anaerobic and  $\epsilon = -1.82\%$  for aerobic biodegradation

The expected carbon isotopic signatures for the observed concentrations do not fit the measured values. In most cases, the observed relative concentrations were too low to explain the observed isotopic values. Hence other processes such as dilution and elimination processes (e.g., volatilization) that do not cause significant isotopic fractionations also have to be taken into account. To correct for dilution processes, MTBE concentrations could be normalized to a suitable conservative tracer. At this site, however, due to the multiple contamination sources and the long history of the disposal site, no tracer could be identified that showed identical sources or a similar concentration decline as MTBE. The lacking correlation of MTBE concentration with chloride and conductivity within the major MTBE plume (Figure 6.6) precludes any cor-

rection for dilution of measured MTBE concentrations along the plume. Hence, a simple Rayleigh-type approach is not appropriate for this particularly complex field site.

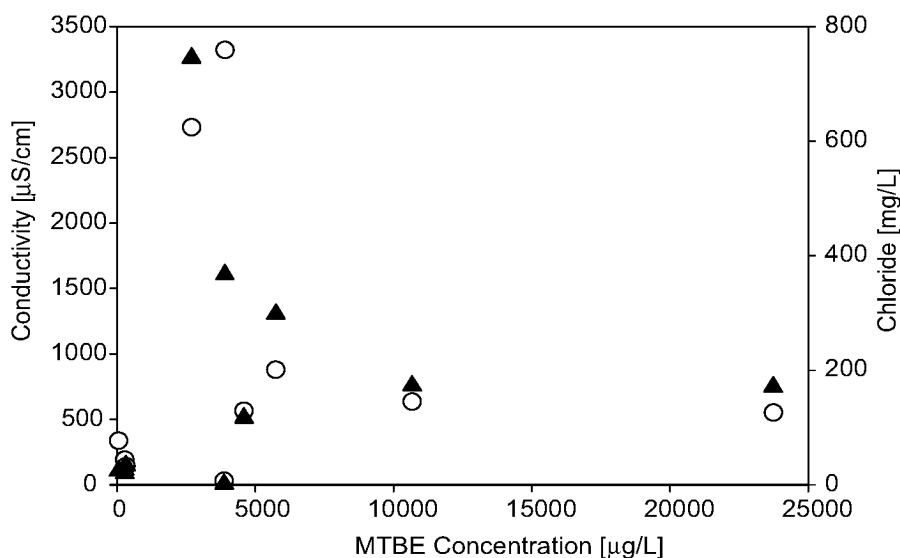


**Figure 6.6: Plot of MTBE Concentration versus Chloride Concentration and Conductivity.** While chloride concentrations (filled triangles) and conductivity (open circles) show a correlation for most samples, no trend with MTBE concentrations could be identified.

An alternative approach suggested to determine the extent of (bio)degradation by calculating the fraction of MTBE that would be expected based on the enrichment in  $^{13}\text{C}$  of MTBE downgradient of the source, assuming a constant  $^{13}\text{C}$ -signature of the MTBE source using Equation (6-3) and Equation (6-4).<sup>46-48,143</sup> This calculated  $f$  represents the concentration decrease that would be expected in a closed or plug flow system where only one reaction with a constant enrichment factor occurs. However, because the nature of the degradation process (i.e., aerobic or anaerobic biodegradation) can not be determined in our case, and because both processes are associated with significantly different enrichment factors ( $\epsilon$ ), an unambiguous determination of  $B$  by Equation (6-4) was not possible. For example, assuming aerobic biodegradation associated with an isotopic enrichment factor of  $-1.82\text{‰}$ , which corresponds to an average of observed  $\epsilon$ -values,<sup>24,36</sup> the extent of biodegradation in wells PZ 06 and PM 23 is calculated to be 95% and 82%, respectively. However, if an isotopic enrichment factor of  $-8.63\text{‰}$  is used, corresponding to the average of reported  $\epsilon$ -values observed under anoxic conditions in laboratory experiments and a field study,<sup>53</sup> biodegradation only accounted for 46% and 30% in the same wells. Thus, an approach has to be adopted that allows to differentiate between anaerobic and aerobic biodegradation of MTBE.

The microbial transformation of MTBE under oxic and anoxic conditions is not only associated with different carbon isotopic enrichments, but also with significantly different hydrogen isotopic enrichments. This observation, which is linked to different reaction mechanisms for anaerobic and aerobic degradation, can be used to differentiate between both processes. With this objective, the remaining fractions of MTBE using Equation (6-3) were *calculated* using the two distinct carbon enrichment factors. For the two cases (e.g., aerobic and anaerobic degradation), the *measured* hydrogen isotopic signatures of MTBE were then plotted against the thus calculated  $f$  are shown in Figure 6.7.

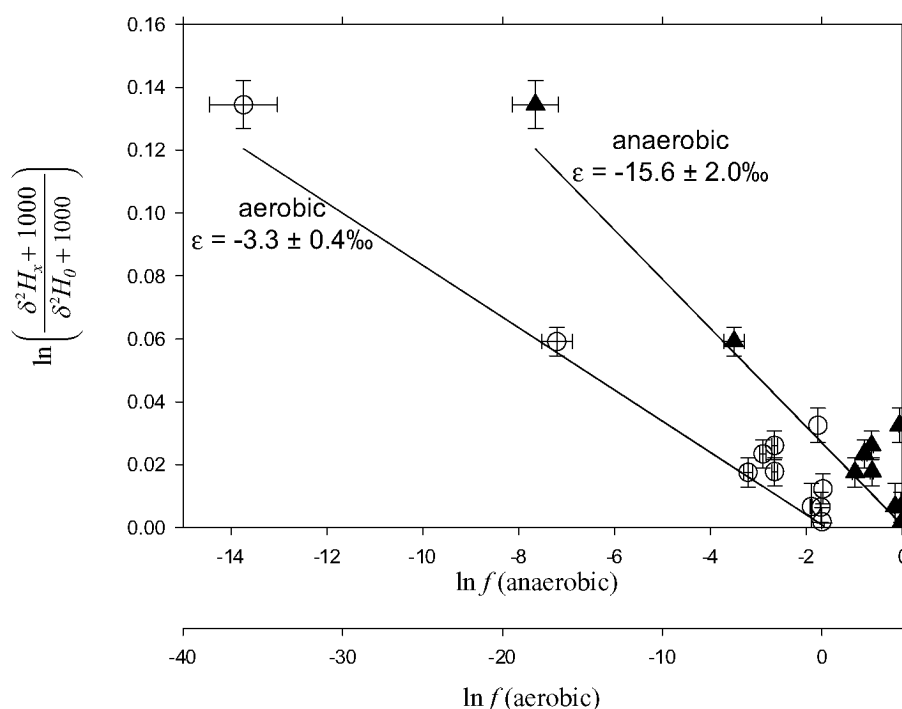


**Figure 6.7: Hydrogen Isotopic Enrichment of MTBE.** Correlation of hydrogen isotopic enrichment with remaining fractions of MTBE calculated for anoxic conditions (filled triangles) and oxic conditions (open circles). The lines correspond to the linear regression of the data. Note the different scales of the x-axis for aerobic respective anaerobic transformation.

As is evident the calculation of  $f$  based on carbon isotopic fractionation did allow to distinguish MTBE concentration decrease associated with *in situ* biodegradation from dilution or other non-fractionating processes. With this approach a strong correlation ( $R^2 = 0.94$ ) was obtained and hydrogen isotopic enrichments factors ( $\epsilon$ ) could be determined for both oxic and anoxic conditions. The obtained hydrogen  $\epsilon$ -values were:  $-3.3 \pm 0.4\text{‰}$  assuming aerobic biodegradation and  $-15.6 \pm 2.0\text{‰}$  with the assumption of anaerobic biodegradation. However, when assuming oxic conditions, the obtained  $\epsilon$  ( $-3.3\text{‰}$ ) is very low compared to previously determined values ( $-29\text{‰}$  to  $-66\text{‰}$ ).<sup>24</sup> Furthermore, the extremely low  $\ln f$

values obtained under the same assumption are not realistic ( $\ln f \ll -10$ ), because such a dramatic decrease would yield concentrations far below the detection limits.

**Table 6.2: Calculated Extent of Biodegradation and Predicted versus Measured MTBE and TBA Concentrations**

Sampling Well	$f$ (MTBE) measured	$f$ (MTBE) <sup>a</sup> calculated	Extent of Biodegradation B [%]	Measured TBA Conc. [ $\mu$ M]	Predicted TBA Conc. [ $\mu$ M]	$\frac{[TBA]_{meas}}{[TBA]_{pred}}$
PM 04 <sup>b</sup>	1.00E+00	9.98E-01	0		38	
PM 09	3.40E-05	3.01E-02	97	25	21	1.2
PM 10 <sup>b</sup>	2.29E-03	9.87E-01	1	83	1	83
PM 19	1.58E-03	8.68E-01	13	139	5	27.8
PZ 01 <sup>c</sup>	1.39E-02	1.01E+00	-1	89	-3	-29.7
PZ 02	2.27E-03	5.33E-01	47	29	38	0.76
PZ 03 <sup>c</sup>	2.75E-03	1.03E+00	-3	70	-2	-35
PZ 04	6.26E-03	9.48E-01	5	119	7	17
PZ 05	1.55E-04	9.38E-01	6	24	0	
PZ 06	3.37E-03	5.36E-01	46	305	56	5.4
PZ 07	2.69E-03	3.76E-01	62	118	86	1.4
PZ 14	1.63E-04	4.78E-04	100	31	6591	$5 \cdot 10^{-3}$
PZ 15	1.87E-04	4.59E-01	54	10	4	2.5
PM 01 <sup>b</sup>	1.00E+00	1.01E+00	-1	138	-1	-138
PM 02	4.46E-02	3.00E-01	70	21	7	3
PM 03	8.35E-02	9.67E-02	90	96	54	1.8
PM 14	6.62E-02	9.55E-01	4	4	0	
PM 16	3.37E-02	5.27E-01	47	5	2	2.5
PZ 11	9.49E-02	6.13E-01	39	27	4	6.7
PZ 13	7.59E-03	2.11E-01	79	21	2	10.5
PB 01	1.03E-01	6.37E-01	36	17	4	4.2
PB 02	8.14E-02	6.73E-01	33	23	3	7.6
PB 03	5.74E-02	8.62E-01	14	4	1	4
PB 05	1.45E-02	6.34E-01	37	1	1	1
PB 06	3.27E-02	6.52E-01	35	2	1	2
PM 23	1.20E-01	6.99E-01	30	6	4	1.5
PM 24	2.34E-01	2.22E-01	78	60	56	1.1

a. Calculated fraction of MTBE remaining assuming that biodegradation is the only important elimination process.

b. Source well.

c. Well adjacent to major MTBE source

However, with the assumption of anaerobic biodegradation the obtained hydrogen enrichment factor corresponds well with the enrichment factors published by Kuder et al. for anoxic conditions (-11.5‰),<sup>53</sup>

and the calculated  $f$  values appear more appropriate. Hence, aerobic biotransformation could be excluded as major degradation pathway of MTBE and the extent of biodegradation was calculated using Equation (6-3) and Equation (6-4) and a carbon isotopic enrichment factor ( $\epsilon$ ) of  $-8.63\text{‰}$  as proposed for anaerobic biodegradation of MTBE.<sup>53</sup> The results of this calculation are shown in Table 6.2.

Hence, based on a plausible hypothesis for the type of process causing the monitored fractionation, it was possible to calculate the extent of biodegradation using Equation (6-4). Furthermore, expected TBA concentrations were calculated for each sampling well, using Equation (6-5). The results of this calculation are also shown in Table 6.2 and are based on the following assumptions (i) no differences in the transport behaviour of MTBE and TBA, (ii) MTBE biodegradation is the only source of TBA formation, (iii) constant isotopic signatures of TBA, and (iv) the absence of TBA biodegradation.

The TBA concentrations were generally underestimated with this approach. Only in well PZ 14, where the highest TBA concentration would be expected based on the large isotopic enrichment of MTBE, much less TBA was found than would be expected. However, the general underestimation can be explained by the fact that the measured MTBE concentrations used for this calculation ( $[\text{MTBE}]_x$ ) are not only lowered by biodegradation (quantified using isotopic fractionation) or dilution (which should be roughly the same for TBA) but by an additional process that does not yield TBA and does not change the isotopic composition of the parent compound. Owing to the relatively high temperature of the groundwater ( $\sim 25\text{ °C}$ ) and the higher air-water partition coefficient of MTBE compared to TBA,<sup>56</sup> volatilization could play a major role in the attenuation of the MTBE concentrations at this particular site. Volatilization is associated with a small inverse isotopic effect, which means that molecules with the heavy isotope preferentially partition into the gas phase.<sup>104,105</sup> For MTBE, this effect is, however, only small ( $+0.17 \pm 0.05\text{‰}$ )<sup>36</sup> compared to the fractionations observed at the field site. The calculated TBA concentration in the source wells is far from the measured concentration. This is due to the fact that even small deviations in isotopic signatures from the average carbon isotopic signature of the 3 source wells lead to high deviations in the calculated TBA concentrations considering the high initial MTBE concentrations. If the isotopic signature of the source well is slightly enriched in  $^{13}\text{C}$  compared to the average value (well PM 01), negative TBA concentrations are calculated. Generally, however, the differences between measured and calculated TBA

concentrations are corroborating the existence of alternative MTBE sinks (such as evaporation), that were already postulated based on the observation of too low MTBE concentrations in the “traditional” Rayleigh analysis.

The discrepancy between estimated and measured TBA concentrations could also be partly due to the heterogeneity of the aquifer. If water from zones with a high MTBE transformation efficiency mixes with water from zones with little microbial activity, one would find relatively high TBA concentrations together with small carbon isotopic enrichments of MTBE. To gain further information on the relative importance of the volatilization of MTBE at the field site, soil air samples should be analyzed for volatile organic compounds.

### 6.3.3 Identification of Mechanism of Anaerobic MTBE Biodegradation

In order to validate the two-element isotopic approach presented above, it is important to show that the correlation of the isotopic fractionations for carbon and hydrogen are not coincidental but may be explained mechanistically. The approach to use carbon isotopic data for the calculation of the concentration decrease due to biodegradation combined with the use of the calculated  $f$  to determine hydrogen isotopic enrichments should only work if both isotope signatures are influenced by the same reaction. In Figure 6.8 carbon and hydrogen isotopic signa-

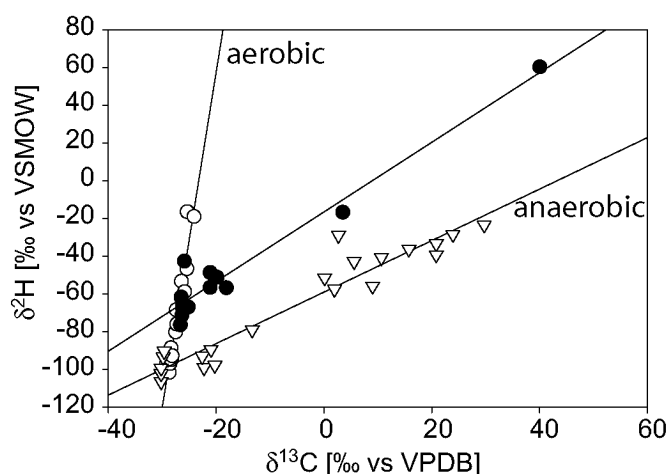


**Figure 6.8: Plot of Hydrogen versus Carbon Isotopic Signatures for Aerobic and Anaerobic Degradation.**  $\delta^{13}\text{C}$  vs  $\delta^2\text{H}$  data for aerobic MTBE degradation<sup>24</sup> in a batch experiment (open circles), anaerobic MTBE degradation observed at different field sites<sup>53</sup> (open triangles), and field data from the major plume of our study (filled circles).

tures observed during aerobic and anaerobic biodegradation are plotted together with the data collected from the investigated field site. A good



correlation of the hydrogen and carbon isotopic shifts was obtained for all three data sets. *Aerobic* biodegradation causes a quite small shift in the carbon isotopic signature but a significant shift in hydrogen isotopic signatures. Conversely, in the case of *anaerobic* biodegradation the carbon

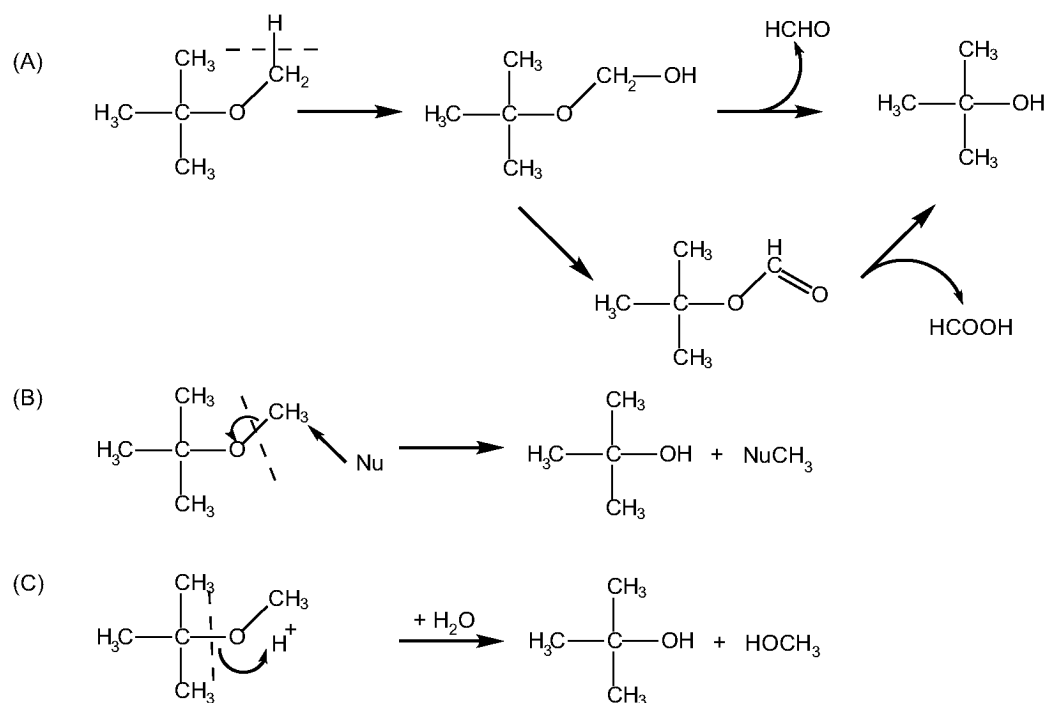


**Figure 6.9: Suggested Reaction Mechanisms for the Enzymatic Degradation of MTBE.** (A) Oxidation of MTBE by monooxygenases. (B)  $S_N2$  Reaction. (C)  $S_N1$  Reaction. The dashed line indicates the chemical bond at which isotopic fractionation will occur during the given reaction.

isotopic enrichment is high and of similar magnitude as the hydrogen effect. The slope of the regression line of our field data is similar to the data collected for anaerobic degradation, corroborating the assumption of anaerobic *in situ* biodegradation. A similar slope could also be obtained if one of the fractionation factors for carbon or hydrogen, would be different from published values for aerobic biodegradation, due to a different commitment to catalysis of the enzyme. The commitment to catalysis corresponds to the tendency of the enzyme-substrate complex to go forward through catalysis rather than to break down to free enzyme and substrate (Appendix A1.3). In the case of a high commitment to catalysis of a given enzyme, the full extent of the intrinsic isotope effect of the first irreversible step of an enzymatic reaction is not detectable.<sup>146</sup> Such a commitment to catalysis would, however, most likely, influence both fractionation factors. Furthermore, they would be influenced in the same way (i.e., an increase or a decrease of  $\epsilon$  for carbon and hydrogen), Hence, the similarity of the regression line from the field

data with the one for anaerobic degradation, can only be obtained by assuming similarities in the reaction mechanism.

The significant difference between the fractionation patterns under oxic versus anoxic conditions is an indicator for the existence of different reaction mechanisms. In the presence of oxygen the most likely degradation pathway from MTBE to TBA starts with an oxidation of the methyl group by monooxygenases (Figure 6.9 case (A)).<sup>160,162,181</sup> The so formed *tert*-butoxy methanol either reacts directly to TBA and formaldehyde or is further oxidized to *tert*-butyl formate which then hydrolyses to form TBA. The reaction mechanism for the formation of TBA from MTBE under *anoxic* conditions has not been elucidated so far. One possibility is a nucleophilic substitution reaction as depicted in Figure 6.9 either via an S<sub>N</sub>2 mechanism (case (B)) or via an S<sub>N</sub>1 mechanism (case(C)). These 3 different cases are also associated with different kinetic isotope effects (KIE, i.e., <sup>12</sup>k/<sup>13</sup>k or <sup>H</sup>k/<sup>D</sup>k). In order to compare the isotopic fractionation observed during the biodegradation of MTBE with KIEs for the different reaction mechanisms, the published data must first be reevaluated using the corrections (Equation (6-6) and Equation (6-7)). Table 6.3 shows the correction factors applied for the different reaction mechanisms.

**Table 6.3: Correction Factors Applied and Expected KIEs for Different Reaction Mechanisms for the Transformation of MTBE**

		Oxidation	S <sub>N</sub> 2	S <sub>N</sub> 1
Carbon	Number of carbon atoms (n)	5	5	5
	Number of carbon atoms in reactive positions (x)	1	1	1 <sup>a</sup>
	Correction for non-reacting sites <sup>b</sup>	n/x = 5	n/x = 5	n/x = 5
	Correction for intramolecular competition (z) <sup>c</sup>	none (z=1)	none (z=1)	none (z=1)
	Expected KIE ( <sup>13</sup> k/ <sup>12</sup> k)	1.01 - 1.02	1.03 - 1.08	1.00 - 1.02
Hydrogen	Number of hydrogen atoms (n)	12	12	12
	Number of hydrogen atoms in reactive positions (x)	3 (primary effect)	3 (secondary effects in α-position)	9 (secondary effects in β-position)
	Correction for non-reacting sites	n/x = 4	n/x = 4	n/x = 4/3
	Correction for intramolecular competition (z)	z = 3, three equal positions of which only one reacts	simultaneous secondary effects, no competition (z = 1)	simultaneous secondary effects, no competition (z = 1)
	Expected KIE ( <sup>2</sup> k/ <sup>1</sup> k)	4 - 6	0.95 - 1.05	1.1 - 1.2

a. The 3 further carbon atoms that could show secondary isotope effects are neglected

b. n/x value used in Equation (6-6)

c. Correction factor z is used in Equation (6-7)

In case A, i.e., the formation of *tert*-butoxy methanol, a carbon-hydrogen bond is broken in the first step of the reaction, hence one would expect a very high primary hydrogen isotope effect combined with a primary carbon isotope effect. The Streitwieser Semiclassical Limits for the breaking of a C-H-bond is 6.4 for  $k^2\text{H}/k^1\text{H}$  and 1.02 for  $k^{13}\text{C}/k^{12}\text{C}$ .<sup>116</sup> In the case of an  $\text{S}_{\text{N}}2$  reaction mechanism, the expected carbon isotope effects are relatively large.<sup>118</sup> The secondary hydrogen isotope effects, in contrast, are very small and may even be inverse, due to a more constrained bending motion of the hydrogen in the transition state.<sup>118,184</sup> The results for  $\text{S}_{\text{N}}1$  reaction mechanisms show the opposite trend, e.g. relatively small carbon isotopic effects and quite large secondary hydrogen isotope effects. The extent of the hydrogen fractionation depends on the nature of the leaving group.<sup>118</sup>

**Table 6.4: Reevaluation of Carbon and Hydrogen Isotope Effects During the Biodegradation of MTBE**

Original Data from	Experimental Conditions	Carbon		Hydrogen	
		$\epsilon$ [‰]	$k^{13}\text{C}/k^{12}\text{C}$	$\epsilon$ [‰]	$k^2\text{H}/k^1\text{H}^a$
Gray et al. <sup>24)</sup>	Aerobic, pure strain PM1	-2.0 - -2.4	1.010 - 1.012	-33 - -37	1.66 - 2.32 <sup>b</sup> 1.15 - 1.23 <sup>c</sup> 1.05-1.08 <sup>d</sup>
Gray et al. <sup>24)</sup>	Aerobic, mixed microcosm	-1.5 - -1.8	1.007 - 1.009	-29 / -66	1.53 / 2.68 <sup>b</sup> 1.13 / 1.26 <sup>c</sup> 1.04 / 1.09 <sup>d</sup>
Hunkeler et al. <sup>36)</sup>	Aerobic, direct or cometabolic degradation	-1.52 - -1.87	1.0083 - 1.011		n.d. <sup>e</sup>
Kolhatkar et al. <sup>42)</sup>	Anaerobic, field and microcosm data	-8.1 - - 9.16	1.0408 -1.0490		n.d. <sup>e</sup>
Kuder et al. <sup>53)</sup>	Anaerobic	n.d. <sup>e</sup>		-11.5	1.14 <sup>b,f</sup> 1.04 <sup>c,f</sup> 1.01 <sup>d,f</sup>
this work	Anaerobic			- 15.6	

a. Values for parameters n, x and z used for the calculation can be found in Table 6.3

b. Oxidation by monooxygenases.

c.  $\text{S}_{\text{N}}2$ .

d.  $\text{S}_{\text{N}}1$ .

e. Not determined.

f. Determined based on  $\epsilon$  published in paper and corrected according to the relation between  $\epsilon$  and  $k^2\text{H}/k^1\text{H}$  from the reevaluation of data obtained from Gray et al.<sup>24)</sup>

The results of the reevaluation of the observed isotope enrichments are shown in Table 6.4. The carbon kinetic isotope data obtained for the aerobic oxidation of MTBE are comparable to the expected KIEs shown in Table 6.3. The assumed reaction mechanism is also supported by the

hydrogen data. Even though they are significantly smaller than the predicted values, they still show a primary isotope effect in case (A). The hydrogen KIEs obtained for case (B) under aerobic conditions are too large to be in agreement with an  $S_N2$  reaction mechanism. They do however, agree with results expected for mechanism (C). While mechanism (C) can not be ruled out based on kinetic isotope effects, an oxidation mechanism (A) seems to be most plausible in the presence of oxygen and has already been postulated.

The carbon isotope effects observed during the anoxic reaction (1.04-1.05) are indicative of an  $S_N2$  reaction mechanism (expected KIE 1.03-1.08), because they are too high compared with the values expected in the case of an oxidation (1.01-1.02) or an  $S_N1$  mechanism (1.00-1.02). This indication is corroborated by the results of the reevaluation for the hydrogen isotope effects. While the obtained hydrogen KIEs for case (A) (1.14 vs 4-6) and (C) (1.01 vs 1.1-1.2) exclude the existence of a primary isotope effect and a  $S_N1$  reaction mechanism respectively, the hydrogen isotope effect obtained by the assumption of an  $S_N2$  mechanism (case (B); 1.04) lies within the theoretically expected KIE-range (0.95-1.05) for this type of reaction. This reevaluation illustrates, that the differing isotopic enrichments observed for aerobic and anaerobic biodegradation are indeed due to mechanistic aspects and can therefore be used as a powerful new tool for the quantification of *in situ* biodegradation of MTBE, since it is applicable independently from mass balances and hydrogeological conditions, as shown in this study.

## 6.4 Conclusions

This example illustrates the potential of using a multiple element approach in CSIA especially in the case of field studies. A quantification of *in situ* biodegradation would have been impossible with data of only one element (for example carbon isotopic signatures). Since we could use the isotopic data of one element (carbon in this case) to correct the concentration data of MTBE for dilution and non-fractionating removal processes, we were able to use the isotopic information of the second element to get hints on the process that is responsible for the observed isotopic fractionation. This new approach relies on the combined evaluation of carbon and hydrogen isotopic data collected at a field site and allows to identify (i) whether the observed isotopic enrichment of carbon and hydrogen isotopes at the site is associated with one single process as well as (ii) the nature of this process. The carbon and hydrogen data determined at the investigated field site are indicative of anaerobic

MTBE degradation, which has only rarely been reported under field conditions so far. Furthermore, the presented evidence for the S<sub>N</sub>2 character of the anoxic biodegradation of MTBE constitutes the first information about the mechanism of the anaerobic MTBE degradation. This finding has to be verified by additional studies, but the isotopic fractionations determined for carbon and hydrogen are already a strong indication for this reaction mechanism.



**REFERENCES**

- (1) Stout, S. A.; Uhler, A. D.; Naymik, T. G.; McCarthy, K. J. *Environmental Forensics: Unraveling Site Liability*, Environ. Sci. Technol. **1998**, 260A-264A.
- (2) Kaplan, I. R.; Galperin, Y.; Lu, S.-T.; Lee, R.-P. *Forensic Environmental Chemistry: Differentiation of Fuel-types, their Sources and Release Times*, Org. Geochem. **1997**, 27, 289-317.
- (3) Johnson, G. W.; Ehrlich, R. *State of the Art Report on Multivariate Chemometric Methods in Environmental Forensics*, Environ. Forensics **2002**, 3, 59-79.
- (4) Rifai, H. S.; Borden, R. C.; Wilson, J. T.; Ward, C. H. *Intrinsic Bioremediation for Sub-surface Restoration*; Batelle Press: Columbus, OH, **1995**.
- (5) Church, C. D.; Tratnyek, P. G.; Pankow, J. F.; Landmeyer, J. E.; Baehr, A. L.; Thomas, M. A.; Schirmer, M. *Effects of Environmental Conditions on MTBE Degradation in Model Column Aquifers*, U.S. Geological Survey, Water Resources Investigations Report, **1999**.
- (6) Schirmer, M.; Barker, J. F. *A Study of Long-term MTBE Attenuation in the Borden Aquifer, Ontario, Canada*, Ground Water Monit. Rem. **1998**, 18, 113-122.
- (7) Landmeyer, J. E.; Vroblesky, D. A.; Chapelle, F. H. *Stable Carbon Isotope Evidence of Biodegradation Zonation in a Shallow Jet-Fuel Contaminated Aquifer*, Environ. Sci. Technol. **1996**, 30, 1120-1128.
- (8) Conrad, M. E.; Daley, P. F.; Fischer, M. L.; Buchanan, B. B.; Leighton, T.; Kashgarian, M. *Combined  $^{14}\text{C}$  and  $\delta^{13}\text{C}$  Monitoring of in Situ Biodegradation of Petroleum Hydrocarbons*, Environ. Sci. Technol. **1997**, 31, 1463-1469.
- (9) Bolliger, C.; Höhener, P.; Hunkeler, D.; Häberli, K.; Zeyer, J. *Intrinsic Bioremediation of a Petroleum Hydrocarbon-contaminated Aquifer and Assessment of Mineralization Based on Stable Carbon Isotopes*, Biodegradation **1999**, 201-217.
- (10) Hunkeler, D.; Höhener, P.; Bernasconi, S.; Zeyer, J. *Engineered In Situ Bioremediation of a Petroleum Hydrocarbon-Contaminated Aquifer: Assessment of Mineralization based on Alkalinity, Inorganic Carbon and Stable Carbon Isotope Balances*, J. Contam. Hydrol. **1999**, 37, 201-223.
- (11) Jackson, A.; Pardue, J. *Quantifying the Mineralization of Contaminants Using Stable Carbon Isotope Ratios*, Org. Geochem. **1999**, 30, 787-792.
- (12) Fang, J.; Barcelona, M. J.; Krishnamurthy, R. V.; Atekwana, E. A. *Stable Carbon Isotope Biogeochemistry of a Shallow Sand Aquifer Contaminated with Fuel Hydrocarbons*, Appl. Geochem. **2000**, 15, 169-181.
- (13) Schmidt, T. C.; Zwank, L.; Elsner, M.; Berg, M.; Meckenstock, R. U.; Haderlein, S. B. *Compound-specific Stable Isotope Analysis of Organic Contaminants in Natural Environments: A Critical Review of the State of the Art, Prospects, and Future Challenges*, Anal. Bioanal. Chem. **2004**, 283-300.
- (14) Dempster, H. S.; Sherwood Lollar, B. S.; Feenstra, S. *Tracing Organic Contaminants in Groundwater: A New Methodology Using Compound-Specific Isotopic Analysis*, Environ. Sci. Technol. **1997**, 31, 3193-3197.
- (15) Smallwood, B. J.; Philp, R. P.; Burgoyne, T. W. *The use of Stable Isotopes to Differentiate Specific Source Markers for MTBE*, Environ. Forensics **2001**, 2, 215-221.
- (16) Yanik, P. J.; Macko, S. A.; Qian, Y.; Il, M. C. K. *Compound Specific Isotope Analysis As a Means Of Tracing the Sources and Fates of PCBs in the Environment*; In: 220th ACS National Meeting; Division of Environmental Chemistry Inc. (ACS): Washington D.C., **2000**; Vol. 40 No. 2, pp 416-417.



- (17) Reddy, C. M.; Heraty, L. J.; Holt, B. D.; Sturchio, N. C.; Eglinton, T. I.; Drenzek, N. J.; Xu, L.; Lake, J. L.; Maruya, K. A. *Stable Chlorine Isotopic Compositions of Aroclors and Aroclor-Contaminated Sediments*, Environ. Sci. Technol. **2000**, 34, 2866-2870.
- (18) Drenzek, N. J.; Tarr, C. H.; Eglinton, T. I.; Heraty, L. J.; Sturchio, N. C.; Shiner, V. J.; Reddy, C. M. *Stable Chlorine and Carbon Isotopic Compositions of Selected Semi-volatile Organochlorine Compounds*, Org. Geochem. **2002**, 33, 437-444.
- (19) Shouakar-Stash, O.; Frape, S. K.; Drimmie, R. J. *Stable Hydrogen, Carbon and Chlorine Isotope Measurements of Selected Chlorinated Organic Solvents*, J. Contam. Hydrol. **2003**, 211-228.
- (20) Coffin, R. B.; Miyares, P. H.; Kelley, C. A.; Cifuentes, L. A.; Reynolds, C. M. *Stable Carbon and Nitrogen Isotope Analysis of TNT: Two-Dimensional Source Identification*, Environ. Toxicol. Chem. **2001**, 20, 2676-2680.
- (21) Rogers, K. M.; Savard, M. M. *Detection of Petroleum Contamination in River Sediments from Quebec City Region using GC-IRMS*, Org. Geochem. **1999**, 30, 1559-1569.
- (22) Beneteau, K. M.; Aravena, R.; Frape, S. K. *Isotopic Characterization of Chlorinated Solvents - Laboratory and Field Results*, Org. Geochem. **1999**, 30, 739-753.
- (23) Ertl, S.; Seibel, F.; Eichinger, L.; Frimmel, F. H.; Kettrup, A. *The  $^{13}\text{C}/^{12}\text{C}$  and  $^2\text{H}/^1\text{H}$  Ratios of Trichloroethene, Tetrachloroethene and their Metabolites*, Isotopes Environ. Health Stud. **1998**, 34, 245-253.
- (24) Gray, J. R.; Lacrampe-Couloume, G.; Deepa, G.; Scow, K. M.; Wilson, R. D.; Mackay, D. M.; Sherwood Lollar, B. S. *Carbon and Hydrogen Isotopic Fractionation during Biodegradation of Methyl tert-Butyl Ether*, Environ. Sci. Technol. **2002**, 36, 1931-1938.
- (25) Mariotti, A.; Germon, J. C.; Hubert, P.; Kaiser, P.; Letolle, R.; Tardieux, A.; P., T. *Experimental Determination of Nitrogen Kinetic Isotope Fractionation: Some Principles; Illustration for the Denitrification and Nitrification Processes*, Plant Soil **1981**, 62, 413-430.
- (26) Slater, G. F.; Sherwood Lollar, B. S.; Spivack, J.; Brennan, M.; Mackenzie, P. *Isotopic Tracers of Degradation of Dissolved Chlorinated Solvents*; In: International Conference on Remediation of Chlorinated and Recalcitrant Compounds; Wickramanayake, G. B., Hinchee, R. E., Eds.; Battelle Press: Monterey, CA, **1998**; Vol. 3, pp 133-138.
- (27) Dayan, H.; Abrajano, T. A. Jr.; Sturchio, N. C.; Winsor, L. *Carbon Isotopic Fractionation during Reductive Dehalogenation of Chlorinated Ethenes by Metallic Iron*, Org. Geochem. **1999**, 30, 755-763.
- (28) Heraty, L. J.; Fuller, M. E.; Huang, L.; Abrajano, T. A. Jr.; Sturchio, N. C. *Isotopic Fractionation of Carbon and Chlorine by Microbial Degradation of Dichloromethane*, Org. Geochem. **1999**, 30, 793-799.
- (29) Hunkeler, D.; Aravena, R.; Butler, B. J. *Monitoring Microbial Dechlorination of Tetrachloroethene (PCE) in Groundwater Using Compound-Specific Stable Carbon Isotope Ratios: Microcosm and Field Studies*, Environ. Sci. Technol. **1999**, 33, 2733-2738.
- (30) Meckenstock, R. U.; Morasch, B.; Warthmann, R.; Schink, B.; Annweiler, E.; Michaelis, W.; Richnow, H. H.  *$^{13}\text{C}/^{12}\text{C}$  Isotope Fractionation of Aromatic Hydrocarbons During Microbial Degradation*, Environ. Microbiol. **1999**, 1, 409-414.
- (31) Poulson, S. R.; Drever, J. I. *Stable Isotope (C, Cl, and H) Fractionation during Vaporization of Trichloroethylene*, Environ. Sci. Technol. **1999**, 33, 3689-3694.

- (32) Sherwood Lollar, B. S.; Slater, G. F.; Ahad, J.; Sleep, B.; Spivack, J.; Brennan, M.; Mackenzie, P. *Contrasting Carbon Isotope Fractionation during Biodegradation of Trichloroethylene and Toluene: Implications for Intrinsic Bioremediation*, *Org. Geochem.* **1999**, 30, 813-820.
- (33) Ahad, J. M. E.; Sherwood Lollar, B. S.; Edwards, E. A.; Slater, G. F.; Sleep, B. E. *Carbon Isotope Fractionation during Anaerobic Biodegradation of Toluene: Implications for Intrinsic Bioremediation*, *Environ. Sci. Technol.* **2000**, 34, 892-896.
- (34) Bloom, Y.; Aravena, R.; Hunkeler, D.; Edwards, E.; Frape, S. K. *Carbon Isotope Fractionation During Microbial Dechlorination of Trichloroethene, cis-1,2-Dichloroethene, and Vinyl chloride: Implications for Assessment of Natural Attenuation*, *Environ. Sci. Technol.* **2000**, 34, 2768-2772.
- (35) Bill, M.; Schütt, C.; Barth, J. A. C.; Kalin, R. M. *Carbon Isotopic Fractionation During Abiotic Reductive Dehalogenation of Trichloroethene (TCE)*, *Chemosphere* **2001**, 44, 1281-1286.
- (36) Hunkeler, D.; Butler, B. J.; Aravena, R.; Barker, J. F. *Monitoring Biodegradation of Methyl tert-Butyl Ether (MTBE) Using Compound-Specific Carbon Isotope Analysis*, *Environ. Sci. Technol.* **2001**, 35, 676-681.
- (37) Hunkeler, D.; Andersen, N.; Aravena, R.; Bernasconi, S. M.; Butler, B. J. *Hydrogen and Carbon Isotope Fractionation during Aerobic Biodegradation of Benzene*, *Environ. Sci. Technol.* **2001**, 35, 3462-3467.
- (38) Miller, L. G.; Kalin, R. M.; McCauley, S. E.; Hamilton, J. T. G.; Harper, D. B.; Millet, D. B.; Oremland, R. S.; Goldstein, A. H. *Large Carbon Isotope Fractionation Associated with Oxidation of Methyl Halides by Methylotrophic Bacteria*, *Proc. Natl. Acad. Sci. U. S. A.* **2001**, 98, 5833-5837.
- (39) Slater, G. F.; Sherwood Lollar, B. S.; Edwards, E. A. *Variability in Carbon Isotopic Fractionation during Biodegradation of Chlorinated Ethenes: Implications for Field Applications*, *Environ. Sci. Technol.* **2001**, 35, 901-907.
- (40) Barth, J. A. C.; Slater, G. F.; Schütt, C.; Bill, M.; Downey, A.; Larkin, M. J.; Kalin, R. M. *Carbon Isotope Fractionation during Aerobic Biodegradation of Trichloroethene by Burkholderia Cepacia G4: a Tool to Map Degradation Mechanisms*, *Appl. Environ. Microbiol.* **2002**, 68, 1728-1734.
- (41) Hunkeler, D.; Aravena, R.; Cox, E. *Carbon Isotopes as a Tool to Evaluate the Origin and Fate of Vinyl Chloride: Laboratory Experiments and Modeling of Isotope Evolution*, *Environ. Sci. Technol.* **2002**, 36, 3378-3384.
- (42) Kolhatkar, R.; Kuder, T.; Philp, R. P.; Allen, J.; Wilson, J. T. *Use of Compound-Specific Stable Carbon Isotope Analysis to Demonstrate Anaerobic Biodegradation of MTBE in Groundwater at a Gasoline Release Site*, *Environ. Sci. Technol.* **2002**, 36, 5139-5146.
- (43) Pond, K. L.; Huang, Y.; Wang, Y.; Kulpa, C. F. *Hydrogen Isotopic Composition of Individual n-Alkanes as an Intrinsic Tracer for Bioremediation and Source Identification of Petroleum Contamination*, *Environ. Sci. Technol.* **2002**, 36, 724-728.
- (44) Brungard, K. L.; Munakata-Marr, J.; Johnson, C. A.; Mandernack, K. W. *Stable Carbon Isotope Fractionation of trans-1,2-dichloroethylene during Co-Metabolic Degradation by Methanotrophic Bacteria*, *Chem. Geol.* **2003**, 195, 59-67.
- (45) Slater, G. F.; Sherwood Lollar, B. S.; Lesage, S.; Brown, S. *Carbon Isotope Fractionation of PCE and TCE During Dechlorination by Vitamin B12*, *Environ. Sci. Technol.* **submitted**.

- (46) Meckenstock, R. U.; Morasch, B.; Kästner, M.; Vieth, A.; Richnow, H. H. *Assessment of Bacterial Degradation Activities in the Environment by Analysis of Stable Carbon Isotope Fractionation*, Soil, Water, Air Pollution **2002**, Focus 2, 141-152.
- (47) Richnow, H. H.; Meckenstock, R. U.; Reitzel, L. A.; Baun, A.; Ledin, A.; Christensen, T. H. *In Situ Biodegradation Determined by Carbon Isotope Fractionation of Aromatic Hydrocarbons in an Anaerobic Landfill Leachate Plume (Vejen, Denmark)*, J. Contam. Hydrol. **2003**, 1-14.
- (48) Richnow, H. H.; Annweiler, E.; Michaelis, W.; Meckenstock, R. U. *Microbial In Situ Degradation of Aromatic Hydrocarbons in a Contaminated Aquifer Monitored by Carbon Isotope Fractionation*, J. Contam. Hydrol. **2003**, 1-20.
- (49) Slater, G. F.; Dempster, H. S.; Sherwood Lollar, B. S.; Ahad, J. *Headspace Analysis: A New Application for Isotopic Characterization of Dissolved Organic Contaminants*, Environ. Sci. Technol. **1999**, 33, 190-194.
- (50) Slater, G. F.; Ahad, J.; Sherwood Lollar, B. S.; Allen-King R.; Sleep, B. *Carbon Isotope Effects Resulting from Equilibrium Sorption of Dissolved VOCs*, Anal. Chem. **2000**, 72, 5669-5672.
- (51) Sherwood Lollar, B. S.; Slater, G. F.; Sleep, B.; Witt, M.; Klecka, G. M.; Harkness, M.; Spivack, J. *Stable Carbon Isotope Evidence for Intrinsic Bioremediation of Tetrachloroethen and Trichloroethen at Area 6, Dover Air Force Base*, Environ. Sci. Technol. **2001**, 35, 261-269.
- (52) Song, D. L.; Conrad, M. E.; Sorenson, K. S.; Alvarez-Cohen, L. *Stable Carbon Isotope Fractionation during Enhanced In Situ Bioremediation of Trichloroethene*, Environ. Sci. Technol. **2002**, 36, 2262-2268.
- (53) Kuder, T.; Philp, R. P.; Kolhatkar, R.; Wilson, J. T.; Allen, J. *Application of Stable Carbon and Hydrogen Isotopic Techniques for Monitoring Biodegradation of MTBE in the Field*; In: NGWA/API Petroleum Hydrocarbons and Organic Chemicals in Ground Water; American Petroleum Institute: Atlanta, **2002**.
- (54) Hunkeler, D.; Aravena, R.; Parker, B. L.; Cherry, J. A.; Diao, X. *Monitoring Oxidation of Chlorinated Ethenes by Permanganate in Groundwater Using Stable Isotopes: Laboratory and Field Studies*, Environ. Sci. Technol. **2003**, 37, 798-804.
- (55) Hunkeler, D.; Aravena, R. *Determination of Compound-Specific Carbon Isotope Ratios of Chlorinated Methanes, Ethanes, and Ethenes in Aqueous Samples*, Environ. Sci. Technol. **2000**, 34, 2839-2844.
- (56) Schmidt, T. C.; Duong, H.-A.; Berg, M.; Haderlein, S. B. *Analysis of Fuel Oxygenates in the Environment*, The Analyst **2001**, 126, 405-413.
- (57) Hanson, J. R.; Ackerman, C. E.; Scow, K. *Biodegradation of Methyl tert-Butyl Ether by a Bacterial Pure Culture*, Appl. Environ. Microbiol. **1999**, 65, 4788-4792.
- (58) Prince, R. C. *Biodegradation of Methyl tertiary-Butyl Ether (MTBE) and Other Fuel Oxygenates*, Crit. Rev. Microbiol. **2000**, 26, 163-178.
- (59) Squillace, P. J.; Zogorski, J. S.; Wilber, W. G.; Price, C. V. *Preliminary Assessment of the Occurrence and Possible Sources of MTBE in Groundwater in the United States, 1993-1994*, Environ. Sci. Technol. **1996**, 30, 1721-1730.
- (60) Baehr, A. L.; Stackelberg, P. E.; Baker, R. J. *Evaluation of the Atmosphere as Source of Volatile Organic Compounds in Shallow Groundwater*, Water Resour. Res. **1999**, 35, 127-136.

- (61) Reuter, J. E.; Allen, B. C.; Richards, R. C.; Pankow, J. F.; Goldman, C. R.; Scholl, R. L.; Seyfried, J. S. *Concentrations, Sources and Fate of the Gasoline Oxygenate Methyl tert-Butyl Ether (MTBE) in a Multiple-Use Lake*, Environ. Sci. Technol. **1998**, *32*, 3666-3672.
- (62) Cline, P. V.; Delfino, J. J.; Rao, P. S. C. *Partitioning of Aromatic Constituents into Water from Gasoline and Other Complex Solvent Mixtures*, Environ. Sci. Technol. **1991**, *25*, 914-920.
- (63) Schwarzenbach, R. P.; Gschwend, P. M.; Imboden, D. M. *Environmental Organic Chemistry*; 2<sup>nd</sup> ed.; John Wiley & Sons, Inc.: New York, **2003**.
- (64) Saraullo, A.; Martos, P. A.; Pawliszyn, J. *Water Analysis by Solid Phase Microextraction Based on Physical Chemical Properties of the Coating*, Anal. Chem. **1997**, *69*, 1992-1998.
- (65) Menéndez, J. C. F.; Sánchez, M. L. F.; Uría, J. E. S.; Martínez, E. F.; Sanz-Medel, A. *Static Headspace, Solid Phase Microextraction and Headspace Solid Phase Microextraction for BTEX Determination in Aqueous Samples by Gas Chromatography*, Anal. Chim. Acta **2000**, *415*, 9-20.
- (66) Langenfeld, J. J.; Hawthorne, S. B.; Miller, D. J. *Quantitative Analysis of Fuel-Related Hydrocarbons in Surface Water and Wastewater Samples by Solid-Phase Microextraction*, Anal. Chem. **1996**, *68*, 144-155.
- (67) Halden, R. U.; Happel, A. M.; Schoen, S. R. *Evaluation of Standard Methods for the Analysis of Methyl tert-Butyl Ether and Related Oxygenates in Gasoline-Contaminated Groundwater*, Environ. Sci. Technol. **2001**, *35*, 1469-1474.
- (68) Cassada, D. A.; Zhang, Y.; Snow, D. D.; Spalding, R. F. *Trace Analysis of Ethanol, MTBE, and Related Oxygenate Compounds in Water Using Solid-Phase Microextraction and Gas Chromatography/Mass Spectrometry*, Anal. Chem. **2000**, *72*, 4654-4658.
- (69) EPA, U. S. *Measurement of Purgeable Organic Compounds in Water by Capillary Column Gas Chromatography/Mass Spectrometry*; U.S. Environmental Protection Agency: Cincinnati, OH, **1992**.
- (70) Gaines, R. B.; Ledford, E. B.; Stuart, J. D. *Analysis of Water Samples for Trace Levels of Oxygenate and Aromatic Compounds Using Headspace Solid-Phase Microextraction and Comprehensive Two-Dimensional Gas Chromatography*, J. Microcol. Sep. **1998**, *10*, 597-604.
- (71) Gorecki, T.; Khaled, A.; Pawliszyn, J. *The Effect of Sample Volume on Quantitative Analysis by Solid Phase Microextraction - Part 2. Experimental Verification*, The Analyst **1998**, *123*, 2819-2824.
- (72) Black, L.; Fine, D. *High Levels of Monoaromatic Compounds Limit the Use of Solid-Phase Microextraction of Methyl tert-Butyl Ether and tert-Butyl Alcohol*, Environ. Sci. Technol. **2001**, *35*, 3190-3192.
- (73) Gurka, D. F.; Pyle, S. M.; Titus, R. *Environmental Analysis by Direct Aqueous Injection*, Anal. Chem. **1992**, *64*, 1749-1754.
- (74) Potter, T. L. *Analysis of Petroleum-Contaminated Water by GC/FID with Direct Aqueous Injection*, Ground Water Monit. Rem. **1996**, *16*, 157-162.
- (75) Church, C. D.; Isabelle, L. M.; Pankow, J. F.; Rose, D. L.; Tratnyek, P. G. *Method for Determination of Methyl tert-Butyl Ether and its Degradation Products in Water*, Environ. Sci. Technol. **1997**, *31*, 3723-3726.
- (76) Hong, S.; Duttweiler, C. M.; Lemley, A. T. *Analysis of Methyl tert-butyl Ether and its Degradation Products by Direct Aqueous Injection onto Gas Chromatography with Mass Spectrometry or Flame Ionization detection systems*, J. Chromatogr. **1999**, *857*, 205-216.

- (77) Landmeyer, J. E.; Chapelle, F. H.; Bradley, P. M.; Pankow, J. F.; Church, C. D.; Tratnyek, P. G. *Fate of MTBE Relative to Benzene in a Gasoline-Contaminated Aquifer (1993-98)*, *Ground Water Monit. Rem.* **1998**, *18*, 93-102.
- (78) Lide, D. R., Ed. *Handbook of Chemistry and Physics*; 76<sup>th</sup> ed.; CRC Press; **1995**.
- (79) Church, C. D.; Pankow, J. F.; Tratnyek, P. G. *Hydrolysis of tert-Butyl Formate : Kinetics, Products and Implications for the Environmental Impact of Methyl tert-Butyl Ether*, *Environ. Toxicol. Chem.* **1999**, *18*, 2789-2796.
- (80) Keith, L. H. *Environmental Sampling and Analysis: A Practical Guide*; Lewis: Chelsea, MI, **1991**.
- (81) Grob, K.; Habich, A. *Effect of Water on Retention Time*, *J. High Resolut. Chromatogr. Chromatogr. Commun.* **1983**, *6*, 34-35.
- (82) Munz, C.; Gälli, R.; Kiayias, G.; Schmid, B. *Risk Assessment, Mass Balance and Successful Remediation of a Major Gasoline Spill in a Residential Area*; In: *Contaminated Soil'98: ConSoil'98, Proceedings of the Sixth International Conference on Contaminated Soil*; 6<sup>th</sup> ed.; Telford, T., Ed.; Thomas Telford: Edinburgh, UK, **1998**; Vol. 2, pp 1067-1068.
- (83) Acero, J. L.; Haderlein, S. B.; Schmidt, T. C.; Suter, M. J.-F.; Gunten, U. v. *MTBE Oxidation by Conventional Ozonation and the Combination Ozone/Hydrogen Peroxide: Efficiency of the Processes and Bromate Formation*, *Environ. Sci. Technol.* **2001**, *35*, 4252-4259.
- (84) Lichtfouse, E. *Compound-Specific Isotope Analysis. Application to Archaeology, Biomedical Sciences, Biosynthesis, Environment, Extraterrestrial Chemistry, Food Science, Forensic Science, Humic Substances, Microbiology, Organic Geochemistry, Soil Science and Sport*, *Rapid Commun. Mass Spectrom.* **2000**, *14*, 1337-1344.
- (85) O'Malley, V. P.; Abrajano, T. A. Jr.; Hellou, J. *Determination of the <sup>13</sup>C/<sup>12</sup>C Ratios of Individual PAH from Environmental Samples: Can PAH Sources Be Apportioned?*, *Org. Geochem.* **1994**, *21*, 809-822.
- (86) Warmerdam, E. M. v.; Frapce, S. K.; Aravena, R.; Drimmie, R. J.; Flatt, H.; Cherry, J. A. *Stable Chlorine and Carbon Isotope Measurements of Selected Chlorinated Organic Solvents*, *Appl. Geochem.* **1995**, *10*, 547-552.
- (87) McRae, C.; Snape, C. E.; Sun, C.-G.; Fabbri, D.; Tartari, D.; Trombini, C.; Fallick, A. E. *Use of Compound-Specific Stable Isotope Analysis to Source Anthropogenic Natural Gas-Derived Polycyclic Aromatic Hydrocarbons in a Lagoon Sediment*, *Environ. Sci. Technol.* **2000**, *34*, 4684-4686.
- (88) Merritt, D. A.; Freeman, K. H.; Ricci, M. P.; Studley, S. A.; Hayes, J. M. *Performance and Optimization of a Combustion Interface for Isotope Ratio Monitoring Gas Chromatography/Mass Spectrometry*, *Anal. Chem.* **1995**, *67*, 2461-2473.
- (89) Hener, U.; Brand, W. A.; Hilker, A. W.; Juchelka, D.; Mosandl, A.; Podebrad, F. *Simultaneous On-line Analysis of <sup>18</sup>O/<sup>16</sup>O and <sup>13</sup>C/<sup>12</sup>C Ratios of Organic Compounds Using GC-Pyrolysis-IRMS*, *Zeitschrift für Lebensmittel-Untersuchung und -Forschung* **1998**, 230-232.
- (90) Hilker, A. W.; Douthitt, C. B.; Schlüter, H. J.; Brand, W. A. *Isotope Ratio Monitoring Gas Chromatography/Mass Spectrometry of D/H by High Temperature Conversion Isotope Ratio Mass Spectrometry*, *Rapid Commun. Mass Spectrom.* **1999**, *13*, 1226-1230.
- (91) Meier-Augenstein, W.; Watt, P. W.; Langhans, C.-D. *Influence of Gas Chromatographic Parameters on Measurements of <sup>13</sup>C/<sup>12</sup>C Isotope Ratios by Gas-Liquid Chromatography-Combustion Isotope Ratio Mass Spectrometry*, *J. Chromatogr.* **1996**, *752*, 233-241.

- (92) Schmitt, J.; Glaser, B.; Zech, W. *Amount-Dependent Isotopic Fractionation during Compound-Specific Isotope Analysis*, Rapid Commun. Mass Spectrom. **2003**, 17, 970-977.
- (93) Górecki, T.; Martos, P.; Pawliszyn, J. *Strategies for the Analysis of Polar Solvents in Liquid Matrixes*, Anal. Chem. **1998**, 70, 19-27.
- (94) Wercinski, S. A. S.; Pawliszyn, J. *Solid Phase Microextraction - A Practical Guide*; Marcel Dekker, Inc: New York, **1999**.
- (95) Goupry, S.; Rochut, N.; Robins, R. J.; Gentil, E. *Evaluation of Solid-Phase Microextraction for the Isotopic Analysis of Volatile Compounds Produced during Fermentation by Lactic Acid Bacteria*, J. Agric. Food Chem. **2000**, 48, 2222-2227.
- (96) Dias, R. F.; Freeman, K. H. *Carbon Isotope Analyses of Semivolatile Organic Compounds in Aqueous Media Using Solid-Phase microextraction and Isotope Ratio Monitoring GC/MS*, Anal. Chem. **1997**, 69, 944-950.
- (97) Munch, J. W.; Eichelberger, J. W. *Evaluation of 48 Compounds for Possible Inclusion in U.S. EPA Method 524.2, Revision 3.0: Expansion of the Analyte List to a Total of 83 Compounds*, J. Chromatogr. Sci. **1991**, 30, 471-477.
- (98) Chambers, L. *Optimization of a Purge-and-trap System for Analysis of VOAs by U.S. EPA Method 524.2, Rev.4*, Am. Lab. **2000**, 32, 40-50.
- (99) Whiticar, M. J.; Snowdon, L. R. *Geochemical Characterization of Selected Western Canada Oils by C5-C8 Compound Specific Isotope Correlation (CSIC)*, Org. Geochem. **1999**, 30, 1127-1161.
- (100) Harris, S. A.; Whiticar, M. J.; Eek, M. K. *Molecular and Isotopic Analysis of Oils by Solid Phase Microextraction of Gasoline Range Hydrocarbons*, Org. Geochem. **1999**, 30, 721-737.
- (101) Zwank, L.; Schmidt, T. C.; Haderlein, S. B.; Berg, M. *Simultaneous Determination of Fuel Oxygenates and BTEX Using Direct Aqueous Injection Gas Chromatography Mass Spectrometry (DAI-GC/MS)*, Environ. Sci. Technol. **2002**, 36, 2054-2059.
- (102) Harrington, R. R.; Poulson, S. R.; Drever, J. I.; Colberg, P. J. S.; Kelly, E. F. *Carbon Isotope Systematics of Monoaromatic Hydrocarbons: Vaporization and Adsorption Experiments*, Org. Geochem. **1999**, 30, 765-775.
- (103) Huang, L.; Sturchio, N. C.; Abrajano T. A., Jr.; Heraty, L. J.; Holt, B. D. *Carbon and Chlorine Isotope Fractionation of Chlorinated Aliphatic Hydrocarbons by Evaporation*, Org. Geochem. **1999**, 30, 777-785.
- (104) Jancso, G.; Van Hook, W. A. *Condensed Phase Isotope Effects (Especially Vapor Pressure Isotope Effects)*, Chem. Rev. **1974**, 74, 689-750.
- (105) Narten, A.; Kuhn, W. *Genaue Bestimmung kleiner Dampfdruckunterschiede isotoper Verbindungen II. Der  $^{13}\text{C}/^{12}\text{C}$ -Isotopieeffekt in Tetrachlorkohlenstoff und in Benzol*, Helv. Chim. Acta **1961**, 44, 1474-1479.
- (106) Davis, A.; Fennemore, G. G.; Peck, C.; Walker, C. R.; McIlwraith, J.; Thomas, S. *Degradation of carbon tetrachloride in a reducing groundwater environment: implications for natural attenuation*, Appl. Geochem. **2003**, 18, 503-525.
- (107) Moran, M. J.; Grady, S.; Zogorski, J. S.; *Occurrence and Distribution of Volatile Organic Compounds in Drinking Water Supplied by Community Water Systems in the Northeast and Mid-Atlantic Regions of the United States, 1993-98* United States Geological Survey, 2001.
- (108) Squillace, P. J.; Scott, J. C.; Moran, M. J.; Nolan, B. T.; Kolpin, D. W. *VOCs, Pesticides, Nitrate, and their mixtures in groundwater used for drinking water in the United States*, Environ. Sci. Technol. **2002**, 36, 1923-1930.

- (109) Haderlein, S. B.; Pecher, K.; *Pollutant Reduction in Heterogeneous Fe(II)/Fe(III)-Systems* In: Kinetics and Mechanisms of Reactions at the Mineral/Water Interface; Sparks, D. L., Grundl, T., Eds.; American Chemical Society: Washington D.C., **1998**; pp 342-345.
- (110) Amonette, J. E.; Workman, D. J.; Kennedy, D. W.; Fruchter, J. S.; Gorby, Y. A. *Dechlorination of Carbon Tetrachloride by Fe(II) Associated with Goethite*, Environ. Sci. Technol. **2000**, 34, 4606-4613.
- (111) Pecher, K.; Haderlein, S. B.; Schwarzenbach, R. P. *Reduction of Polyhalogenated Methanes by Surface Bound Fe(II) in Aqueous Suspensions of Iron Oxides*, Environ. Sci. Technol. **2002**, 36, 1734-1741.
- (112) Rügge, K.; Hofstetter, T.; Haderlein, S. B.; Bjerg, P. L.; Knudsen, S.; Zraunig, C.; Mosbaek, H.; Christensen, T. *Characterization of Predominant Reductants in an Anaerobic Leachate-Contaminated Aquifer by Nitroaromatic Probe Compounds*, Environ. Sci. Technol. **1998**, 32, 23-31.
- (113) Kenneke, J. F.; Weber, E. J. *Reductive Dehalogenation of Halomethanes in Iron- and Sulfate-Reducing Sediments. 1. Reactivity Pattern Analysis*, Environ. Sci. Technol. **2003**, 37, 713-720.
- (114) Stehmeier, L. G.; Francis, M. M.; Jack, T. R.; Diegor, E.; Winsor, L.; Abrajano, T. A. Jr. *Field and in vitro Evidence for in-situ Bioremediation Using Compound-Specific  $^{13}\text{C}/^{12}\text{C}$  Ratio Monitoring*, Org. Geochem. **1999**, 30, 821-833.
- (115) Pause, L.; Robert, M.; Savéant, J.-M. *Reductive Cleavage of Carbon Tetrachloride in a Polar Solvent. An Example of a Dissociative Electron Transfer with Significant Attractive Interaction between the Caged Product Fragments*, J. Am. Chem. Soc. **2000**, 122, 9829-9835.
- (116) Huskey, W. P.; *Origins and Interpretations of Heavy-Atom Isotope Effects* In: Enzyme Mechanisms from Isotope Effects; Cook, P. F., Ed.; CRC Press: Boca Raton, FL, **1991**.
- (117) Elsner, M.; Haderlein, S. B.; Schwarzenbach, R. P. *Reactivity of Fe(II)-Bearing Minerals towards Reductive Transformation of Organic Contaminants*, Environ. Sci. Technol. **2004**, 38, 799.
- (118) Melander, L.; Saunders, W. H. J. *Reaction Rates of Isotopic Molecules*; 2<sup>nd</sup> ed.; John Wiley & Sons: New York, **1980**.
- (119) Elsner, M.; Schwarzenbach, R. P.; Kellerhals, T.; Luzi, S.; Zwank, L.; Angst, W. *Mechanisms and Products of Surface-Mediated Reductive Dehalogenation of Carbon Tetrachloride by Fe(II) on Goethite*, Environ. Sci. Technol. **in press**.
- (120) Elsner, M. *Reductive Dehalogenation of Chlorinated Hydrocarbons by Surface-Bound Fe(II) - Kinetic and Mechanistic Aspects*; In: Departement für Umweltnaturwissenschaften; Eidgenössisch Technische Hochschule Zürich; ETH Diss.Nr. 14955: Zürich, **2002**
- (121) Fadrus, H.; Maly, J. *Suppression of Iron(III) Interferences in the Determination of Iron(II) in Water by the 1,10-Phenanthroline Method*, The Analyst **1975**, 549-554.
- (122) Graf, T. *Produktion kosmogener Nuklide in Meteoriten*; Eidgenössisch Technische Hochschule Zürich; ETH Diss. Nr. 8515: Zurich, **1988**.
- (123) Zhang, Y.; Charlet, L.; Schindler, P. W. *Adsorption of Protons, Fe(II), and Al(III) on Lepidocrocite ( $\gamma\text{-FeOOH}$ )*, Colloids and Surfaces **1992**, 63, 259-268.
- (124) Coughlin, B. R.; Stone, A. T. *Nonreversible Adsorption of Divalent Metal Ions (Mn(II), Co(II), Ni(II), Cu(II), and Pb(II)) onto Goethite: Effects of Acidification. Fe(II) Addition and Picolinic Acid Addition*, Environ. Sci. Technol. **1995**, 29, 2445-2455.

- (125) Liger, E.; Charlet, L.; Van Capellen, P. *Surface Catalysis of Uranium(VI) Reduction by Iron(II)*, *Geochim. Cosmochim. Acta* **1999**, *63*, 2939-2955.
- (126) Jeon, B.-H.; Dempsey, B. A.; Burgos, W. D.; A., R. R. *Reactions of Ferrous Iron with Hematite*, *Colloids and Surfaces A: Physicochemical and Engineering Aspects* **2001**, *191*, 41-55.
- (127) Kriegman-King, M. R.; Reinhard, M. *Transformation of Carbon Tetrachloride by Pyrite in Aqueous Solution*, *Environ. Sci. Technol.* **1994**, *28*, 692-700.
- (128) Roberts, A. L.; Totten, L. A.; Arnold, W. A.; Burris, D. R.; Campbell, T. J. *Reductive Elimination of Chlorinated Ethylenes by Zero-Valent Metals*, *Environ. Sci. Technol.* **1996**, *30*, 2654-2659.
- (129) Scherer, M. M.; Johnson, K. M.; Westall, J. C.; Tratnyek, P. G. *Mass Transport Effects on the Kinetics of Nitrobenzene Reduction by Iron Metal*, *Environ. Sci. Technol.* **2001**, *35*, 2804-2811.
- (130) Arnold, W. A.; Roberts, A. L. *Pathways and Kinetics of Chlorinated Ethylene and Chlorinated Acetylene Reaction with Fe(0) Particles*, *Environ. Sci. Technol.* **2000**, *34*, 1794-1805.
- (131) Lee, W.; Batchelor, B. *Abiotic Reductive Dechlorination of Chlorinated Ethylenes by Iron-Bearing Soil Minerals. 1. Pyrite and Magnetite*, *Environ. Sci. Technol.* **2002**, *36*, 5147-5154.
- (132) Lee, W.; Batchelor, B. *Abiotic Reductive Dechlorination of Chlorinated Ethylenes by Iron-Bearing Soil Minerals. 2. Green Rust*, *Environ. Sci. Technol.* **2002**, *36*, 5348-5354.
- (133) Butler, E. C.; Hayes, K. F. *Kinetics of the Transformation of Trichloroethylene and Tetrachloroethylene by Iron Sulfide*, *Environ. Sci. Technol.* **1999**, *33*, 2021-2027.
- (134) Weerasooriya, R.; Dharmasena, B. *Pyrite-Assisted Degradation of Trichloroethene (TCE)*, *Chemosphere* **2001**, *42*, 389-396.
- (135) Holliger, C.; Hahn, D.; Harmsen, H.; Ludwig, W.; Schumacher, W.; Tindall, B.; Vazquez, F.; Weiss, N.; Zehnder, A. J. B. *Dehalobacter Restrictus gen. nov. and sp. nov., a Strictly Anaerobic Bacterium that Reductively Dechlorinates Tetra- and Trichloroethene in an Anaerobic Respiration*, *Arch. Microbiol.* **1998**, *169*, 313-321.
- (136) Mayo-Gatell, X.; Chien, Y.-t.; Gossett, J. M.; Zinder, S. H. *Isolation of a Bacterium that Reductively Dechlorinates Tetrachloroethene to Ethene*, *Science* **1997**, *276*, 1568-1571.
- (137) Middeldorp, P. J. M.; Luijten, M. L. G. C.; van de Pas, B. A.; van Eekert, M. H. A.; Kengen, S. W. M.; Schraa, G.; Stams, A. J. M. *Anaerobic Microbial Reductive Dehalogenation of Chlorinated Ethenes*, *Bioremediation J.* **1999**, *3*, 151-169.
- (138) Herbert Jr, R. B.; Benner, S. G.; Pratt, A. R.; Blowes, D. W. *Surface Chemistry and Morphology of Poorly Crystalline Iron Sulfides Precipitated in Media Containing Sulfate-Reducing Bacteria*, *Chem. Geol.* **1998**, *144*, 87-97.
- (139) Butler, E. C.; Hayes, K. F. *Kinetics of the Transformation of Halogenated Aliphatic Compounds by Iron Sulfide*, *Environ. Sci. Technol.* **2000**, *34*, 422-429.
- (140) Butler, E. C.; Hayes, K. F. *Effects of Solution Composition and pH on the Reductive Dechlorination of Hexachloroethane by Iron Sulfide*, *Environ. Sci. Technol.* **1998**, *32*, 1276-1284.
- (141) Butler, E. C.; Hayes, K. F. *Factors Influencing Rates and Products in the Transformation of Trichloroethylene by Iron Sulfide and Iron Metal*, *Environ. Sci. Technol.* **2001**, *35*, 3884-3891.



- (142) Poulson, S. R.; Naraoka, H. *Carbon Isotope Fractionation during Permanganate Oxidation of Chlorinated Ethylenes (cDCE, TCE, PCE)*, Environ. Sci. Technol. **2002**, 36, 3270-3274.
- (143) Richnow, H. H.; Meckenstock, R. U. *Isotopen-geochemisches Konzept zur in-situ-Erfassung des biologischen Abbaus in kontaminiertem Grundwasser*, TerraTech **1999**, 38-41.
- (144) Glod, G.; Angst, W.; Holliger, C.; Schwarzenbach, R. P. *Corrinoid-Mediated Reduction of Tetrachloroethene, Trichloroethene, and Trichlorofluoroethene in Homogeneous Aqueous Solution: Reaction Kinetics and Reaction Mechanisms*, Environ. Sci. Technol. **1997**, 31, 253-260.
- (145) Northrop, D. B.; *Intrinsic Isotope Effects in Enzyme-Catalyzed Reactions* In: Enzyme Mechanism from Isotope Effects; Cook, P. F., Ed.; CRC Press: Boca Raton, FL, **1991**.
- (146) Hunkeler, D.; Aravena, R. *Evidence of Substantial Carbon Isotope Fractionation among Substrate, Inorganic Carbon, and Biomass during Aerobic Mineralization of 1,1-Dichloroethane by Xanthobacter Autotrophicus*, Appl. Environ. Microbiol. **2000**, 66, 4870-4876.
- (147) Neumann, A.; Scholz-Muramatsu, H.; Diekert, G. *Tetrachloroethene Metabolism of Dehalospirillum Multivorans*, Arch. Microbiol. **1994**, 162, 295-301.
- (148) Rickard, D. T. *The Chemistry of Iron Sulphide Formation at Low Temperatures*, Stockholm Contributions in Geology **1969**, 26, 49-66.
- (149) Slater, G. F.; Sherwood Lollar, B. S.; King, R. A.; O'Hannesin, S. *Isotopic Fractionation during Reductive Dechlorination of Trichloroethene by Zero-Valent Iron: Influence of Surface Treatment*, Chemosphere **2002**, 49, 587-596.
- (150) Sessions, A. L.; Burgoyne, T. W.; Schimmelfmann, A.; Hayes, J. M. *Fractionation of Hydrogen Isotopes in Lipid Biosynthesis*, Org. Geochem. **1999**, 30, 1193-1200.
- (151) Krayer von Krauss, M.; Harremoës, P., Eds. *MTBE in Petrol as a Substitute for Lead*; Office for Official Publications of the European Communities: Copenhagen, **2001**; Vol. Environmental Issue Report 22.
- (152) European Fuel Oxygenates Association (EFOA); *MTBE Resource Guide*, EFOA, 2002.
- (153) Ekwurzel, B.; Moran, J. E.; Koester, C. J.; Davisson, M. L.; Eaton, G. F.; *Nonpoint Source Methyl tert-Butyl Ether Movement through the Environment: Ultra Low Level (ppt) Measurements in California* In: Oxygenates in Gasoline: Environmental Aspects; Diaz, A. F., Drogos, D. L., Eds.; American Chemical Society: Washington, D.C., **2002**; pp 17-27.
- (154) Pankow, J. F.; Thomson, N. R.; Johnson, R. L.; Baehr, A. L.; Zogorski, J. S. *The Urban Atmosphere as a Non-Point Source for the Transport of MTBE and Other Volatile Organic Compounds (VOCs) to Shallow Groundwater*, Environ. Sci. Technol. **1997**, 31, 2821-2828.
- (155) Schmidt, T. C.; Morgenroth, E.; Schirmer, M.; Effenberger, M.; Haderlein, S. B.; *Use and Occurrence of Fuel Oxygenates in Europe* In: Oxygenates in Gasoline: Environmental Aspects; Diaz, A. F., Drogos, D. L., Eds.; American Chemical Society: Washington, D.C., **2002**; pp 58-79.
- (156) Deeb, R. A.; Scow, K. M.; Alvarez-Cohen, L. *Aerobic MTBE Biodegradation: An Examination of Past Studies, Current Challenges and Future Research Directions*, Biodegradation **2000**, 11, 171-186.
- (157) Fayolle, F.; Vandecasteele, J.-P.; Monot, F. *Microbial Degradation and Fate in the Environment of Methyl tert-Butyl Ether and Related Fuel Oxygenates*, Appl. Microbiol. Biotechnol. **2001**, 56, 339-349.

- (158) Salanitro, J. P.; Diaz, L. A.; Williams, M. P.; Wisniewski, H. L. *Isolation of a Bacterial Culture that Degrades Methyl tert-Butyl Ether*, *Appl. Environ. Microbiol.* **1994**, *60*, 2593-2596.
- (159) Mo, K.; Iora, C. O.; Wanken, A. E.; Javanmardian, K.; Yang, X.; Kulpa, C. F. *Biodegradation of Methyl tert-Butyl Ether by Pure Bacterial Cultures*, *Appl. Microbiol. Biotechnol.* **1997**, *47*, 69-72.
- (160) Steffan, R. J.; McClay, K.; Vainberg, S.; Condee, C. W.; Zhang, D. *Biodegradation of the Gasoline Oxygenates Methyl tert-Butyl Ether, Ethyl tert-Butyl Ether, and tert-Amyl Methyl Ether by Propane-Oxidizing Bacteria*, *Appl. Environ. Microbiol.* **1997**, *63*, 4216-4222.
- (161) Bradley, P. M.; Landmeyer, J. E.; Chapelle, F. H. *Aerobic Mineralization of MTBE and tert-Butyl Alcohol by Stream-Bed Sediment Microorganisms*, *Environ. Sci. Technol.* **1999**, *33*, 1877-1879.
- (162) Hardison, L. K.; Curry, S. S.; Ciufetti, L. M.; Hyman, M. R. *Metabolism of Diethyl Ether and Cometabolism of Methyl tert-Butyl Ether by a Filamentous Fungus, a Graphium sp.*, *Appl. Environ. Microbiol.* **1997**, *63*, 3059-3067.
- (163) Garnier, P. M.; Auria, R.; Augur, C.; Revah, S. *Cometabolic Biodegradation of Methyl tert-Butyl Ether by Pseudomonas Aeruginosa Grown on Pentane*, *Appl. Microbiol. Biotechnol.* **1999**, *51*, 498-503.
- (164) Garnier, P. M.; Auria, R.; Augur, C.; Revah, S. *Cometabolic Biodegradation of Methyl tert-Butyl Ether by a Soil Consortium: Effect of Components Present in Gasoline*, *J. Gen. Appl. Microbiol.* **2000**, 79-84.
- (165) Deeb, R. A.; Hu, H.-Y.; Hanson, J. R.; Scow, K. M.; Alvarez-Cohen, L. *Substrate Interactions in BTEX and MTBE Mixtures by an MTBE-Degrading Isolate*, *Environ. Sci. Technol.* **2001**, *35*, 312-317.
- (166) Bradley, P. M.; Chapelle, F. H.; Landmeyer, J. E. *Effect of Redox Conditions on MTBE Biodegradation in Surface Water Sediments*, *Environ. Sci. Technol.* **2001**, *35*, 4643-4647.
- (167) Bradley, P. M.; Chapelle, F. H.; Landmeyer, J. E. *Methyl t-Butyl Ether Mineralization in Surface-Water Sediment Microcosms under Denitrifying Conditions*, *Appl. Environ. Microbiol.* **2001**, *67*, 1975-1978.
- (168) Somsamak, P.; Cowan, R. M.; Häggblom, M. M. *Anaerobic Biotransformation of Fuel Oxygenates under Sulfate-Reducing Conditions*, *FEMS Microbiol. Ecol.* **2001**, *37*, 259-264.
- (169) Finneran, K. T.; Lovley, D. R. *Anaerobic Degradation of Methyl tert-Butyl Ether (MTBE) and tert-Butyl Alcohol (TBA)*, *Environ. Sci. Technol.* **2001**, *35*, 1785-1790.
- (170) Mormile, M. R.; Liu-Shi; Suflita, J. M. *Anaerobic Biodegradation of Gasoline Oxygenates: Extrapolation of Information to Multiple Sites and Redox Conditions*, *Environ. Sci. Technol.* **1994**, *28*, 1727-1732.
- (171) Yeh, C. K.; Novak, J. T. *Anaerobic Biodegradation of Gasoline Oxygenates in Soils*, *Water Environment Research* **1994**, *66*, 744-752.
- (172) Wilson, J. T.; Cho, J. S.; Wilson, B. H.; Vardy, J. A. *Natural Attenuation of MTBE in the Subsurface under Methanogenic Conditions*, U.S. Environmental Protection Agency, National Risk Assessment Research Laboratory, 2000.
- (173) O'Reilly, K. T.; Moir, M. E.; Taylor, C. D.; Smith, C. A.; Hyman, M. R. *Hydrolysis of tert-Butyl Methyl Ether (MTBE) in Dilute Aqueous Acid*, *Environ. Sci. Technol.* **2001**, *35*, 3954-3961.

- (174) Schmidt, T. C.; Schirmer, M.; Weiss, H.; Haderlein, S. B. *Microbial Degradation of Methyl tert-Butyl Ether (MTBE) and tert-Butyl Alcohol (TBA) in the Subsurface*, J. Contam. Hydrol. **2004**, in press.
- (175) Landmeyer, J. E.; Chapelle, F. H.; Herlong, H. H.; Bradley, P. M. *Methyl tert-Butyl Ether Biodegradation by Indigenous Aquifer Microorganisms under Natural and Artificial Oxidic Conditions*, Environ. Sci. Technol. **2001**.
- (176) Bradley, P. M.; Landmeyer, J. E.; Chapelle, F. H. *TBA Biodegradation in Surface-Water Sediments under Aerobic and Anaerobic Conditions*, Environ. Sci. Technol. **2002**, 36, 4087-4090.
- (177) Schirmer, M.; Butler, B. J.; Barker, J. F.; Church, C. D.; Schirmer, K. *Evaluation of Biodegradation and Dispersion as Natural Attenuation Processes of MTBE and Benzene at the Borden Field Site*, Phys. Chem. Earth B **1999**, 24, 557-560.
- (178) Stout, S. A.; Uhler, R. M.; Philp, R. P.; Allen, J.; Uhler, A. D. *Source Differentiation of Individual Chlorinated Solvents Dissolved in Groundwater using Compound Specific Carbon Isotopic Analysis*; Proceedings of the 216<sup>th</sup> American Chemical Society National Meeting, Boston, MA, **1998**, ACS.
- (179) Sturchio, N. C.; Clausen, J. L.; Heraty, L. J.; Huang, L.; Holt, B. D.; Abrajano, T. A. Jr. *Chlorine Isotope Investigation of Natural Attenuation of Trichloroethene in an Aerobic Aquifer*, Environ. Sci. Technol. **1998**, 32, 3037-3042.
- (180) Day, M.; Aravena, R.; Hunkeler, D.; Gulliver, T. *Application of Carbon Isotopes to Document Biodegradation of tert-Butyl Alcohol under Field Conditions*, Contaminated Soil Sediment and Water **2002**, 88-92.
- (181) Hernandez-Perez, G.; Fayolle, F.; Vandecasteele, J.-P. *Biodegradation of Ethyl t-Butyl Ether (ETBE), Methyl t-Butyl Ether (MTBE) and t-Amyl Methyl Ether (TAME) by Gordonia Terrae*, Appl. Microbiol. Biotechnol. **2001**, 55, 117-121.
- (182) Zwank, L.; Schmidt, T. C.; Berg, M.; Haderlein, S. B. *Compound-specific Carbon Isotope Analysis of Volatile Organic Compounds in the Low  $\mu\text{g/L}$ -Range*, Anal. Chem. **2003**, 75, 5575-5583.
- (183) Elsner, M.; Zwank, L.; Hunkeler, D.; Schwarzenbach, R. P. Environ. Sci. Technol. **in preparation**.
- (184) Willi, A. V. *Isotopeneffekte bei chemischen Reaktionen*; Georg Thieme Verlag: Stuttgart; New York, **1983**.



# ***APPENDIX A1***

## **THEORETICAL BACKGROUND**

## A1.1 Definitions and Calculations<sup>1</sup>

CSIA yields data of the isotopic distribution of an element  $A$  in a single compound  $x$  relative to an international standard that are usually expressed as  $\delta$  values in permil [‰] according to <sup>2</sup>

$$\delta A_x = \left( \frac{R_x - R_{Reference}}{R_{Reference}} \right) \times 1000 \quad [\text{‰}] \quad (\text{A1-1})$$

where  $R_x$  and  $R_{reference}$  are the ratios of the heavy isotope to the light isotope (e.g.  $^{13}\text{C}/^{12}\text{C}$  or D/H) in compound  $x$  and an international standard, respectively. Thus, rather than absolute values, the differences in relative ratios are reported to allow a correction for mass-discriminating effects in a single instrument and to facilitate the comparison of published GC/IRMS data. Only such relative isotope ratios can be determined with the required precision. A  $\delta^{13}\text{C}$  value of +10‰ then corresponds to a sample with an isotope ratio one percent higher than that of the international standard (usually Vienna Peedee Belemnite, VPDB). For VPDB a ratio of  $^{13}\text{C}$  versus  $^{12}\text{C}$  of 0.011180 has been reported.<sup>2</sup> The  $\delta^{13}\text{C}$  value of +10‰ for the sample then corresponds to a  $^{13}\text{C}$ -to- $^{12}\text{C}$  ratio of 0.011292, which demonstrates the very subtle changes that need to be measured. Details of referencing strategies in IRMS can be found in a review of Werner and Brand.<sup>2</sup> It is important to emphasize that accurate isotopic data for single compounds in a complex matrix/mixture can only be obtained if the corresponding peaks are well resolved. The isotope fractionation between two compounds (e.g., a substrate and its degradation product) can be expressed either with the fractionation factor  $\alpha$  or the enrichment factor  $\epsilon$  according to Equation (A1-2)

$$\alpha_{p-r} = \frac{R_{product}}{R_{reactant}} = \frac{\delta A_p + 1000}{\delta A_r + 1000} \quad (\text{A1-2})$$

- 
1. The following section has been taken from a review submitted to Analytical and Bioanalytical Chemistry<sup>1</sup>
  2. The notations used in this section are chosen to be as general as possible, hence in the case of carbon

isotopic data for example Equation (A1-1) corresponds to:  $\delta^{13}\text{C}_x = \left( \frac{\left( \frac{^{13}\text{C}}{^{12}\text{C}} \right)_x - \left( \frac{^{13}\text{C}}{^{12}\text{C}} \right)_{Reference}}{\left( \frac{^{13}\text{C}}{^{12}\text{C}} \right)_{Reference}} \right) \times 1000$

and Equation (A1-3)

$$\varepsilon_{p-r} = \left( \frac{R_{product}}{R_{reactant}} - 1 \right) \times 1000 = (\alpha - 1) \times 1000 \quad [\%] \quad (\text{A1-3})$$

where subscripts  $r$  and  $p$  refer to reactant and product, respectively, and  $R_{reactant}$  and  $R_{product}$  are the ratios of the heavy isotope to the light isotope in the substrate and the degradation product, respectively, that appear in an infinitely short period of time.<sup>3,4</sup> For small molecules in which all isotopes are located in the same reactive position,  $\alpha$  can also be interpreted according to Equation (A1-4).

$$\alpha = \frac{^{heavy}k}{^{light}k} = \frac{1}{KIE} \quad (\text{A1-4})$$

where  $^{heavy}k$  and  $^{light}k$  are the rate constants of compounds containing heavy and light isotopes at the reactive position and  $KIE = \frac{^{light}k}{^{heavy}k}$ , which is the kinetic isotope effect of the reaction.

The isotopic enrichment factor  $\varepsilon$  or the fractionation factor  $\alpha$  is usually determined by using the relationship between substrate concentration change and isotope fractionation given in Equation (A1-5)

$$\frac{R_t}{R_0} = \left[ f \cdot \frac{(1 + R_0)^{-(\alpha - 1)}}{(1 + R_t)} \right] = \left[ f \cdot \frac{(1 + R_0)}{(1 + R_t)} \right]^\varepsilon \quad (\text{A1-5})$$

where  $R_t$  and  $R_0$  are the ratios of the heavy isotope to the light isotope in the reactant  $r$  at time  $t = 0$  and  $t$ , respectively, and  $f$  is the remaining fraction of the reactant at time  $t$  according to Equation (A1-6)

$$f = \frac{L_t + H_t}{L_0 + H_0} = \frac{L_t \cdot (1 + R_t)}{L_0 \cdot (1 + R_0)} \quad (\text{A1-6})$$

where  $L_0$  and  $H_0$  are the concentrations of light isotope and the heavy isotope at time  $t = 0$ , respectively, and  $L_t$  and  $H_t$  are the concentrations of the light isotope and the heavy isotope at time  $t$ , respectively.

If studies at the low natural abundance level of the heavy isotopes are carried out (i.e.,  $H + L \approx L$ ) or the fractionation is very small (i.e.,  $1 + R_t \approx 1 + R_0$ ), Equation (A1-5) can be approximated by the following

classical Rayleigh-type equation originally derived by Lord Rayleigh to describe fractional distillation of mixed liquids:

$$\frac{R_t}{R_0} = f^{(\alpha-1)} \quad (\text{A1-7})$$

After ln transformation and combination with Equation (A1-3) we obtain:

$$\ln\left(\frac{R_t}{R_0}\right) = (\alpha - 1) \cdot \ln f = \frac{\varepsilon}{1000} \cdot \ln f \quad (\text{A1-8})$$

which yields:

$$1000 \cdot \ln\left(\frac{\delta A_{r,t} + 1000}{\delta A_{r,0} + 1000}\right) = \varepsilon \cdot \ln f \quad (\text{A1-9})$$

where  $\delta_{r,0}$  and  $\delta_{r,t}$  are the ratios of the heavy isotope to the light isotope in the reactant  $r$  at time  $t = 0$  and  $t$ , respectively, expressed in the  $\delta$  notation.

## A1.2 General Rules for the Correction of “Statistical” Effects in the Reevaluation of $\varepsilon$ -Data.<sup>1</sup>

### A1.2.1 Ratios of Isotopes and Isotopic Molecules

The natural isotopic ratio  $R = \text{heavy } A / \text{light } A$  of a given element  $A$  is assumed to be very small where  $\text{light } A$  and  $\text{heavy } A$  are the abundance of the lighter and the heavier isotope, respectively. Molecules with more than one heavy isotope can then be neglected so that only compounds, where all isotopes of  $A$  are light,  $[\text{light } A_n]$ , and molecules with just one heavy isotope present,  $[\text{heavy } A \text{ light } A_{n-1}]$ , need to be considered in the following derivations.

Because the Rayleigh equation describes whole reacting molecules rather than single isotopes inside a compound, the ratio  $R = \text{heavy } A / \text{light } A$  of total isotopes measured by CSIA must, strictly speaking, first be converted into the ratio of isotopic molecules before mathematical manipu-

---

1. The following section has been adapted from a critical review in preparation for submission to Environmental Science and Technology.<sup>5</sup>



lations can be performed. With  $n$  being the number of atoms in molecule  $A$  and assuming, that at natural abundance, a given molecule  $A$  comprises no or only one single isotopic atom of a given element,  $R$  can be written:

$$R = \frac{[{}^{heavy}A^{light}A_{n-1}]}{[{}^{light}A_n]} \quad (\text{A1-10})$$

The following equations apply:

$${}^{heavy}A = [{}^{heavy}A^{light}A_{n-1}] \quad (\text{A1-11})$$

$${}^{light}A = n \cdot [{}^{light}A_n] + (n-1) \cdot [{}^{heavy}A^{light}A_{n-1}] \quad (\text{A1-12})$$

Therefore,

$$R = \frac{{}^{heavy}A}{{}^{light}A_n} = \frac{[{}^{heavy}A^{light}A_{n-1}]}{n \cdot [{}^{light}A_n] + (n-1) \cdot [{}^{heavy}A^{light}A_{n-1}]} = \frac{R'}{n + (n-1) \cdot R'} \quad (\text{A1-13})$$

and

$$R' = \frac{n \cdot R}{1 - (n-1) \cdot R} \quad (\text{A1-14})$$

However, if values of  $R$  are small, the approximation  $R \approx n \cdot R'$  can be made so that, the Rayleigh equation can be written as:

$$\frac{R'}{R'_0} = \left[ f \cdot \frac{(1 + n \cdot R'_0)}{(1 + n \cdot R')} \right]^{(\alpha-1)} \approx f^{(\alpha-1)} \approx f^\varepsilon \quad (\text{A1-15})$$

Again, if  $R'$  is very small this expression can be approximated by the commonly known Rayleigh expression:

$$\ln\left(\frac{R'}{R'_0}\right) \approx (\alpha-1) \cdot \ln f \approx \varepsilon \cdot \ln f \quad (\text{A1-16})$$

In the following, all equations will be derived for isotopic molecules  $R=[{}^{heavy}A^{light}A_{n-1}]/[{}^{light}A_n]$  rather than isotope ratios that can be measured by CSIA after complete combustion,  $R={}^{heavy}A/{}^{light}A$ . In

cases of low natural abundance the outcome will be the same in both cases. If however, isotopic abundance is large, if fractionation becomes very strong and/or if only  $n$  becomes sufficiently large, Equation (A1-10) through Equation (A1-15) provide the framework that must be used to convert the ratios of  $R'$  into values of  $R$ .

### A1.2.2 Zero Fractionation at Non-Reacting Positions Inside a Molecule

If a molecule contains  $n$  atoms of an element  $A$  and only  $x$  of them are located at reacting positions, changes in the average isotope ratio  $\Delta\delta A_{average}$  can be converted into relevant changes at the reacting site  $\Delta\delta A_{reactive\ site}$  by:

$$\Delta\delta A_{reactivesite} = \frac{n}{x} \cdot \Delta\delta A_{average} \quad (\text{A1-17})$$

where  $A$  stands for the investigated element. The appropriate Rayleigh equation from which position specific isotope enrichment factors  $\varepsilon$  can be calculated is then:

$$\begin{aligned} \ln \frac{R}{R_0} &= \ln \frac{1000 + \delta A_0 + \Delta\delta A_{reactivesite}}{1000 + \delta A_0} \\ &= \ln \frac{1000 + \delta A_0 + \frac{n}{x} \cdot \Delta\delta A_{average}}{1000 + \delta A_0} \approx \frac{\varepsilon_{reactivesite}}{1000} \cdot \ln f \end{aligned} \quad (\text{A1-18})$$

In cases where the changes in isotope signatures  $\Delta\delta A_{reactive\ site} = n/x \cdot \Delta\delta A_{average}$  are not too large, an approximate conversion can be accomplished according to

$$\varepsilon_{reactivesite} \approx \frac{n}{x} \cdot \varepsilon_{average} \quad (\text{A1-19})$$

For these corrections, one has to assume that the isotopic signatures are initially the same for every position.

### A1.2.3 Intramolecular Isotopic Competition

If there are  $z$  indistinguishable reactive positions inside a molecule, data of these positions can be inserted in the Rayleigh equation. This will result in an enrichment factor  $\varepsilon$  that has the physical meaning of:

$$\varepsilon = \frac{1}{z} \cdot \left( \frac{\text{heavy } k}{\text{light } k} - 1 \right) = \frac{1}{z} \cdot \left( \frac{1}{KIE} - 1 \right) \quad (\text{A1-20})$$

Hence the intrinsic kinetic isotope effect can then be calculated from the isotopic enrichment factor  $\varepsilon$  by::

$$KIE = \frac{1}{z \cdot \varepsilon + 1} \quad (\text{A1-21})$$

For this correction two assumptions are necessary: (i) the heavy isotope is of low natural abundance, so that at most only one of the  $z$  positions is occupied by the heavy isotope and (ii) secondary isotope effects are neglected. The first assumption is generally valid for hydrogen, carbon, nitrogen and oxygen. If no extensive changes in bonding take place at distant positions (neighboring group participation or hyperconjugation), secondary effects are generally by at an order of magnitude smaller than primary effects, so that relative errors in KIE introduced by the second assumption are <10%.

### A1.2.4 General derivation of the proposed evaluation scheme

Considered is the arbitrary case of a molecule with  $n$  atoms of the element  $A$ , of which  $x$  are equivalent and located at reactive positions  $[A_{(n-x)}A_x]$ . It is assumed that heavy isotopes of  $A$  are of low natural abundance. In the following derivations, heavy isotopomers are written in general as  $^{\text{heavy}}[A_{(n-x)}A_x]$ , those with heavy isotopes in the non-reacting position are denoted as  $[^{\text{heavy}}A_{(n-x)}A_x]$  and those with the heavy isotope in the reactive position as  $[A_{(n-x)}^{\text{heavy}}A_x]$ . Molecules without heavy isotopes are written as  $[A_{(n-x)}A_x]$ .

The following equations apply:

$$R = \frac{^{\text{heavy}}([A_{(n-x)}A_x])}{[A_{(n-x)}A_x]} = \frac{[^{\text{heavy}}A_{(n-x)}A_x]}{[A_{(n-x)}A_x]} + \frac{[A_{(n-x)}^{\text{heavy}}A_x]}{[A_{(n-x)}A_x]} \quad (\text{A1-22})$$

$$\frac{d^{heavy}([A_{(n-x)}A_x])}{d[A_{(n-x)}A_x]} = \frac{d[{}^{heavy}A_{(n-x)}A_x]}{d[A_{(n-x)}A_x]} + \frac{d[A_{(n-x)}{}^{heavy}A_x]}{d[A_{(n-x)}A_x]} \quad (\text{A1-23})$$

In other words, both isotopic molecules react essentially independent of each other, and the observed isotopic enrichment is the *average* of the two reactions. This is important, because they can now be considered in two separate mathematical treatments, and then the effect on the average value can be calculated. In the case of  $[A_{(n-x)}{}^{heavy}A_x]$  a primary isotope effect can be expected, accompanied by intramolecular competition in situations where  $x > 1$ :

$$\frac{d[A_{(n-x)}{}^{heavy}A_x]}{d[A_{(n-x)}A_x]} = \frac{{}^{heavy}k_{primeff} + (x-1) \cdot {}^{heavy}k_{seceff}}{x \cdot {}^{light}k} \cdot \frac{[A_{(n-x)}{}^{heavy}A_x]}{[A_{(n-x)}A_x]} \quad (\text{A1-24})$$

Where the subscripts *primeff.* and *seceff.* stand for primary and secondary isotope effects, respectively. In the case of  $[{}^{heavy}A_{(n-x)}A_x]$  there will be no isotope effect:

$$\frac{d[{}^{heavy}A_{(n-x)}A_x]}{d[A_{(n-x)}A_x]} = \frac{x \cdot {}^{light}k}{x \cdot {}^{light}k} \cdot \frac{[{}^{heavy}A_{(n-x)}A_x]}{[A_{(n-x)}A_x]} = 1 \cdot \frac{[{}^{heavy}A_{(n-x)}A_x]}{[A_{(n-x)}A_x]} \quad (\text{A1-25})$$

Introduction of Equation (A1-24) and Equation (A1-25) in Equation (A1-23) gives

$$\begin{aligned} \frac{d^{heavy}([A_{(n-x)}A_x])}{d[A_{(n-x)}A_x]} &= \frac{{}^{heavy}k_{primeff} + (x-1) \cdot {}^{heavy}k_{seceff}}{x \cdot {}^{light}k} \cdot \frac{[{}^{heavy}A_{(n-x)}A_x]}{[A_{(n-x)}A_x]} \\ &\quad + \frac{[{}^{heavy}A_{(n-x)}A_x]}{[A_{(n-x)}A_x]} \end{aligned} \quad (\text{A1-26})$$

Integration of Equation (A1-25), finally, gives

$$\left( \frac{[{}^{heavy}A_{(n-x)}A_x]}{[A_{(n-x)}A_x]} \right)_t = \left( \frac{[{}^{heavy}A_{(n-x)}A_x]}{[A_{(n-x)}A_x]} \right)_0 \quad (\text{A1-27})$$

which means that molecules with the isotope in a non-reacting position  $[{}^{heavy}A_{(n-x)}A_x]$  are over the whole reaction in a constant ratio to non-labelled molecules  $[A_{(n-x)}A_x]$  in the substrate fraction and that this ratio is identical to the ratio at time 0. Knowledge about the initial isotope distribution therefore very helpful. Often, however, there is no

information about initial position-specific isotope ratios so that as a working hypothesis it must be assumed that at time 0 isotopes are statistically distributed within the molecule. Equation (A1-1) can then be rewritten for time 0:

$$R_0 = \left( \frac{[{}^{heavy}A_{(n-x)}A_x]}{[A_{(n-x)}A_x]} \right)_0 + \left( \frac{[A_{(n-x)}{}^{heavy}A_x]}{[A_{(n-x)}A_x]} \right)_0 = \frac{(n-x)}{n} \cdot R_0 + \frac{x}{n} \cdot R_0 \quad (\text{A1-28})$$

and also for any given time of conversion:

$$R = \left( \frac{[{}^{heavy}A_{(n-x)}A_x]}{[A_{(n-x)}A_x]} \right) + \left( \frac{[A_{(n-x)}{}^{heavy}A_x]}{[A_{(n-x)}A_x]} \right) = \frac{(n-x)}{n} \cdot R_0 + \left( \frac{[A_{(n-x)}{}^{heavy}A_x]}{[A_{(n-x)}A_x]} \right) \quad (\text{A1-29})$$

Hence:

$$\left( \frac{[{}^{heavy}A_{(n-x)}A_x]}{[A_{(n-x)}A_x]} \right) = \frac{(n-x)}{n} \cdot R_0 \quad (\text{A1-30})$$

and

$$\left( \frac{[A_{(n-x)}{}^{heavy}A_x]}{[A_{(n-x)}A_x]} \right) = R - \frac{(n-x)}{n} \cdot R_0 \quad (\text{A1-31})$$

If both expressions are introduced in Equation (A1-26), the result is

$$\frac{d^{heavy}([A_{(n-x)}A_x])}{d[A_{(n-x)}A_x]} = \frac{{}^{heavy}k_{primeff} + (x-1) \cdot {}^{heavy}k_{seceff}}{x \cdot {}^{light}k} \cdot \left( R - \frac{(n-x)}{n} \cdot R_0 \right) + \frac{(n-x)}{n} \cdot R_0 \quad (\text{A1-32})$$

or with

$$\frac{{}^{heavy}k_{primary\ effect} + (x-1) \cdot {}^{heavy}k_{secondary\ effect}}{x \cdot {}^{light}k} = \alpha \quad (\text{A1-33})$$

and

$$R = \frac{{}^{heavy}([A_{(n-x)}A_x])}{[A_{(n-x)}A_x]} \quad (\text{A1-34})$$

one obtains

$$\begin{aligned} \frac{d{}^{heavy}([A_{(n-x)}A_x])}{d[A_{(n-x)}A_x]} &= \alpha \cdot \left( \frac{{}^{heavy}([A_{(n-x)}A_x])}{[A_{(n-x)}A_x]} - \frac{(n-x)}{n} \cdot R_0 \right) + \frac{(n-x)}{n} \cdot R_0. \\ &= \alpha \cdot \frac{{}^{heavy}([A_{(n-x)}A_x])}{[A_{(n-x)}A_x]} + \frac{(n-x)}{n} \cdot R_0 \cdot (1 - \alpha) \end{aligned} \quad (\text{A1-35})$$

so that, finally

$$\frac{d{}^{heavy}([A_{(n-x)}A_x])}{d[A_{(n-x)}A_x]} - \alpha \cdot \frac{{}^{heavy}([A_{(n-x)}A_x])}{[A_{(n-x)}A_x]} = \frac{(n-x)}{n} \cdot R_0 \cdot (1 - \alpha). \quad (\text{A1-36})$$

The general solution of this first-order inhomogeneous differential equation is

$${}^{heavy}([A_{(n-x)}A_x]) = \kappa \cdot [A_{(n-x)}A_x]^\alpha + \frac{(n-x)}{n} \cdot R_0 \cdot [A_{(n-x)}A_x]. \quad (\text{A1-37})$$

where  $\kappa$  is an arbitrary constant introduced by integration. Division by  $[A_{(n-x)}A_x]$  gives

$$\frac{{}^{heavy}([A_{(n-x)}A_x])}{[A_{(n-x)}A_x]} = R = \kappa \cdot [A_{(n-x)}A_x]^{(\alpha-1)} + \frac{(n-x)}{n} \cdot R_0. \quad (\text{A1-38})$$

or, after subtraction of  $(n-x)/n \cdot R_0$ ,

$$R - \frac{(n-x)}{n} \cdot R_0 = \kappa \cdot [A_{(n-x)}A_x]^{(\alpha-1)}. \quad (\text{A1-39})$$

This can be expressed for  $t = 0$ ,

$$R_0 - \frac{(n-x)}{n} \cdot R_0 = \frac{x}{n} \cdot R_0 = \kappa \cdot [A_{(n-x)}A_x]^{(\alpha-1)}. \quad (\text{A1-40})$$

Division of the two equations gives

$$\frac{R - \frac{(n-x)}{n} \cdot R_0}{\frac{x}{n} \cdot R_0} = \left( \frac{[A_{(n-x)}A_x]}{[A_{(n-x)}A_x]_0} \right)^{(\alpha-1)} \quad (\text{A1-41})$$

or

$$\frac{\frac{n}{x} \cdot R - \frac{(n-x)}{x} \cdot R_0}{R_0} = \frac{R_0 + \frac{n}{x} \cdot (R - R_0)}{R_0} = \frac{R_0 + \frac{n}{x} \cdot \Delta R}{R_0} = \left( \frac{[A_{(n-x)}A_x]}{[A_{(n-x)}A_x]_0} \right)^{(\alpha-1)} \quad (\text{A1-42})$$

The proposed correction for non-reacting positions (A1-18) that was introduced in Chapter 6 as Equation (6-6) has been now derived as outcome of a stringent mathematical treatment. The term  $n/x$  that was introduced by the assumption that isotopes are initially distributed statistically in the molecule, can anytime be replaced by an experimentally determined distribution. (If, for example, SNIF-NMR measurements give the result that 20% of the deuterium is present in reactive positions,  $n/x$  can be replaced by the factor  $1 / 0.2 = 5$ ).

The correction for intramolecular competition, finally is present in the factor  $\alpha$  (Equation (A1-33)).

### A1.3 Enzymatic Effect on Kinetic Isotope Effects - “Commitment to Catalysis”<sup>1</sup>

In the case of enzymatic reactions, the measured isotope effect is not only linked to the intrinsic isotope effect, occurring during the first irreversible step of the reaction but also to other parameters that characterize the kinetics of the investigated enzyme. This effect is often referred to as “commitment to catalysis”.<sup>7</sup> This effect has been explained in the case of the aerobic mineralization of 1,2-dichloroethane by the well studied haloalkane dehalogenase.<sup>6</sup>

The isotopic fractionation factor  $\alpha$  for enzymatic reactions is often defined by:

$$\alpha = \frac{d^{13}P/d^{12}P}{^{13}S/^{12}S} \quad (\text{A1-43})$$

---

1. The following section has been adapted from Hunkeler & Aravena.<sup>6</sup>

where  $d^{13}P$  and  $d^{12}P$  are increments of product containing  $^{13}C$  and  $^{12}C$ , respectively, which appear in an infinitely short period of time and  $^{13}S$  and  $^{12}S$  are the concentrations of substrate with  $^{12}C$  and  $^{13}C$ , respectively.

If substrate with  $^{12}C$  and  $^{13}C$  at the reactive center is available, the amount of product with  $^{12}C$  ( $d^{12}P$ ) that is formed during an infinitely short period  $dt$  is given by:

$$\frac{d^{12}P}{dt} = \frac{{}^{12}V \cdot {}^{12}S}{{}^{12}S + {}^{12}K_m \cdot \left(1 + \frac{{}^{13}S}{{}^{13}K_m}\right)} \quad (\text{A1-44})$$

where  ${}^{12}V$  is the limiting rate for substrate with  $^{12}C$  at the reactive center,  ${}^{12}S$  and  ${}^{13}S$  are the concentrations of substrate with  $^{12}C$  and  $^{13}C$ , respectively, at the reactive center, and  ${}^{12}K_m$  and  ${}^{13}K_m$  are the Michaelis Menten constants for substrate with  $^{12}C$  and  $^{13}C$ , respectively at the reactive center. By inserting Equation (A1-44) and an analogous equation for  $d^{13}P$  into Equation (A1-43), the following expression for  $\alpha$  is obtained:

$$\alpha = \frac{d^{13}P/d^{12}P}{{}^{13}S/{}^{12}S} = \frac{{}^{13}V/{}^{13}K_m}{{}^{12}V/{}^{12}K_m} = \frac{1}{{}^{13}(V/K)} \quad (\text{A1-45})$$

where  ${}^{13}(V/K)$  is defined by:

$${}^{13}(V/K) = \frac{{}^{12}V/{}^{12}K_m}{{}^{13}V/{}^{13}K_m} \quad (\text{A1-46})$$

and stands for the isotopic effect on  $V/K$ . For the haloalkane dehalogenase, for example,  $V/K$  is given by:

$$V/K = \frac{k_1 \cdot k_2 \cdot E_t}{k_{-1} + k_2} \quad (\text{A1-47})$$

where  $k_1$  and  $k_{-1}$  are the rates of formation and dissociation of the enzyme-substrate complex,  $k_2$  the rate of the first irreversible catalytic step and  $E_t$  is the total enzyme concentration (see also Figure A1.1).

Commitment to catalysis (C) represents the tendency of the enzyme-substrate complex to go forward through catalysis rather than to break down to free enzyme and substrate ( $C = {}^{12}k_2/k_{-1}$ )(Figure A1.1). The



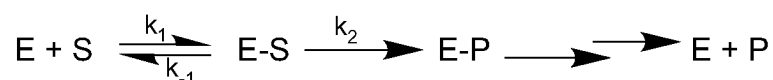


**Figure A1.1: Reaction Scheme for Haloalkane Dehalogenase (modified from Hunkeler & Aravena<sup>6</sup>).** *E*, *E-S* and *E-P* stand for the enzyme, the enzyme substrate complex and the enzyme product complex, respectively.

intrinsic fractionation factor is defined as the relative reaction rates of the substrates containing the heavy isotopes compared to the ones with the light isotopes in the first irreversible step of the reaction ( $^{13}k_2/^{12}k_2$ ). Assuming that the isotopic fractionation associated with the formation and dissociation of the enzyme-substrate complex one obtains by inserting Equation (A1-47) into Equation (A1-45): Equation (A1-48)

$$\frac{1}{\alpha} = {}^{13}(V/K) = \frac{{}^{12}k_2/{}^{13}k_2 + C}{1 + C} \quad (\text{A1-48})$$

As can be seen from the magnitude of the isotopic fractionation depends on the commitment of catalysis. The larger the rate of catalysis ( $k_2$ ) compared to  $k_{-1}$  (e.g., the larger  $C$ ) the smaller is the measured isotopic fractionation for a given intrinsic isotope effect. Hence, depending on this affinity of the enzyme for different substrates, differences between microbial and abiotic reactions can be more or less pronounced, complicating the differentiation between abiotic and microbial reactions at field sites.

## A1.4 References

- (1) Schmidt, T. C.; Zwank, L.; Elsner, M.; Berg, M.; Meckenstock, R. U.; Haderlein, S. B.; *Compound-specific Stable Isotope Analysis of Organic Contaminants in Natural Environments - State of the Art, Prospects and Future Challenges*; Analytical and Bioanalytical Chemistry; **2004**, 283-300.
- (2) Werner, R. A.; Brand, W. A.; *Referencing Strategies and Techniques in Stable Isotope Ratio Analysis*; Rapid Communications in Mass Spectrometry; **2001**, (15) 501-519.
- (3) Clark, I. D.; Fritz, P.; *Environmental Isotopes in Hydrogeology*, 1<sup>st</sup> ed.; Lewis Publishers (CRC Press): Boca Raton, **1997**.
- (4) Mariotti, A.; Germon, J. C.; Hubert, P.; Kaiser, P.; Letolle, R.; Tardieux, A.; P., T.; *Experimental Determination of Nitrogen Kinetic Isotope Fractionation: Some Principles; Illustration for the Denitrification and Nitrification Processes*; Plant and Soil; **1981**, (62) 413-430.
- (5) Elsner, M.; Zwank, L.; Hunkeler, D.; Schwarzenbach, R. P.; *Environmental Science & Technology*; **in preparation**,
- (6) Hunkeler, D.; Aravena, R.; *Evidence of Substantial Carbon Isotope Fractionation among Substrate, Inorganic Carbon, and Biomass during Aerobic Mineralization of 1,1-Dichloroethane by Xanthobacter autotrophicus*; Applied and Environmental Microbiology; **2000**, (66) 11, 4870-4876.
- (7) Northrop, D. B. In *Enzyme Mechanism from Isotope Effects*; Cook, P. F., Ed.; CRC Press: Boca Raton, Fl., **1991**.

# ***APPENDIX A2***

## **ISOTOPIC ENRICHMENT FACTORS REPORTED FOR TRANSFORMATION REACTIONS OF ENVIRONMENTAL CONTAMINANTS**

**Table A2.1: Reported Enrichment Factors for Carbon, Hydrogen and Chloride from Laboratory Degradation Experiments**

Compound	Reaction	Enrichment factor $\epsilon$ [‰]			Details	Ref.
		C	H	Cl		
1,1,2-trichloroethane	Microbial reduction	-2				(1)
1,1-dichloroethylene	Microbial reduction	-7.3				(1)
1,2 dichloroethane	Aerobic biodegradation	-27; -28; -30; -29; -30; -32			<i>Xanthobacter autotrophicus</i>	(2)
1,2-dichloroethane	Microbial reduction	-32.1				(1)
1,2-dichloroethane				-4.5	Haloalkane dehalogenase from <i>Xanthobacter autotrophicus</i>	(3)
1-chloro-butane				-6.6	Haloalkane dehalogenase from <i>Xanthobacter autotrophicus</i>	(3)
2,3,4,5- tetrachloro-biphenyl	Microbial reduction	prob. 0				(4)
Benzene	Aerobic biodegradation	-1.46	-12.8		<i>Acinetobacter sp.</i>	(5)
Benzene	Aerobic biodegradation	-3.53	-11.2		<i>Burkholderia sp.</i>	(5)
Benzene	Anaerobic biodegradation	-2.4; -2.2	-29; -35		Mixed consortium (from field site); nitrate reducing	(6)
Benzene	Anaerobic biodegradation	-3.6	-79		Mixed consortium (from field site); sulfate reducing	(6)
Benzene	Anaerobic biodegradation	-1.9; 2.1	-60; -59		Mixed consortium (from field site); methanogenic	(6)
Benzene	Anaerobic biodegradation	-2.0	-59		Mixed consortium (from field site); methanogenic	(6)
Benzylchloride	Abiotic	-7.2; -7.6			$S_N2$ reduction by sodium borhydride;	(7)
<i>cis</i> -1,2-dichloroethylene	Abiotic oxidation with permanganate	-21.1				(8)
<i>cis</i> -1,2-dichloroethylene	Abiotic reduction with Fe(0)	-14.4				(9)
<i>cis</i> -1,2-dichloroethylene	Microbial reduction	-12			estimated from $\delta^{13}C_{\text{precursor}} - \delta^{13}C_{\text{product}}$	(10)
<i>cis</i> -1,2-dichloroethylene	Microbial reduction	-20.4			Mixed consortium (KB-1)	(11)
<i>cis</i> -1,2-dichloroethylene	Microbial reduction	-14.1; -16.1			2 separate batch experiments	(12)
<i>cis</i> -1,2-dichloroethylene	Microbial reduction	-19.9				(1)
DDT	Abiotic dehydrochlorination			-9		(13)

**Table A2.1: Reported Enrichment Factors for Carbon, Hydrogen and Chloride from Laboratory Degradation Experiments**

Compound	Reaction	Enrichment factor $\epsilon$ [‰]			Details	Ref.
		C	H	Cl		
Dichloromethane	Aerobic biodegradation	-42.4		-38	<i>MC8b</i>	(14)
Ethene	Microbial reduction	-4.0; -2.6; -2.3			TCE-, DCE, and VC-degraders, respectively	(12)
Methyl <i>tert</i> -butyl ether	Aerobic biodegradation	-2.0; -2.4	-33; -37		<i>PM1</i> ; 2 replicates	(15)
Methyl <i>tert</i> -butyl ether	Aerobic biodegradation	-1.5; -1.8	-29; -66		Mixed consortium; 2 replicates	(15)
Methyl <i>tert</i> -butyl ether	Aerobic biodegradation	-1.97; -1.87; -1.64; -1.84			Mixed consortium; MTBE as only substrate	(16)
Methyl <i>tert</i> -butyl ether	Aerobic biodegradation	-1.52			Mixed consortium; cometabolic with 3-methylpentane as primary substrate	(16)
Methyl <i>tert</i> -butyl ether	Anaerobic biodegradation	-8.1			Mixed consortium	(17)
Methyl <i>tert</i> -butyl ether	Anaerobic biodegradation	-9.16	-11.5		Field data	(18)
Methylbromide	Aerobic biodegradation	-66; -72			<i>IMB-1</i> ; different cell density	(19)
Methylbromide	Aerobic biodegradation	-63; -57			<i>MB-2</i> ; different cell density	(19)
Methylbromide	Aerobic biodegradation	-4			<i>CC495</i> ; high cell density	(19)
Methylchloride	Abiotic oxidation	-21			Enzyme isolated from <i>CC495</i>	(19)
Methylchloride	Aerobic biodegradation	-50; -47			<i>IMB-1</i> ; different cell density	(19)
Methylchloride	Aerobic biodegradation	-44			<i>MB-2</i>	(19)
Methylchloride	Aerobic biodegradation	-42			<i>CC495</i> ; high cell density	(19)
Methyl iodide	Aerobic biodegradation	-40; -29			<i>IMB-1</i> ; different cell density	(19)
Methyl iodide	Aerobic biodegradation	-30			<i>MB-2</i>	(19)
Methyl iodide	Aerobic biodegradation	-9			<i>CC495</i> ; high cell density	(19)
n-alkane (C15)	Aerobic biodegradation		-7.1		Activated sewage sludge	(20)
n-alkane (C16)	Aerobic biodegradation		-18.9		Activated sewage sludge	(20)
n-alkane (C17)	Aerobic biodegradation		-12.3		Activated sewage sludge	(20)

**Table A2.1: Reported Enrichment Factors for Carbon, Hydrogen and Chloride from Laboratory Degradation Experiments**

Compound	Reaction	Enrichment factor $\epsilon$ [‰]			Details	Ref.
		C	H	Cl		
n-alkane (C18)	Aerobic biodegradation		-3.8		Activated sewage sludge	(20)
Perchlorate	Aerobic biodegradation			-16.6; -12.9	<i>Dechlorosoma suillum</i> ;	(21)
<i>tert</i> -butanol	Aerobic biodegradation	-4.21			Mixed consortium; cometabolic with 3-methylpentane as primary substrate	(16)
Tetrachloroethylene	Abiotic oxidation with permanganate	-17.7; -15.7; -17.6				(8)
Tetrachloroethylene	Abiotic reduction with Fe(0)	-25.3				(9)
Tetrachloroethylene	Abiotic reduction with vitamin B12	-16.5; -15.8				(22)
Tetrachloroethylene	Microbial reduction	-2			estimated from $\delta^{13}\text{C}_{\text{precursor}} - \delta^{13}\text{C}_{\text{product}}$	(10)
Tetrachloroethylene	Microbial reduction	-5.5			Mixed consortium (KB-1)	(11)
Tetrachloroethylene	Microbial reduction	"-5,1; -5.2; -2.7"			Isolate from treatment plant	(11)
Tetrachloroethylene	Microbial reduction			-9; -12	3 different mixed consortia	(23)
Toluene	Aerobic biodegradation	-2.6			<i>Pseudomonas putida</i>	(24)
Toluene	Aerobic biodegradation		-4.98		<i>Pseudomonas putida</i> ; tol- $d_8$ and tol- $d_3$	(25)
Toluene	Aerobic biodegradation		-956.4		<i>Pseudomonas putida</i> ; tol- $d_3$ and nonlabeled toluene	(25)
Toluene	Aerobic biodegradation		-926.4		<i>Pseudomonas putida</i> ; tol- $d_8$ and tol- $d_5$	(25)
Toluene	Aerobic biodegradation		-89.25		<i>Pseudomonas putida</i> ; tol- $d_5$ and nonlabeled toluene	(25)
Toluene	Aerobic biodegradation		-943.8		<i>Pseudomonas putida</i> ; tol- $d_8$ and nonlabeled toluene	(25)
Toluene	Anaerobic biodegradation	-0.5			Sulfate reducing culture	(26)
Toluene	Anaerobic biodegradation	-0.8			Methanogenic culture	(26)
Toluene	Anaerobic biodegradation	-1.7			<i>Thauera aromatica</i> ; nitrate reducing	(24)
Toluene	Anaerobic biodegradation	-1.8			<i>Geobacter metallireducens</i> ; iron reducing	(24)
Toluene	Anaerobic biodegradation	-1.7			<i>TRM1</i> , sulfate reducing	(24)

**Table A2.1: Reported Enrichment Factors for Carbon, Hydrogen and Chloride from Laboratory Degradation Experiments**

Compound	Reaction	Enrichment factor $\epsilon$ [‰]			Details	Ref.
		C	H	Cl		
Toluene	Anaerobic biodegradation	-1.5			Non sterile soil column (sulfate reducing)	(24)
Toluene	Anaerobic biodegradation		-198.1		<i>Desulfobacterium cetonicum</i>	(25)
Toluene	Anaerobic biodegradation		4.016		<i>Desulfobacterium cetonicum</i> ; tol- $d_8$ and tol- $d_3$	(25)
Toluene	Anaerobic biodegradation		-734.9		<i>Desulfobacterium cetonicum</i> ; tol- $d_3$ and nonlabeled toluene	(25)
Toluene	Anaerobic biodegradation		-514.1		<i>Desulfobacterium cetonicum</i> ; tol- $d_8$ and tol- $d_5$	(25)
Toluene	Anaerobic biodegradation		-8.92		<i>Desulfobacterium cetonicum</i> ; tol- $d_5$ and nonlabeled toluene	(25)
Toluene	Anaerobic biodegradation		-691.7		<i>Desulfobacterium cetonicum</i> ; tol- $d_8$ and nonlabeled toluene	(25)
Toluene	Anaerobic biodegradation		-726		TRM1; sulfate reducing	(25)
Toluene	Anaerobic biodegradation		129.9		TRM1; sulfate reducing; tol- $d_8$ and tol- $d_3$	(25)
Toluene	Anaerobic biodegradation		-704.5		TRM1; sulfate reducing; tol- $d_3$ and nonlabeled toluene	(25)
Toluene	Anaerobic biodegradation		-516.9		TRM1; sulfate reducing; tol- $d_8$ and tol- $d_5$	(25)
Toluene	Anaerobic biodegradation		-13.81		TRM1; sulfate reducing; tol- $d_5$ and nonlabeled toluene	(25)
Toluene	Anaerobic biodegradation		-694.7		TRM1; sulfate reducing; tol- $d_8$ and nonlabeled toluene	(25)
Toluene	Anaerobic biodegradation		-606.8		<i>Thauera aromatica</i> ; nitrate reducing; tol- $d_8$ and nonlabeled toluene	(25)
Toluene	Anaerobic biodegradation		-607.8		<i>Geobacter metallireducens</i> ; iron reducing; tol- $d_8$ and nonlabeled toluene	(25)
Toluene	Anaerobic biodegradation		-65 to -12		Methanogenic culture	(27)
<i>trans</i> -1,2-dichloroethylene	Anaerobic biodegradation	-3.5			<i>Methylomonas methanica</i> ; methanogenic; cometabolic	(28)
<i>trans</i> -1,2-dichloroethylene	Anaerobic biodegradation	-6.7			<i>Methylosinus trichosporium</i> ; methanogenic; cometabolic	(28)
<i>trans</i> -1,2-dichloroethylene	Microbial reduction	-30.3				(1)

**Table A2.1: Reported Enrichment Factors for Carbon, Hydrogen and Chloride from Laboratory Degradation Experiments**

Compound	Reaction	Enrichment factor $\epsilon$ [‰]			Details	Ref.
		C	H	Cl		
Trichloroethylene	Abiotic oxidation with permanganate	-20.9; -21.3; -26.3; -18.5; -22.0				(8)
Trichloroethylene	Abiotic oxidation with permanganate	-25.1; -26.8			1 exp. with excess permanganate; 1 exp. with limited permanganate	(29)
Trichloroethylene	Abiotic reduction with Fe(0)	-16				(30)
Trichloroethylene	Abiotic reduction with Fe(0)	-8.6				(9)
Trichloroethylene	Abiotic reduction with Fe(0)	-7.6				(31)
Trichloroethylene	Abiotic reduction with hydrogen on palladium catalyst	-4.8				(31)
Trichloroethylene	Abiotic reduction with vitamin B12	-17.2; -16.6				(22)
Trichloroethylene	Microbial oxidation	-18.2; -20.4; -20.7			different cell density	(32)
Trichloroethylene	Microbial reduction	-7.1				(33)
Trichloroethylene	Microbial reduction	-4			estimated from $\delta^{13}\text{C}_{\text{precursor}} - \delta^{13}\text{C}_{\text{product}}$	(10)
Trichloroethylene	Microbial reduction	-13.8			Mixed consortium (KB-1)	(11)
Trichloroethylene	Microbial reduction	-6.6; -2.5				(12)
Trichloroethylene	Microbial reduction			-5; -6	3 different mixed consortia	(23)
Vinyl Chloride	Microbial reduction	-26			estimated from $\delta^{13}\text{C}_{\text{precursor}} - \delta^{13}\text{C}_{\text{product}}$	(10)
Vinyl Chloride	Microbial reduction	-22.4			Mixed consortium (KB-1)	(11)
Vinyl Chloride	Microbial reduction	-26.6; -21.5				(12)



## References

- (1) Hunkeler, D.; Aravena, R.; Cox, E.; *Carbon Isotopes as a Tool to Evaluate the Origin and Fate of Vinyl Chloride: Laboratory Experiments and Modeling of Isotope Evolution*; Environmental Science and Technology; **2002**, (36) 15, 3378-3384.
- (2) Hunkeler, D.; Aravena, R.; *Evidence of Substantial Carbon Isotope Fractionation among Substrate, Inorganic Carbon, and Biomass during Aerobic Mineralization of 1,1-Dichloroethane by Xanthobacter autotrophicus*; Applied and Environmental Microbiology; **2000**, (66) 11, 4870-4876.
- (3) Lewandowicz, A.; Rudzinski, J.; Tronstad, L.; Widersten, M.; Ryberg, P.; Matsson, O.; Paneth, P.; *Chlorine Kinetic Isotope Effects on the Haloalkane Dehalogenase Reaction*; Journal of the American Chemical Society; **2001**, (123) 4550-4555.
- (4) Drenzek, N. J.; Eglinton, T. I.; Wirsén, C. O.; May, H. D.; Wu, Q.; Sowers, K. R.; Reddy, C. M.; *The Absence and Application of Stable Carbon Isotopic Fractionation during the Reductive Dechlorination of Polychlorinated Biphenyls*; Environmental Science and Technology; **2001**, (35) 16, 3310-3313.
- (5) Hunkeler, D.; Andersen, N.; Aravena, R.; Bernasconi, S. M.; Butler, B. J.; *Hydrogen and Carbon Isotope Fractionation during Aerobic Biodegradation of Benzene*; Environmental Science and Technology; **2001**, (35) 17, 3462-3467.
- (6) Mancini, S. A.; Ulrich, A. C.; Lacrampe-Couloume, G.; Sleep, B. E.; Edwards, E. A.; Lollar, B. S.; *Carbon and hydrogen isotopic fractionation during anaerobic biodegradation of benzene*; Applied and Environmental Microbiology; **2003**, (69) 1, 191-198.
- (7) Westaway, K. C.; Koerner, T.; Fang, Y.-R.; Rudzinski, J.; Paneth, P.; *A New Method of Determining Chlorine Kinetic Isotope Effects*; Analytical Chemistry; **1998**, (70) 3548-3552.
- (8) Poulson, S. R.; Naraoka, H.; *Carbon Isotope Fractionation during Permanganate Oxidation of Chlorinated Ethylenes (cDCE, TCE, PCE)*; Environmental Science and Technology; **2002**, (36) 15, 3270-3274.
- (9) Dayan, H.; Abrajano, T. A.; Sturchio, N. C.; Winsor, L.; *Carbon Isotopic Fractionation during Reductive Dehalogenation of Chlorinated Ethenes by Metallic Iron*; Organic Geochemistry; **1999**, (30) 8A, 755-763.
- (10) Hunkeler, D.; Aravena, R.; Butler, B. J.; *Monitoring Microbial Dechlorination of Tetrachloroethene (PCE) in Groundwater Using Compound-Specific Stable Carbon Isotope Ratios: Microcosm and Field Studies*; Environmental Science and Technology; **1999**, (33) 16, 2733-2738.
- (11) Slater, G. F.; Lollar, B. S.; Edwards, E. A.; *Variability in Carbon Isotopic Fractionation during Biodegradation of Chlorinated Ethenes: Implications for Field Applications*; Environmental Science and Technology; **2001**, (35) 5, 901-907.
- (12) Bloom, Y.; Aravena, R.; Hunkeler, D.; Edwards, E.; Frappe, S. K.; *Carbon Isotope Fractionation During Microbial Dechlorination of Trichloroethene, cis-1,2-Dichloroethene, and Vinyl chloride: Implications for Assessment of Natural Attenuation*; Environmental Science and Technology; **2000**, (34) 13, 2768-2772.
- (13) Reddy, C. M.; Drenzek, N. J.; Eglinton, T. I.; Heraty, L. J.; Sturchio, N. C.; Shiner, V. J.; *Stable Chlorine Intramolecular Kinetic Isotope Effects from the Abiotic Dehydrochlorination of DDT*; Environmental Science and Pollution Research; **2002**, (9) 3, 183-186.

- (14) Heraty, L. J.; Fuller, M. E.; Huang, L.; Abrajano, T. J.; Sturchio, N. C.; *Isotopic Fractionation of Carbon and Chlorine by Microbial Degradation of Dichloromethane*; *Organic Geochemistry*; **1999**, (30) 793-799.
- (15) Gray, J. R.; Lacrampe-Couloume, G.; Deepa, G.; Scow, K. M.; Wilson, R. D.; Mackay, D. M.; Sherwood Lollar, B.; *Carbon and Hydrogen Isotopic Fractionation during Biodegradation of Methyl tert-Butyl Ether*; *Environmental Science and Technology*; **2002**, (36) 9, 1931-1938.
- (16) Hunkeler, D.; Butler, B. J.; Aravena, R.; Barker, J. F.; *Monitoring Biodegradation of Methyl tert-Butyl Ether (MTBE) Using Compound-Specific Carbon Isotope Analysis*; *Environmental Science and Technology*; **2001**, (35) 4, 676-681.
- (17) Kolhatkar, R.; Kuder, T.; Philp, R. P.; Allen, J.; Wilson, J. T.; *Use of Compound-Specific Stable Carbon Isotope Analysis to Demonstrate Anaerobic Biodegradation of MTBE in Groundwater at a Gasoline Release Site*; *Environmental Science & Technology*; **2002**, (36) 5139-5146.
- (18) Kuder, T.; Philp, R. P.; Kolhatkar, R.; Wilson, J. T.; Allen, J. *NGWA/API Petroleum Hydrocarbons and Organic Chemicals in Ground Water*, Atlanta, **2002**.
- (19) Miller, L. G.; Kalin, R. M.; McCauley, S. E.; Hamilton, J. T. G.; Harper, D. B.; Millet, D. B.; Oremland, R. S.; Goldstein, A. H.; *Large Carbon Isotope Fractionation Associated with Oxidation of Methyl Halides by Methylophilic Bacteria*; *Proceedings of the National Academy of Sciences of the United States of America*; **2001**, (98) 10, 5833-5837.
- (20) Pond, K. L.; Huang, Y.; Wang, Y.; Kulpa, C. F.; *Hydrogen Isotopic Composition of Individual n-Alkanes as an Intrinsic Tracer for Bioremediation and Source Identification of Petroleum Contamination*; *Environmental Science and Technology*; **2002**, (36) 4, 724-728.
- (21) Sturchio, N. C.; Hatzinger, P. B.; Arkins, M. D.; Suh, C.; Heraty, L. J.; *Chlorine Isotope Fractionation during Microbial Reduction of Perchlorate*; *Environmental Science & Technology*; **2003**, (37) 17, 3859-3863.
- (22) Slater, G. F.; Lollar, B. S.; Lesage, S.; Brown, S.; *Carbon Isotope Fractionation of PCE and TCE During Dechlorination by Vitamin B12*; *Environmental Science & Technology*; **submitted**.
- (23) Numata, M.; Nakamura, N.; Koshikawa, H.; Terashima, Y.; *Chlorine Isotope Fractionation during Reductive Dechlorination of Chlorinated Ethenes by Anaerobic Bacteria*; *Environmental Science & Technology*; **2002**, (36) 4389-4394.
- (24) Meckenstock, R. U.; Morasch, B.; Warthmann, R.; Schink, B.; Annweiler, E.; Michaelis, W.; Richnow, H. H.;  *$^{13}\text{C}/^{12}\text{C}$  Isotope Fractionation of Aromatic Hydrocarbons During Microbial Degradation*; *Environmental Microbiology*; **1999**, (1) 5, 409-414.
- (25) Morasch, B.; Richnow, H. H.; Schink, B.; Meckenstock, R. U.; *Stable Hydrogen and Carbon Isotope Fractionation during Microbial Toluene Degradation: Mechanistic and Environmental Aspects*; *Applied and Environmental Microbiology*; **2001**, (67) 10, 4842-4849.
- (26) Ahad, J. M. E.; Lollar, B. S.; Edwards, E. A.; Slater, G. F.; Sleep, B. E.; *Carbon Isotope Fractionation during Anaerobic Biodegradation of Toluene: Implications for Intrinsic Bioremediation*; *Environmental Science and Technology*; **2000**, (34) 5, 892-896.
- (27) Ward, J. A. M.; Ahad, J. M. E.; Lacrampe-Couloume, G.; Slater, G. F.; Edwards, E. A.; Lollar, B. S.; *Hydrogen Isotope Fractionation during Methanogenic Degradation of Toluene: Poten-*

- tial for Direct Verification of Bioremediation*; Environmental Science and Technology; **2000**, (34) 4577-4581.
- (28) Brungard, K. L.; Munakata-Marr, J.; Johnson, C. A.; Mandernack, K. W.; *Stable Carbon Isotope Fractionation of trans-1,2-dichloroethylene during Co-Metabolic Degradation by Methanotrophic Bacteria*; Chemical Geology; **2003**, (195) 1-4, 59-67.
- (29) Hunkeler, D.; Aravena, R.; Parker, B. L.; Cherry, J. A.; X., D.; *Monitoring Oxidation of Chlorinated Ethenes by Permanganate in Groundwater Using Stable Isotopes: Laboratory and Field Studies*; Environmental Science & Technology; **2003**, (37) 4, 798-804.
- (30) Slater, G. F.; B., H. D. S. L.; Spivack, J.; Brennan, M.; Mackenzie, P. International Conference on Remediation of Chlorinated and Recalcitrant Compounds, Monterey, CA, **1998**; p 133-138.
- (31) Bill, M.; Schütt, C.; Barth, J. A. C.; Kalin, R. M.; *Carbon Isotopic Fractionation During Abiotic Reductive Dehalogenation of Trichloroethene (TCE)*; Chemosphere; **2001**, (44) 1281-1286.
- (32) Barth, J. A. C.; Slater, G. F.; Schüth, C.; Bill, M.; Downey, A.; Larkin, M. J.; Kalin, R. M.; *Carbon Isotope Fractionation during Aerobic Biodegradation of Trichloroethene by Burkholderia cepacia G4: a Tool to Map Degradation Mechanisms*; Applied and Environmental Microbiology; **2002**, (68) 4, 1728-1734.
- (33) Sherwood Lollar, B.; Slater, G. F.; Ahad, J.; Sleeb, B.; Spivack, J.; Brennan, M.; Mackenzie, P.; *Contrasting Carbon Isotope Fractionation during Biodegradation of Trichloroethylene and Toluene: Implications for Intrinsic Bioremediation*, Organic Geochemistry; **1999**, (30), 813-820.



# ***APPENDIX A3***

## **HYDROGEN ISOTOPIC SIGNATURES OF PRODUCTS FROM THE MICROBIAL DEGRADATION OF PER AND TCE BY DEHALOSPIRILLUM MULTIVORANS**

### A 3.1 Experiments Spiked with Tetrachloroethene (PER)

The results from the preliminary experiment shown in Table A5.1 could be reproduced in a second degradation experiment (see Table A3.1). Again it is shown that TCE as well *cis*-DCE produced

**Table A3.1:Compound-Specific Hydrogen Isotopic Data of Degradation Products and Bulk H<sub>2</sub>O**

Experiment	$\delta^2\text{H}$		
	TCE [‰ vs VSMOW]	<i>cis</i> -DCE [‰ vs VSMOW]	H <sub>2</sub> O [‰ vs VSMOW]
Microbial 1	-121 ± 53	-206 ± 36	n.d. <sup>a</sup>
Microbial 2	n.d. <sup>a</sup>	-150 ± 79	n.d. <sup>a</sup>
Microbial 3	-228 ± 20	n.d. <sup>a</sup>	n.d. <sup>a</sup>
Microbial 4	-165 ± 125	n.d. <sup>a</sup>	n.d. <sup>a</sup>
Standard	+549 ± 27	+295 ± 27	

a. Not determined.

by the microbial degradation of PER are significantly depleted in deuterium as compared to anthropogenic sources, hence allowing a distinction of the sources of these contaminants in groundwater.

### A 3.2 Experiments Spiked with Trichloroethene (TCE)

In addition to the above mentioned experiments, experiments were carried out by initially spiking TCE instead of PER. The results found during these experiments are resumed in Table A3.2. The high scattering of the hydrogen isotopic data of TCE can not be explained and does not allow an identification. The isotopic signatures of *cis*-DCE, however, are becoming enriched in deuterium as the reaction proceeds (Figure A3.1). This effect did not appear in either experiment previously spiked with PER and could not be explained so far. Different aspects including the conservation method with NaOH, purge and trap extraction as well as the GC-method have to be reevaluated for their influence on the hydrogen isotopic composition of the target analytes. After this evaluation an additional degradation experiment focussed on the course of hydrogen isotopic signatures (i.e. more replicate measurements as well as a higher sampling rate in the PER experiment) during the degradation should be carried out.

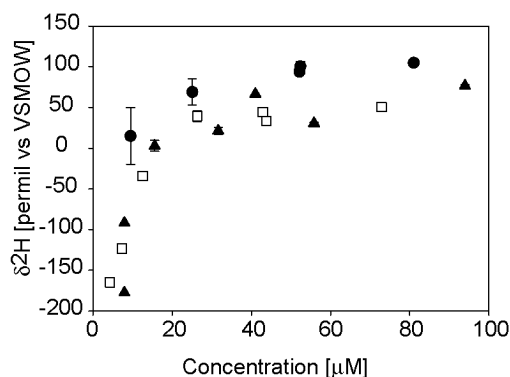
**Table A3.2: Compound-Specific Hydrogen Isotopic Signatures Observed during the Microbial Dehalogenation of TCE**

Replicate	Time [h]	TCE		cis-DCE	
		Concentration [ $\mu\text{M}$ ]	$\delta^2\text{H}$ [‰ vs VSMOW]	Concentration [ $\mu\text{M}$ ]	$\delta^2\text{H}$ [‰ vs VSMOW]
1	14.5	63.7	-133 $\pm$ 16	9.5	15 $\pm$ 35
	20	45.3	-120 $\pm$ 0.8	25.1	69 $\pm$ 16
	23.25	33.4	-115 $\pm$ 1.5	52.2	94 $\pm$ 5
	26.5	10.3	-54 $\pm$ 12	52.4	100 $\pm$ 6
	29.5	n.f. <sup>a</sup>	n.d. <sup>b</sup>	81	105 $\pm$ 4
2	0	90.4	-330 <sup>c</sup>	4.3	-160 <sup>c</sup>
	5.5	102	-220 <sup>c</sup>	7.3	-120 <sup>c</sup>
	14.5	81.3	-410 <sup>c</sup>	12.5	-34 <sup>c</sup>
	20	53.9	n.d. <sup>b</sup>	26.3	39 $\pm$ 6
	23.25	32.1	n.d. <sup>b</sup>	43.8	33 $\pm$ 6
	26.5	10.3	n.d. <sup>b</sup>	42.9	44 $\pm$ 4
	29.5	n.f. <sup>a</sup>	n.d. <sup>b</sup>	72.9	50
3	0	195	194	7.9	-177 <sup>c</sup>
	5.5	195	-69	7.9	-92 <sup>c</sup>
	14.5	169	67	15.5	3 $\pm$ 7
	20	139	n.d. <sup>b</sup>	31.6	21 $\pm$ 4
	23.25	110	n.d. <sup>b</sup>	41.0	66 <sup>c</sup>
	26.5	87.6	n.d. <sup>b</sup>	55.8	31 $\pm$ 1
	29.5	34.7	269	93.9	76 $\pm$ 1

a. Not found

b. Not determined

c. n = 1

**Figure A3.1: Hydrogen Isotopic Enrichment of cis-DCE Produced During Microbial Dehalogenation of TCE.** The results of three different replicate experiments (filled triangles, circles and empty squares) are shown.





# CURRICULUM VITAE

Luc Zwank

geboren am 2. Januar 1975 in Luxemburg

## Ausbildung

1981-1987            Grundschule, Lintgen

1987-1994            Gymnasium, Athénée de Luxembourg, Luxemburg

1994-2000            Diplomstudium in Umweltnaturwissenschaften mit  
Fachvertiefung Chemie an der Eidgenössischen  
Technischen Hochschule Zürich (ETHZ)

1995/1996            Erstes und Zweites Vordiplom, ETHZ

1998            Berufspraktikum an der Umweltverwaltung in  
Luxemburg mit dem Ziel der Bestimmung der  
Umwelteinflüsse durch die Weinherstellung in  
Luxemburg in Zusammenarbeit mit dem staatli-  
chen Weinbauinstitut.

2000            Diplomarbeit: *The Fate and Distribution of cis-Dichlo-  
roethylene and Trichloroethylene in a Small Lake Adja-  
cent to a Superfund Site in the Aberjona Watershed*;  
durchgeführt am Ralph M. Parsons Laboratory am  
Massachusetts Institute of Technology (MIT), Cam-  
bridge, MA, in der Forschungsgruppe von Prof. Dr.  
Philip M. Gschwend.

2000-2003            Doktorarbeit an der Eidgenössischen Anstalt für  
Wasserbau, Abwasser und Gewässerschutz,  
EAWAG, Dübendorf und an der ETHZ unter der  
Betreuung von Prof. René P. Schwarzenbach und  
Prof. Stefan B. Haderlein.

seit 2000            Assistent am Departement Umweltnaturwissen-  
schaften der ETHZ